

AN ABSTRACT OF THE THESIS OF

Travis J. Woolley for the degree of Master of Science in Forest Science presented on December 5, 2005.

Title: Inter-annual Variability of Net Primary Productivity Across Multiple Spatial Scales in the Western Oregon Cascades: Methods of Estimation and Examination of Spatial Coherence

Abstract Approved:

Mark E. Harmon

Kari E. O'Connell

Quantifying and modeling processes involved in the global carbon cycle is important to evaluate the temporal and spatial variability of these processes and understand the effect of this variability on future response to changing climate and land use patterns. Biomass accumulation and Net Primary Productivity (NPP) are large components of ecosystem carbon exchange with the atmosphere and thus are the focus of many modeling efforts. When scaling estimates of NPP temporally from days to years and spatially from square meters to landscapes and regions the spatial coherence of these processes through time must be taken into account. Spatial coherence is the degree to which pairs of sites across space are synchronous (i.e., correlated) through time with respect to a given process or variable. In this thesis I

determined the spatial coherence of a major component of NPP, tree bole productivity (NPP_B), and examine how it influences scaling and our ability to predict NPP and forecast change of this flux.

In Chapter 2 I developed and tested a method modeling radial tree increment growth from sub-sampled trees and estimating annual site-level biomass accumulation that allows quantification of the uncertainty in these estimates. Results demonstrated that a simple model using the mean and standard deviation of growth increments underestimated bole biomass increment in all three age classes examined by 1% at the largest sample sizes and up to 15% at the smallest sample sizes. The long term average NPP_B and inter-annual variability were also underestimated by as much as 10% and 22%, respectively. Stratification of trees by size in sampling and modeling methods increased accuracy and precision of estimates markedly. The precision of both models was sufficient to detect patterns of inter-annual variability. To estimate bole biomass accumulation with acceptable levels of accuracy and precision our results suggest sampling at least 64 trees per site, although one site required a sample size of more than 100 trees.

In Chapter 3 I compared year to year variability of NPP for tree boles (NPP_B) for two adjacent small watersheds (second-growth and old-growth) in the western Cascades of Oregon using the methods developed in Chapter 2. Spatial coherence of NPP_B within and between watersheds was assessed using multivariate analysis techniques. NPP_B was found to be less coherent between watersheds than within watersheds, indicating decreased spatial coherence with differences in age class and

increased spatial scale. However, a larger degree of spatial coherence existed within the old-growth watershed compared to the second-growth watershed, which may be a result of the smaller degree of variation in environmental characteristics in the former watershed. Within a watershed, potential annual direct incident radiation and heat load were more strongly associated with the variation of NPP_B than climate. Climatic factors correlated with the temporal variation of annual NPP_B varied between the two watersheds. Results suggest that inter-annual variability and spatial coherence of forest productivity is a result of both internal (e.g., environment and stand dynamics) and external (climate) factors. An unexpected conclusion was that spatial coherence was not consistent and changed through time. Therefore, the coherence of sites over time is not a simple relationship. Instead the patterns of spatial coherence exhibit complex behaviors that have implications for scaling estimates of productivity. This result also indicates that a correlation coefficient alone may not capture the complexity of change through time across space.

In Chapter 4 I estimated year to year variation of NPP_B for eleven sites of varying age, elevation, moisture, and species composition in the Western Cascades of Oregon. Spatial coherence of tree growth within sites and NPP_B between sites was assessed using Pearson's product-moment correlation coefficient (r). Results suggest that spatial coherence is highly variable between sites ($r=-0.18$ to 0.92). The second-growth sites exhibited the greatest temporal variability of annual NPP_B due to the large accumulation of biomass during stand initiation, but old-growth sites exhibited the greatest variation of coherence of NPP_B between sites. In some years all sites behaved

similarly, but for other years some sites were synchronous while others were not. As growth of individual trees and NPP_B at the site scale increased, inter-annual variability of those variables increased. Climate in part affected annual NPP_B , but intrinsic factors and spatial proximity also affected the coherence between sites in this landscape.

©Copyright by Travis J. Woolley
December 5, 2005
All Rights Reserved

Inter-annual Variability of Net Primary Productivity Across Multiple Spatial Scales in
the Western Oregon Cascades: Methods of Estimation and Examination of Spatial
Coherence

by
Travis J. Woolley

A THESIS

Submitted to

Oregon State University

in partial fulfillment of
the requirements for the
degree of

Master of Science

Presented on December 5, 2005
Commencement June 2006

Master of Science thesis of Travis J. Woolley presented on December 5, 2005.

APPROVED:

Co-Major Professor, representing Forest Science

Co-Major Professor, representing Forest Science

Head of the Department of Forest Science

Dean of the Graduate School

I understand that my thesis will become part of the permanent collection of Oregon State University libraries. My signature below authorizes release of my thesis to any reader upon request.

Travis J. Woolley, Author

ACKNOWLEDGEMENTS

I would like to first thank Mark E. Harmon and Kari E. O'Connell for giving me the opportunity to take on this project and for funding me through the process. I would like to thank Mark for challenging me to think outside of the box with my project, for which I have become a better scientist. I would like to thank Kari for being an understanding mentor and friend and keeping me sane through this whole process. I would also like to thank Jack Morgan for his contribution and creation of the scholarship in which funded my first year at Oregon State University.

I would like to thank all the people (too many to name) who helped in every way possible to help with the completion of this project. This includes all of the people involved in the H.J. Andrews Experimental Forest, especially Howard Bruner for his logistical support, coring trees in the snow, and the confidence he maintained in my abilities since I worked on his vegetation crew. I would also like to thank the Forest Service and the Long-Term Ecological Research program for providing such a unique and wonderful place to conduct research.

I would like to thank all of the graduate students in the Department of Forest Science that have worked along beside me for grueling hours in the computer lab, you guys and gals are the best. I would like to especially thank Stephanie Hart for her friendship first and foremost, as well as her staunch statistical advice and overall support through our time together as graduate students.

I would most of all like to thank my Mother for putting me in a position to succeed in life, I will forever be grateful. Last but certainly not least I would like to

thank my son Keiran for being a constant inspiration to do the best I can in all aspects of my life; I Love you bud.

CONTRIBUTION OF AUTHORS

Lisa Ganio and Manuela Huso provided much needed statistical advice throughout my project, and were both responsible for teaching me SAS and helping me to write endless amounts of code. Bruce McCune fostered ideas and provided guidance on statistical analysis for the second chapter.

TABLE OF CONTENTS

	<u>Page</u>
Chapter 1: General Introduction.....	1
Chapter 2: Estimating Annual Bole Biomass Increment: Determining Sampling and Modeling Methodology Using Uncertainty Analysis	6
Abstract	7
Introduction.....	9
Methods.....	11
Study Area.....	11
Data Collection	12
Biomass Calculation	13
Increment Modeling.....	13
Simple Random Model (SR).....	14
Stratified Simple Random Model (SRQ).....	15
Monte Carlo Uncertainty Analysis	15
Results.....	17
Simple Random Model (SR).....	18
Accuracy	18
Precision.....	19
Stratified Random Model (SRQ)	20
Accuracy	20
Precision.....	21
Discussion	21
Conclusions.....	24
Literature Cited	26
Chapter 3: Inter-annual variation and spatial coherence of Net Primary Productivity within and between a second-growth and an old-growth small watershed	51
Abstract	52
Introduction.....	54
Methods.....	55
Study Area.....	55
Data Collection	56
Tree Increment Dating Accuracy.....	57
Calculating Annual NPP _B and Plot-level Environmental Variables.....	58
Data Adjustments	60
Data Analysis	61
Results.....	62
Climate.....	62

TABLE OF CONTENTS (continued)

	<u>Page</u>
Environment and Topography	63
Discussion	67
Conclusions.....	70
Literature Cited	73
Chapter 4: Inter-annual variation and spatial coherence of Net Primary Productivity within and between sites across a Western Oregon Cascades landscape	99
Abstract	100
Introduction.....	102
Methods.....	104
Study Area.....	104
Data Collection	105
Tree Increment Dating Accuracy.....	105
Calculating Annual Net Primary Productivity (NPP _B)	106
Statistical Analysis.....	107
Results.....	108
Discussion	112
Conclusions.....	116
Literature Cited	117
CHAPTER 5: General Conclusions	127
Bibliography	129

LIST OF TABLES

<u>Table</u>	<u>Page</u>
2.1 Site Characteristics for the old-growth, mature, and second-growth sites.....	29
2.2 Allometric equations used to calculate total stem biomass (BST) in g for eight tree species	29
2.3 Mean biomass increment over entire time series and inter-annual variability of model estimates	30
3.1 Site Characteristics for second-growth and old-growth watersheds	76
3.2 Outlier Statistics for both watersheds	76
3.3 Summary Statistics for plots and years including outliers for both the second-growth and old-growth watersheds.....	76
3.4 PCA statistics for the first 4 axes corresponding to Figures 3.4 and 3.5	77
3.5 Correlation coefficients for climatic variables and associated axes for the second-growth and old-growth watersheds.....	78
3.6 A-statistics from MRPP of pair-wise comparisons of <i>a priori</i> groups in the second-growth watershed.....	79
3.7 PCA statistics with outliers for the first 4 axis corresponding to Figures 3.8 and 3.9	80
3.8 Correlation coefficients for measured environmental variables and associated axis for the second-growth and old-growth watersheds	80
3.9 PCA statistics with outliers for the first 4 axis corresponding to Figure 3.10	80
3.10 Correlation coefficients for measured environmental variables and associated axis for the comparison of old-growth and second-growth watersheds corresponding to Figure 3.10	81
3.11 PCA statistics for the first 4 axes corresponding to Figures 3.11 and 3.12	81
3.12 Correlation coefficients for measured environmental variables and associated axis for the second-growth and old-growth watersheds corresponding to Figures 3.11 and 3.12	81
3.13 Correlation coefficients for years of NPP _B and associated axis for the second-growth and old-growth watersheds corresponding to Figures 3.11 and 3.12	82
3.14 Response (+/-) of north and south facing zones in the second-growth watershed for different years.....	82

3.16 Correlation coefficients for years of NPP_B and associated axis for the comparison of second-growth and old-growth watersheds corresponding to Figure 3.13	83
3.17 PCA statistics for the first 4 axes corresponding to Figure 3.13.....	83
3.18 Correlation coefficients for measured environmental variables and associated axis for old-growth and second-growth watersheds together corresponding to Figure 3.13	84
4.1 Values of NPP_B for 11 sites sampled in the western Cascades, H.J. Andrews Experimental Forest, Oregon.....	120

LIST OF FIGURES

<u>Figure</u>	<u>Page</u>
2.1 Random Sampling and Radial Increment Growth Modeling Simulation Process	31
2.2 Distributions of radial growth increment of trees within the second-growth site	32
2.3 Distributions of radial growth increment of trees within the mature site	33
2.4 Distributions of radial growth increment of trees within the old-growth site.....	34
2.5 Distributions of Monte Carlo Simulation Estimates for varying sample sizes and years for the old-growth site using a simple random model (SR)	35
2.6 Distributions of Monte Carlo Simulation Estimates for varying sample sizes and years for the mature site using a simple random model (SR).....	36
2.7 Distributions of Monte Carlo Simulation Estimates for varying sample sizes and years for the second-growth site using a simple random model (SR)	37
2.8 Distributions of Monte Carlo Simulation Estimates for varying sample sizes and years for the old-growth site using a simple random model with quartiles (SRQ)	38
2.9 Distributions of Monte Carlo Simulation Estimates for varying sample sizes and years for the mature site using a simple random model with quartiles (SRQ).....	39
2.10 Distributions of Monte Carlo Simulation Estimates for varying sample sizes and years for the second-growth site using a simple random model with quartiles (SRQ)	40
2.11 Box plots showing distributions of biomass increment estimates at varying sample levels for four different years for the second-growth site	41
2.12 Box plots showing distributions of biomass increment estimates at varying sample levels for four different years for the mature site	42
2.13 Box plots showing distributions of biomass increment estimates at varying sample levels for four different years for the old-growth site	43
2.14 Box plots showing distributions of biomass increment estimates at varying sample levels for four different years for the second-growth site	44

LIST OF FIGURES (continued)

<u>Figure</u>	<u>Page</u>
2.15 Box plots showing distributions of biomass increment estimates at varying sample levels for four different years for the mature site	45
2.16 Box plots showing distributions of biomass increment estimates at varying sample levels for four different years for the old-growth site	46
2.17 Linear regressions comparing estimated annual biomass increment and true biomass increment	47
2.18 Plot of time series comparing true biomass increment and estimates from both models	48
2.19 Plot of time series comparing true biomass increment and estimates from both models (SR and SRQ) for the mature site.....	49
2.20 Plot of time series comparing true biomass increment and estimates from both models (SR and SRQ) for the old-growth site	50
3.1 Ordination of years of NPP_B across all plots for the second-growth watershed	85
3.2 Residual NPP_B (Mg/ha/yr) for two outlier plots	86
3.3 Average residual NPP_B (Mg/ha/yr) for riparian plots with and without outliers.....	87
3.4 Years of NPP_B across all plots for the second-growth watershed.....	88
3.5 Years of NPP_B across all plots for the second-growth watershed with an overlay of climatic variables	89
3.6 Years of NPP_B across all plots for the old-growth watershed.....	90
3.7 Years of NPP_B across all plots for the old-growth watershed with an overlay of climatic variables	91
3.8 Ordination of plots in the second-growth watershed in annual NPP_B space.....	92
3.9 Ordination of plots in the old-growth watershed in annual NPP_B space.....	93
3.10 Ordination of plots in both watersheds, in annual NPP_B space	94
3.11 Ordination of plots in the second-growth watershed in environmental space.....	95
3.12 Ordination of plots in the old-growth watershed in environmental space	96
3.13 Ordination of plots in both watersheds in environmental space	97

LIST OF FIGURES (continued)

<u>Figure</u>	<u>Page</u>
3.14 Average annual residual NPP _B for both the second-growth and old-growth watersheds	98
4.1 Residual annual radial growth increments	121
4.2 Linear regressions illustrating the relationship of increasing inter-annual variability of annual growth increment as mean growth rate increases	122
4.3 Box plots of annual NPP _B (Mg/ha/yr) vs. site and age class for 11 sites	123
4.4 Linear regression illustrating the relationship of increasing inter-annual variability of annual NPP _B (Mg/ha/yr).as mean annual NPP _B (Mg/ha/yr) increases across sites on the landscape	124
4.5 Annual NPP _B (Mg/ha/yr) over time for all sites	125
4.6 Average annual NPP _B across all sites	126

LIST OF APPENDIX FIGURES

<u>Figure</u>	<u>Page</u>
1.1 Map of H.J. Andrews Experimental Forest showing sampling sites	134

LIST OF APPENDIX TABLES

<u>Table</u>	<u>Page</u>
1.2 Sample Sizes used for uncertainty analysis for each age class	135
1.3 D-statistics and associated p-values from a Kolmogorov-Smirnov test for normality for Monte Carlo distributions	136
1.4 Four different years illustrating the estimate, standard deviation, and upper and lower bounds of biomass increment at varying sample sizes for the second-growth site using the SR model	137
1.5 Four different years illustrating the estimate, standard deviation, and upper and lower bounds of biomass increment at varying sample sizes for the mature site using the SR model.....	139
1.6 Four different years illustrating the estimate, standard deviation, and upper and lower bounds of biomass increment at varying sample sizes for the old-growth site using th SR model.....	141
1.7 Four different years illustrating the estimate, standard deviation, and upper and lower bounds of biomass increment at varying sample sizes for the second-growth site using the SRQ model	143
1.8 Four different years illustrating the estimate, standard deviation, and upper and lower bounds of biomass increment at varying sample sizes for the mature site using the SRQ model.....	145
1.9 Four different years illustrating the estimate, standard deviation, and upper and lower bounds of biomass increment at varying sample sizes for the old-growth site using the SRQ model	147
1.10 Coefficients for equations used to calculate volume and total stem biomass in Mg for five conifer species in the second-growth watersheds.....	149
1.11 Coefficients for equations used to calculate wood and bark volume and total stem biomass in Mg for seven conifer species in old-growth sites.....	150
1.12 Allometric equations used to calculate height (HT) for three hardwood tree species in both second-growth and old-growth watersheds	151
1.13 Allometric equations used to calculate total stem biomass (BST) in g for three hardwood tree species in both second-growth and old-growth watersheds	151
1.14 Allometric equations used to calculate total stem wood volume in g for three hardwood tree species in both second-growth and old-growth watersheds	151

LIST OF APPENDIX TABLES (continued)

<u>Table</u>	<u>Page</u>
1.15 Example SAS code for modeling of increment growth and estimation of NPP _B for a single site.....	152

Dedication

I would like to dedicate this thesis to Keiran R. Woolley, the single greatest inspiration in my life.

Chapter 1: General Introduction

This research was part of the Long-Term Ecological Research (LTER) program at the H.J. Andrews Experimental Forest. This program provides unprecedented opportunities to understand ecological phenomena at multiple temporal and spatial scales (Kratz et al. 2003). To understand ecological systems they must be studied over varying temporal and spatial scales (Magnuson 1990, Swanson and Sparks 1990) and predicting response of these systems to future change will require studying processes at varying locations across space (Kratz et al. 2003).

This study contributes to the understanding of temporal and spatial variability of annual tree productivity across different scales, which will in turn allow for better modeling of Net Primary Productivity (NPP) in these and other forested ecosystems. NPP is the net gain of biomass or carbon by vegetation after losses to plant respiration are accounted for. Carbon dynamics are important in terrestrial ecosystems and have consequences for predicting ecosystem response to future land use and climate change. These dynamics are directly influenced by NPP at multiple spatial and temporal scales. The importance of forests in the global carbon cycle, and their ability to act as sources or sinks of atmospheric carbon in the future in relation to climate change and land use (Dixon et al. 1994 and Clark et al. 2001), has been a topic of extensive research for over two decades (Huxman et al. 2004, Graumlich et al. 2004, Knapp and Smith 2001, Turner et al. 2000, Schimel et al., Turner and Koerper 1995, Webb et al. 1983). Understanding the inter-annual variability of NPP at multiple scales (i.e., watershed, landscape, region, biome) is critical in determining the

response of ecosystem processes to global change (Knapp and Smith 2001; Huxman et al. 2004).

To estimate NPP at broad scales or over long periods of time models are often used. Many ecosystem process models are driven by known physiological responses of plants to climate. Therefore, they assume a great deal of spatial coherence, at least as much coherence as expressed by the underlying climatic driving variables. However, similar sites or systems can respond differently to changes in identical drivers, depending on site history and spatial location (Kratz et al. 2003). There are other processes and factors affecting NPP that are not accounted for in these models. These factors as well as physiology can vary by species composition, age class, competitive status, local micro-site characteristics, etc. These factors are likely to reduce coherence of NPP spatially. Therefore, the actual correlations between biological processes across space may not be as high as the correlations between climatic variables across space. An initial step in understanding spatial correlations of biological processes is to determine spatial coherence of NPP through time. Spatial coherence can be defined as the degree to which temporal variation in processes or variables are synchronous or correlated among pairs of sites across space (definition altered from Magnuson et al. 1990; Baron and Caine 2000; Soranno et al. 1999; and Baines et al. 2000).

Several approaches are used to measure NPP in forests (Clark et al. 2001). Site-level estimates of annual NPP from ground-based measurements are likely to be the most accurate and precise, but can be costly, making sampling/coverage of an adequate temporal resolution and spatial extent difficult. Some studies have measured

and examined annual NPP on smaller scales, by collecting tree cores from small plots where all trees could be sampled (e.g., Graumlich et al. 2004). Alternatively a sub-sample can be taken (Campbell et al. 2004), although the sample size required for relatively accurate and precise estimates has not been determined.

In the second chapter I investigated a method for using increment cores in combination with long-term permanent plots and remeasurement records to estimate annual bole diameter increment. The larger objective of this analysis was to develop a method of sub-sampling trees and modeling radial increment growth to estimate annual tree bole productivity (NPP_B) and to examine the uncertainty produced in our estimates.

In the third chapter I examined the spatial coherence of annual tree NPP_B within and between two adjacent small watersheds of contrasting ages, so as to try and better understand how climate and environmental factors may be affecting this process spatially and temporally at the scale of small watersheds.

In the fourth chapter I investigated the inter-annual variability and spatial coherence of site level NPP_B across the landscape to gain an increased understanding of how extrinsic (climate) and intrinsic (e.g., disturbance, mortality) factors influence the fluctuations of NPP_B over time at an annual scale. Comparisons of variability at the site and landscape scale were also made.

Literature Cited

- Baines, S. B., K. E. Webster, T. K. Kratz, S. R. Carpenter, and J. J. Magnuson. 2000. Synchronous behavior of temperature, calcium, and chlorophyll in lakes of northern Wisconsin. *Ecology* **81**:815-825.
- Baron, J. S., and N. Caine. 2000. Temporal coherence of two alpine lake basins of the Colorado Front Range, U.S.A. *Freshwater Biology* **43**:463-476.
- Campbell, J., O. Sun, and B. E. Law. 2004. Disturbance and net ecosystem production across three climatically distinct forest landscapes. *Global Biogeochemical Cycles* **18**:1-11.
- Clark, D. A., S. Brown, D. W. Kicklighter, J. Q. Chambers, J. R. Thomlinson, and J. Ni. 2001. Measuring Net Primary Production in Forests. *Ecological Applications* **11**:356-370.
- Dixon, R. K., Brown S., Houghton, R.A., Solomon, A.M., Trexler, M.C., and Wisniewski, J. 1994. Carbon Pools and Flux of Global Forest Ecosystems. *Science* **263**:185-190.
- Graumlich, L. J., L. B. Brubaker, and C. C. Grier. 1989. Long-term trends in forest Net primary productivity: Cascade Mountains, Washington. *Ecology* **70**:405-410.
- Huxman, T. E., M. D. Smith, P. A. Fay, A. K. Knapp, R. M. Shaw, M. E. Lolk, S. D. Smith, D. T. Tissue, J. C. Zak, J. F. Weltzin, W. T. Pockman, O. E. Sala, B. M. Haddad, J. Harte, G. W. Koch, S. Schwinning, E. E. Small, and D. G. Williams. 2004. Convergence across biomes to a common rain use efficiency. *Nature* **429**:651-654.
- Knapp, K. A., and Smith, M.D. 2001. Variation among biomes in temporal dynamics of aboveground primary production. *Science* **291**:481-484.
- Kratz, T. K., Deegan, L.A., Harmon, M.E., Lauenroth, W.K. 2003. Ecological Variability in space and time: Insights gained from the US LTER program. *BioScience* **53**:57-67.
- Magnuson, J.J. 1990. Long-Term Ecological Research and the Invisible Present. *BioScience* **40**:495-501.
- Magnuson, J. J., B. J. Benson, and T. K. Kratz. 1990. Temporal coherence in the limnology of a suite of lakes in Wisconsin, USA. *Freshwater Biology* **23**:145-159.

- Schimel, D., Melillo, J., Tian, H., McGuire, D.A., Kicklighter, D., Kittel, T., Rosenbloom, N., Running, S., Thornton, P., Ojima, D., Parton, W., Kelly, R., Skyes, M., Neilson, R., Rizzo, B. 2000. Contribution of Increasing CO₂ and Climate to Carbon Storage by Ecosystems in the United States. *Science* **287**:2004-2006.
- Soranno, P. A., K. E. Webster, J. L. Riera, T. K. Kratz, J. S. Baron, P. A. Bukaveckas, G. W. Kling, D. S. White, N. Caine, R. C. Lathrop, and P. R. Leavitt. 1999. Spatial Variation among Lakes within Landscapes: Ecological Organization along Lake Chains. *Ecosystems* **2**:395-410.
- Swanson, F. J., and R. E. Sparks. 1990. Long-Term Ecological Research and the Invisible Place. *BioScience* **40**:502-508.
- Turner, D. P., Cohen W.B., Kennedy, R.E. 2000. Alternative spatial resolutions and estimation of carbon flux over a managed forest landscape in Western Oregon. *Landscape Ecology* **15**:441-452.
- Turner, D. P., and G. J. Koerper. 1995. A Carbon Budget for the Conterminous United States. *Ecological Applications* **5**:421-436.
- Webb, W. L., Lauenroth, W.K., Szarek, S.R., Kinerson, R.S. 1983. Primary production and abiotic controls in forests, grasslands, and desert ecosystems in the United States. *Ecology* **64**:134-151.

Chapter 2: Estimating Annual Bole Biomass Increment: Determining Sampling and Modeling Methodology Using Uncertainty Analysis

Travis J. Woolley, Mark E. Harmon, and Kari E. O'Connell

Prepared for submission to the *Canadian Journal of Forest Research*

Abstract

When estimating annual site level productivity in forests, it is important to determine the sample size necessary to obtain an accurate (no significant bias) and precise estimate (no greater than a defined percentage of the estimate) of annual biomass increment. It is also useful to estimate the error that arises from predicting growth increments for non-sampled trees. The objectives of this analysis were to: 1) develop a system for sub-sampling sites, 2) determine the adequate sample sizes needed to obtain an estimate of average annual radial growth increments, and 3) test simple models for applying sampled radial growth rates to non-sampled trees to estimate site level annual bole biomass increment (Mg/ha/yr). An uncertainty analysis using Monte Carlo methods was conducted using data from three Douglas-fir (*Pseudotsuga menziesii*) dominated sites of varying age classes (second-growth, mature, and old-growth) at the H.J. Andrews Experimental Forest, Oregon. Increment cores were extracted from all trees ≥ 5 cm diameter at breast height in each site and measured for annual growth increment (cm). A simple statistical model based on the mean and standard deviation of measured annual radial increment growth from sampled trees was used to predict increments for trees that were not sampled. This simple model was applied with and without stratified sampling by four size classes. This process was iterated 10,000 times and repeated for varying sample sizes. The mean and variance of these 10,000 biomass estimates were compared among different sample sizes for models with or without stratification. Results indicate that a simple model using the mean and standard deviation of growth increments underestimates bole biomass increment in all 3 age classes by 1% at the largest sample sizes and up to

15% at the smallest sample sizes. The long term average biomass production and inter-annual variability were also underestimated by as much as 10% and 22%, respectively. Applying stratification increased accuracy and precision of estimates markedly. The precision of both models was sufficient to detect patterns of inter-annual variability. Results suggest that second-growth and old-growth sites required similar sample sizes (~64 trees) to gain accuracy and precision of biomass estimates, while the mature site required a larger sample (~112 trees) to obtain similar accuracy and precision. This analysis has shown that sub-sampling and predicting radial increment growth by size class is a valid approach, but that more trees may need to be sampled than often assumed.

Introduction

The importance of forests in the global carbon cycle, and their ability to act as sources or sinks of atmospheric carbon in the future in relation to climate change and land use (Dixon et al. 1994 and Clark et al. 2001) has been a topic of extensive research for over two decades (Huxman et al. 2004, Graumlich et al. 2004, Knapp and Smith 2001, Turner et al. 2000, Schimel et al., Turner and Koerper 1995, Webb et al. 1983). Net Ecosystem Productivity (NEP) of forests has been a recent focus of much of this research (e.g., Van Tuyl et al. 2005, Law et al. 2004, Law et al. 2003, Harmon et al. 2004, Turner et al. 2003, Janisch and Harmon 2002, Goulden et al. 1996). NEP determines the nature of forests as sources or sinks of carbon from the atmosphere, and is the balance between Net Primary Productivity (NPP) and losses of carbon through heterotrophic respiration. The production of woody tissue by trees is a large component of NPP of forests. Thus understanding variations in tree bole productivity (NPP_B) is an important component in determining carbon sequestration in forests. The variability and behavior of NPP has implications for ecosystem response to future changes in climate (Knapp and Smith 2001).

Several approaches are used to measure NPP in forests (Clark et al. 2001). Site-level estimates of annual NPP from ground-based measurements are likely to be the most accurate and precise, but can be costly, making sampling/coverage of an adequate temporal resolution and spatial extent difficult. Permanent study plots (Acker et al. 1998) have been used to measure growth and mortality to estimate long-term trends in NPP, although the long measurement intervals do not lend themselves to accurate and precise annual estimates. Some studies have measured and examined

annual NPP on smaller scales, by collecting tree cores from small plots where all trees could be sampled (e.g., Graumlich and Brubaker 2004). Alternatively a sub-sample of tree cores can be taken (Campbell et al. 2004), although the sample size required for relatively accurate and precise estimates has not been determined. The small plot-based approach is difficult to apply over larger spatial scales, and can have limitations in estimating NPP (see Campbell et al. 2004 and Bond-Lamberty 2004). Satellite remote sensing combined with simulation modeling has also been used in a variety of ways to estimate components of the terrestrial carbon budget, including NPP, in a spatially explicit manner (Turner et al. 2000).

Here a method for using increment cores in combination with long-term permanent plots and remeasurement records to estimate annual bole biomass increment was explored. The objective of this analysis was to develop a method of sub-sampling trees and modeling radial increment growth to estimate annual tree bole biomass and to examine the uncertainty produced in our estimates. Estimates derived from this method can then be used to ask questions regarding climatic variability and behaviors of NPP_B across different spatial scales. This method will be applied across permanent forest plots to better understand temporal and spatial variability of tree NPP regionally. This method will also be a viable approach for estimating NPP in other types of plots and forested regions.

Given live bole biomass increment is a large component of tree NPP; we focused explicitly on production of biomass by tree boles for this analysis. I specifically asked the following questions: 1) What sub-sample sizes of tree increment cores are required to accurately and precisely (+/- 10%) estimate live annual bole

biomass increment?; 2) Is a simple model for increment prediction of non-sampled trees adequate to estimate site-level annual bole biomass increment with the desired level of accuracy and precision ($\pm 10\%$); and 3) How can accuracy and precision of our estimates of annual bole biomass increment be determined as a function of sample size?

Methods

Study Area

Data collection was conducted in three long-term permanent study plots within the H.J. Andrews Experimental Forest, Blue River, OR (Appendix 1.1). The experimental forest covers a 6,400 hectare (ha) drainage located in the western Oregon Cascades. Elevation ranges from 410 to 1630 meters (m). The maritime climate consists of cool wet winters and dry hot summers. Average annual precipitation ranges from 230 centimeters (cm) at lower elevations to 355 cm at higher elevations. Annual average daily temperatures range from 0.6° C in January, to 17.8° C in July (Bierlmaier and McKee 1989). The lower elevations are dominated by Douglas-fir (*Pseudotsuga menzeisii*), western hemlock (*Tsuga heterophylla*), and western red-cedar (*Thuja plicata*). As elevation increases, Douglas-fir and western hemlock dominance decrease, and are replaced by noble fir (*Abies procera*), mountain hemlock (*Tsuga mertensiana*), and Pacific silver-fir (*Abies amabilis*).

Each of the three sites represents a different age class (second-growth, mature, and old-growth) and elevation with similar species composition (Table 2.1). All three sites are within the *Tsuga heterophylla* forest zone (Franklin and Dyrness 1973). The old-growth site (RS07) was sampled in the summer of 2000 (Fraser 2001). The

second-growth site (WS06) was sampled in the summer 2001 during regular measurement of the permanent plot, and the mature site (RS32) was sampled in the summer 2003. All three sites are part of a long-term permanent study plot network designed to monitor changes in forest composition, structure, and function (Acker et al. 1998). The old-growth and mature sites are 0.25 ha square reference stands divided into 4 equal-sized plots. The second-growth site is a small watershed study area that contains transects with small circular sampling plots (0.1 ha) spaced at regular intervals. Although these sites were not randomly selected, they are representative of the age classes in this forested landscape.

Data Collection

Within the two reference stands (mature and old-growth), all live trees ≥ 5 cm diameter at breast height (DBH) were sampled. Within the second-growth site, samples were taken from tagged trees ≥ 5 cm in the north half of each upland plot and the half of each riparian plot in the direction away from the gauging station. Sampling consisted of coring a tree at breast height, and recording DBH to the nearest 0.1 cm. In both the mature and old-growth sites, trees ≥ 10 cm DBH were cored twice, at approximate right angles (preferentially the side-slope and upslope sides of the tree). In the second-growth site, only 1 core per tree was collected due to the smaller size of the trees. Increment cores were stored in paper straws and taken to the lab for preparation and measurement.

Increment core preparation consisted of mounting individual cores on routed blocks with wood glue, allowing them to dry sufficiently, and sanding them with a grit of 240, with a belt sander. All cores were then measured for annual radial increment

growth (mm), and measurements were then converted to centimeters for subsequent analyses. Cores from the old-growth site were measured by hand using a microscope, and radial increment growth was averaged between the two samples for trees ≥ 10 cm DBH. Increment cores from the mature and second-growth sites were measured using WinDendroTM image analysis software. All cores from these two sites were scanned to obtain an image for measurement, and the image was then digitally archived.

Biomass Calculation

Annual tree bole biomass was calculated using species and site-specific allometric equations (Table 2.2) from the BIOPAK equation library (Means et al. 1994). Annual stem diameter was calculated using the last remeasurement DBH, combined with measured annual growth increment from tree cores (similar to Graumlich et al. 2004). Diameters for each year were used in the bole biomass equations to estimate bole biomass. Annual tree bole biomass was calculated for all trees sampled in the field, and was summed to determine the annual bole biomass increment of the whole site (bole biomass change for all trees). This quantity of annual bole biomass increment will be referred to as the true annual bole biomass increment, as all individuals within the population of interest (≥ 5 cm DBH) were sampled. This quantity was used to compare to modeled outcomes with different sample sizes to evaluate accuracy and precision in an analysis of uncertainty (Figure 2.1).

Increment Modeling

To predict radial increment growth for non-sampled individuals two models were evaluated by examining the distribution of estimates produced by each model using a Monte Carlo simulation method (10,000 iterations). Simulated sampling of

tree growth increments was accomplished by sampling the population of trees using a uniform probability function (SAS v9.0). These sampled trees were used to estimate the mean and standard deviation used in modeling radial increment growth. All modeling and uncertainty analyses were done using SAS v9.0. A description of each model follows.

Simple Random Model (SR)

The simple random model uses the mean growth rate of all sampled trees in a given year, and the variation about that mean to predict increments for non-sampled trees (Figure 2.1). Specifically this model was:

Equation 2.1

$$\hat{G}_{ij} = \mu_j + \epsilon_{ij}$$

Where:

\hat{G}_{ij} = Predicted annual growth increment for the i^{th} tree, for the j^{th} year

μ_j = Mean growth increment for the j^{th} year

$\epsilon_{ij} \sim N(\mu_j, \sigma_j^2)$ = Random error term based on mean and variance for the j^{th} year.

The growth increment (\hat{G}_{ij}) of a non-sampled tree (i) for a given year (j) is predicted by adding a random error term (ϵ_{ij}) to the mean growth rate (μ_j) of sampled trees for that year. The random error term is based on the mean and variance (σ_j^2) of the sampled distribution. This model assumes that the increments from a site for a given year are normally distributed with constant variance. Secondly, it assumes that growth increment between trees is independent, and furthermore that increments between years within a tree are independent of one another. While the data used in this

analysis do not completely meet the assumptions of normality (Figures 2.2, 2.3, and 2.4), this assumption allows the model to be relatively simple.

Stratified Simple Random Model (SRQ)

In the second model stratified sampling by tree size was used, which more closely met the assumptions of normality. Therefore, the simple model was modified to predict increments by size class. Simulated stratified sampling was accomplished by dividing the population into quartiles based on the most recent measurements of diameter, and each quartile was sampled separately using a uniform probability function (SAS v9.0). All calculations necessary for increment modeling, as well as the prediction of increments, were completed independently for each quartile. Specifically this model was:

Equation 2.2

$$\hat{G}_{ijq} = \mu_{qj} + \epsilon_{ijq}$$

Where:

\hat{G}_{ijq} = Predicted annual growth increment for the i^{th} tree, from the q^{th} quartile, for the j^{th} year

μ_{qj} = Mean growth increment of the q^{th} quartile, for the j^{th} year

$\epsilon_{ijq} \sim N(\mu_{qj}, \sigma_{qj}^2)$ = Random error term based on mean and variance of the q^{th} quartile in the j^{th} year.

Monte Carlo Uncertainty Analysis

To determine both accuracy and precision of estimates of the models, an analysis of uncertainty was performed using Monte Carlo methods (Figure 2.1). Simulated random sampling of individual tree increments from the population, increment model applications, and tree biomass calculations were repeated 10,000

times, resulting in 10,000 estimates of site level bole biomass increment (Mg/ha/yr) for each sample size at each site. Basic rules of thumb suggest that for standard error estimates 100 to 200 iterations are necessary, but 1,000 or more iterations would be necessary for estimating confidence intervals (Chernick 1999). Distributions produced by 1,000 iterations tended to be highly variable in terms of normality, and that 10,000 iterations led to more consistent normality of distributions. The more normal distributions are, the better simple parameters such as standard deviations approximate distributions of estimates. Random sampling was conducted using a uniform distribution so all individuals had an equal probability of selection for each simulation. Simulated sampling sizes were 90%, 80%, 70%, 60%, 50%, 40%, 30%, 20%, and 10% of the entire population (for actual numbers of trees sampled for each site see Appendix 1.2). The mean and standard deviation of these 10,000 estimates were used to compare to the true population bole biomass increment. The error of our mean estimate was calculated as the standard deviation of the 10,000 estimates multiplied by 1.645, to capture 90% of the distribution of our estimates. This range was compared to +/- 10% of the true biomass increment which was our desired level of precision. Distributions of Monte Carlo estimates were tested for normality using the Kolmogorov-Smirnov test for normality – SAS v9.0. This test computes a *D*-statistic, based on the largest vertical difference between the proportion of observations less than or equal to the distribution function and the probability of an observation less than or equal to the distribution function. The *D*-statistic is then used to test against a normal distribution with mean and variance equal to the mean and variance of the distribution in question.

The calculation of the Coefficient of Variation (%CV) of inter-annual variability and error of estimates is shown in equations 2.3 and 2.4 below.

Equation 2.3

$$\%CV = (SD_j / \mu_{1...j}) * 100$$

Where:

%CV= Coefficient of Variation expressed as a percent

SD_j= Standard deviation of estimated biomass increment of the **jth** year

μ_{1...j}= Average estimated biomass increment over entire time series (**jth** years)

Equation 2.4

$$\%CV = (SD_{1...j} / \mu_{1...j}) * 100$$

Where:

%CV= Coefficient of Variation expressed as a percent

SD_{1...j}= Standard deviation of true biomass increment over entire time series (**jth** years)

μ_{1...j}= Average true biomass increment over entire time series (**jth** years)

Results

Given the large number of years within each of the three time series, a subset of four years was used to present results from all the years. Comparisons of model estimates of annual biomass increment (average of 10,000 estimates) with the true annual biomass increment, as well as the range of the model estimates are shown for these years.

Summaries are presented for the inter-annual variability (i.e., standard deviation) of average annual biomass increment over the entire time series (i.e.,

average of all years) for each site and how modeling results compare to the long-term trends of the true average biomass increment over time for each site.

The assumption that the distributions of Monte Carlo simulations are normally distributed were not met statistically for either model (SR or SRQ) using the Kolmogorov-Smirnov test for normality (Appendix 1.3). However, the distributions visually appear approximately normal at higher sample sizes, although they become slightly skewed at the lowest sample sizes (Figures 2.5, 2.6, 2.7, 2.8, 2.9, and 2.10). The statistical significance indicating non-normality was a consequence of the large sample size (10,000) of the population of estimates, allowing extremely small departures from normality (e.g., skewness and kurtosis) to be detected. The distributions were considered normal because these departures seemed small visually.

Simple Random Model (SR)

Accuracy

Results from the uncertainty analysis indicate that a simple random model (SR) underestimates annual bole biomass increment for all age classes (second-growth, mature, and old-growth) at all sample sizes (Figures 2.11, 2.12, 2.13). For example, the mean estimate of bole biomass increment at the highest sample size fell below the true bole biomass increment of the entire population, for all sites in almost all years reported, with the exception of 1985 for the old-growth site (for estimates of annual biomass increment and error of estimates at varying sample sizes for each age class see Appendix 1.4-1.9). Estimates for the four years reported were on average 0.044, 0.062, and 0.030 Mg/ha/yr below the true bole biomass increment (3.55, 4.30, and 3.22 Mg/ha/yr) at the highest sample size for second-growth, mature, and old-growth

sites, respectively. This underestimation was as much as 15% of the true biomass increment.

Results from linear regressions of estimates against the true annual biomass increment (Figure 2.20) illustrate an increasing bias in estimates as annual biomass increment increases for all three age classes. Intercepts were statistically different from zero (two-sided p-value \leq 0.0001, 0.0006, and 0.0003 for second-growth, mature, and old-growth sites respectively), and slopes were significantly less than one (two-sided p-value \leq 0.0001 for all three sites). The resulting bias indicates that this model was not as accurate as desired, and was inadequate for predicting annual bole biomass increment. The increasing bias as biomass increment increases (Figures 2.17, 2.18 and 2.19) led to underestimates of the inter-annual variability of average annual bole biomass increment (Table 2.3).

Precision

The SR model only met the desired level of precision (\pm 10%) at the highest sample sizes for all three age classes. As expected, the precision of the estimates decreases (i.e., increased variability around the mean estimate of bole biomass increment annually) as sample sizes become smaller for all age classes (Figure 2.11, 2.12, and 2.13). The uncertainty analysis, however, did confirm that even with underestimation, the SR model was precise enough to be within \pm 10% for sample sizes \geq 90% of the total population at each age class.

The coefficient of variation (%CV) of estimates (Equation 2.3) ranged from 3-7% across all three age classes. As compared to %CV of the true biomass increment (Equation 2.4) of 12.5 %, 16%, and 13.5% for the second-growth, mature, and old-

growth site, respectively. This comparison of precision and inter-annual variability indicated that the error of the estimates was within the bounds of inter-annual variability.

Stratified Random Model (SRQ)

Accuracy

The addition of stratification to the simple random model resulted in improved accuracy of bole biomass increment estimates. For both the second-growth and old-growth sites, the model estimated live bole biomass increment with a sample size of approximately 64 trees with increased accuracy over the SR model (Figures 2.14, 2.15, and 2.16). Again as with the SR model, the SRQ model estimates did not equal the true bole biomass increment. Estimates for the four years reported were on average 0.014 (second-growth) and 0.044 (old-growth) Mg/ha/yr above the true bole biomass increment (3.55 and 3.22 Mg/ha/yr second-growth and old-growth, respectively). Similar patterns held true for the mature site, with an average overestimation of 0.028 Mg/ha/yr for the (true biomass increment of 4.30 Mg/ha/yr). Across all sites, the average overestimation of the model increased with increased age of the site.

Linear regressions (Figure 2.17) show that the intercept for the old-growth site was still significantly different from zero (intercept=0.074, two-sided p-value=0.0005) confirming a slight but consistent overestimation (slope=1, two sided p-value=0.205). However, slopes and intercepts were not statistically different from one or zero, respectively, for either the second-growth (two-sided p-value for slope=0.1522 and intercept=0.1663) or mature sites (two-sided p-value for slope=0.5662 and intercept=0.095). The stratified model (SRQ) did necessitate a much larger sample

size for the mature site than the second-growth and old sites, requiring a sample size of more than 112 trees for three of the four years reported, and 96 trees for the other year. These larger sample sizes were due to lack of precision and not a large decrease in the accuracy of the estimate at lower levels of sampling.

Precision

The range of estimates fell within +/-10% of the true bole biomass increment at lower sample sizes than the SR model for both the second-growth and mature site, but not for the old-growth site. The increase in precision for the second-growth and mature site was caused by a decrease in the standard deviation of the estimate compared to the SR model, while a small decrease in accuracy and precision for the old-growth site led to similar sample size requirements for both the SR and SRQ models. As with the SR model the precision of estimates decreases as sample sizes decrease.

The coefficient of variation (%CV) of estimates ranged from 3-7% across all three age classes as compared to %CV of the true biomass increment of 12.5%, 16%, and 13.5% for the second-growth, mature, and old-growth sites, respectively. This comparison of precision and inter-annual variability indicates that the error of the estimates was comparable to the SR model, thus adequate to detect patterns of inter-annual variability (Figures 2.18, 2.19, and 2.20).

Discussion

Trees were sub-sampled and radial increment growth was modeled for non-sampled trees in long-term permanent plots to estimate annual biomass increment. The

goals of this analysis were: 1) to develop a sampling methodology and a model that was simple and could be used for varying age classes; 2) to determine approximately what sample sizes necessary to estimate annual biomass increment precisely; and 3) to capture the inter-annual variability of annual biomass increment.

Monte Carlo methods provided a technique to estimate the accuracy and precision of estimates using a simple model, with and without stratified sampling. We determined that without stratification by tree size, the model did not accurately estimate biomass increment, and showed an increasing bias as annual biomass increment increased for all three age classes. This bias caused an underestimation of the long-term average annual biomass increment and the inter-annual variability of that average. When stratification was applied to the model estimates of annual biomass increment were highly accurate, with the only bias being a slight and consistent overestimation of 0.074 Mg/ha/yr for the old-growth site.

Using this method the approximate sample sizes necessary to estimate annual biomass increment precisely and to capture the inter-annual variability of annual biomass increment were determined. The use of stratification resulted in decreased sample sizes for all sites. Second-growth and old-growth sites essentially required the same sample sizes, while the mature site needed a much larger sample size. The latter site could have higher variability of growth rates compared to other mature sites, or it could be that this stage of succession has greater inter-annual variability of growth between trees than that of second-growth and old-growth sites. The lack of replication of ages in this analysis does not allow us to determine if this is atypical of mature sites in the study area.

An important outcome of our analysis was the attainment of estimates of annual biomass increment that could be used to examine patterns of inter-annual variability of NPP. The variation in our estimates was much lower than the variation over time of biomass increments (indicated by lower %CV). This ensures that the error in our estimates will not have an undue affect on patterns seen in inter-annual variability of biomass increment, and thus subsequent estimates of NPP.

Different models or parameters may be necessary for estimating bole biomass increment of different age classes more accurately. Since the bias of estimates for the old-growth site was consistent, it would be possible to add an adjustment to the model or the estimates produced by the model if desired. Given that this analysis involved time series, autocorrelation may need to be considered, and therefore autoregressive models may hold the key to better prediction of individual tree growth, estimation of site level bole biomass increment, and inter-annual variability using smaller sample sizes.

Annual biomass increment values from this study are comparable to those found in previous studies (Grier and Logan 1977, and Gholz 1982), but lower than reported by Van Tuyl and others (2005). The largest source of error when estimating tree biomass production has been shown to be the prediction of radial growth increment of non-sampled trees (Campbell et al. 2004). Some studies have sampled entire plots of trees to remove this source of error (Graumlich et al. 1989), but this approach is often not feasible for sampling large stands and/or for large numbers of plots across a larger study area. Different methods have been developed to deal with the variation created by sub-sampling trees. For example, Jenkins and others (2001)

used linear regression models correlating diameter and radial growth to predict radial growth for non-sampled trees. Although this method is useful for making generalized estimates at the plot level, it may not maintain within plot or between plot variability (Campbell et al. 2004). Thus the value of this technique for examining temporal patterns between sites across space is limited. Campbell and others (2004) used a DBH quartile method similar to our method, where mean radial growth increment for the trees in a quartile was assigned to the unmeasured trees in that quartile. Our study used a very similar approach, but by using Monte Carlo methods and assigning radial growth increment randomly based on the mean and variance of a given quartile's distribution we were able to estimate the uncertainty of our biomass estimates. With information about uncertainty this method allows the researcher to decide on sample size accordingly.

The method developed in this analysis may not be appropriate for all objectives and our results indicate alterations in model structure and complexity may be needed. Although we have shown it can be a useful tool to predict radial growth for non-sampled trees. Moreover it can be used to predict radial growth of trees lost to mortality in previous years. This will be particularly useful for permanent plots where a record of mortality for individual trees exists.

Conclusions

This analysis has shown that sub-sampling radial growth increment using stratification by tree size and application of a relatively simple random model is a valid approach to estimating annual bole biomass increment. However, more trees may need to be sampled than previously sampled in other studies. Improvements on

the model structure and complexity may allow increased accuracy and precision, as well as smaller sample sizes. The error of estimates associated with predicting growth increment of non-sampled trees was determined at varying sample sizes by using Monte Carlo uncertainty analysis. This methodology was also sufficient in replicating the patterns of inter-annual variability of live bole biomass increment, a major component of the inter-annual variability of NPP. By using this methodology one can now begin to further answer questions regarding patterns of annual NPP at the site, landscape, and regional scales in forests of the Pacific Northwest and elsewhere.

Literature Cited

- Acker, S. A., Halpern, C.B., Harmon, M.E., and Dyrness, C.T. (2002). "Trends in Biomass accumulation, net primary production, and tree mortality in *Psuedotsuga menziesii* forest of contrasting age." *Tree Physiology* **22**: 213-217.
- Acker, S. A., W. A. McKee, et al. (1998). Long-term research on forest dynamics in the Pacific Northwest: a network of permanent forest plots. Forest biodiversity in North, Central, and South America and the Caribbean: Research and Monitoring, Washington, DC, The Parthenon Publishing Group.
- Bierlmaier, F. A., and McKee, A. (1989). Climatic Summaries and Documentation for the Primary Meteorological Station, H.J. Andrews Experimental Forest, 1972 to 1984. Gen. Tech. Rep. PNW-GTR-242. Portland, OR, Department of Agriculture, Forest Service, Pacific Northwest Research Station: 56 p.
- Bond-Lamberty, B., C. Wang, et al. (2004). "Net primary production of a black spruce wildfire chronosequence." *Global Change Biology* **10**: 473-487.
- Campbell, J., O. Sun, et al. (2004). "Disturbance and net ecosystem production across three climatically distinct forest landscapes." *Global Biogeochemical Cycles* **18**: 1-11.
- Chernick, M. R. (1999). *Bootstrap Methods: A Practitioner's Guide*. New York, John Wiley & Sons, Inc.
- Clark, D. A., S. Brown, et al. (2001). "Measuring Net Primary Production in Forests." *Ecological Applications* **11**(2): 356-370.
- Dixon, R. K., Brown S., Houghton, R.A., Solomon, A.M., Trexler, M.C., and Wisniewski, J. (1994). "Carbon Pools and Flux of Global Forest ecosystems." *Science* **263**: 185-190.
- Franklin, J. F. and C. T. Dyrness (1973). Natural vegetation of Oregon and Washington, USDA Forest Service General Technical Report PNW 8. Pacific Northwest Forest and Range Experiment Station.
- Fraser, V. D. (2001). Biomass and productivity in an old-growth Douglas-fir/western hemlock stand in the western Cascades of Oregon. Project in Ecology.
- Gholz, H. L. (1982). "Environmental limits on aboveground net primary production, leaf area and biomass production in vegetation zones of the pacific northwest." *Ecology* **63**(2): 469-481.

- Goulden, M. L., J. W. Munger, et al. (1996). "Exchange of Carbon Dioxide by a deciduous forest: Response to interannual climate variability." *Science* **271**: 1576-1578.
- Graumlich, L. J., Brubaker, L.B., and Grier, C.C. (1989). "Long-term trends in forest Net primary productivity: Cascade Mountains, Washington." *Ecology* **70**(2): 405-410.
- Grier, C. C., and Logan, R.S. (1977). "Old-growth *Pseudotsuga menziesii* communities of a western Oregon watershed: Biomass distribution and production budgets." *Ecological Monographs* **47**: 373-400.
- Harmon, M. E., Bible K., Ryan, M.G., Shaw, D.C., Chen, H., Klopatek, J., and Xia, L. (2004). "Production, respiration, and overall Carbon Balance in an old-growth *Pseudotsuga-Tsuga* Forest Ecosystem." *Ecosystems* **7**: 498-512.
- Huxman, T. E., M. D. Smith, et al. (2004). "Convergence across biomes to a common rain use efficiency." *Nature* **429**: 651-654.
- Janisch, J. E. a. H., M.E. (2002). "Successional changes in live and dead wood carbon stores: implications for net ecosystem productivity." *Tree Physiology* **22**: 77-89.
- Jenkins, J. C., R. A. Birdsey, et al. (2001). "Biomass and NPP estimation for the mid-atlantic region (USA) using plot-level forest inventory data." *Ecological Applications* **11**(4): 1174-1193.
- Knapp, K. A., and Smith, M.D. (2001). "Variation among biomes in temporal dynamics of aboveground primary production." *Science* **291**: 481-484.
- Law, B. E., O. J. Sun, et al. (2003). "Changes in carbon storage and fluxes in a chronosequence of Ponderosa Pine." *Global Change Biology* **9**: 510-524.
- Law, B. E., D. P. Turner, et al. (2004). "Disturbance and climate effects on carbon stocks and fluxes across western Oregon, USA." *Global Change Biology* **10**: 1429-1444.
- SAS Institute (2002). SAS Version 9.1. SAS Inc. Carey N.C.
- Schimel, D., Melillo, J., Tian, H., McGuire, D.A., Kicklighter, D., Kittel, T., Rosenbloom, N., Running, S., Thornton, P., Ojima, D., Parton, W., Kelly, R., Skyes, M., Neilson, R., Rizzo, B. (2000). "Contribution of Increasing CO₂ and Climate to Carbon Storage by Ecosystems in the United States." *Science* **287**: 2004-2006.

- Turner, D. P., Cohen W.B., Kennedy, R.E. (2000). "Alternative spatial resolutions and estimation of carbon flux over a managed forest landscape in Western Oregon." *Landscape Ecology* **15**: 441-452.
- Turner, D. P., Guxy, M., Lefsky, M.A., Van Tuyl, S., Sun, O., Daly, C., Law, B.E. (2003). "Effects of land use and fine scale environmental heterogeneity on net ecosystem production over a temperate coniferous forest landscape." *Tellus* **55(B)**: 657-668.
- Turner, D. P. and G. J. Koerper (1995). "A Carbon Budget for the Conterminous United States." *Ecological Applications* **5(2)**: 421-436.
- Van Tuyl, S., Law, B.E., Turner, D.P., Gitelman, A.I. (2005). "Variability in net primary production and carbon storage in biomass across Oregon forests-an assessment integrating data from forest inventories, intensive sites, and remote sensing." *Forest Ecology and Management* **209**: 273-291.
- Webb, W. L., Lauenroth, W.K., Szarek, S.R., Kinerson, R.S. (1983). "Primary production and abiotic controls in forests, grasslands, and desert ecosystems in the United States." *Ecology* **64(1)**: 134-151.

Tables

Table 2.1 Site Characteristics for the old-growth, mature, and second-growth sites.

Site	Age Class (yrs)	Elevation (m)	Dominant Tree Species	Area Sampled (ha)	# of trees \geq 5cm DBH
RS07	Old-growth (460)	460	<i>Pseudotsuga menziesii</i> / <i>Tsuga heterophylla</i>	0.25	71
RS32	Mature (145)	650	<i>Pseudotsuga menziesii</i> / <i>Tsuga heterophylla</i>	0.25	160
WS06	Second-growth (35)	900-1000	<i>Pseudotsuga menziesii</i>	0.51	311

Table 2.2 Allometric equations used to calculate total stem biomass (BST) in g for eight tree species, using diameter at breast height measurements (DBH). All equations are in the following form – $\ln(\text{BST}) = B_0 + B_1 * \ln(\text{DBH})$.

Species	Site(s)	BIOPAK Equation #	(B ₀)	(B ₁)
<i>Pseudotsuga menziesii</i>	RS07/RS32/WS06	256	4.660412	2.4247
<i>Tsuga heterophylla</i>	RS07/RS32/WS06	259	3.968674	2.5989
<i>Thuja plicata</i>	RS07/RS32/WS06	332	4.077376	2.4024
<i>Taxus brevifolia</i>	RS32	259	3.968674	2.5989
<i>Calocedrus decurrens</i>	RS32	386	2.112422	2.7818
<i>Acer macrophyllum</i>	WS06	35	-4.574	2.574
<i>Prunus emarginata</i>	WS06	43	3.1998	2.658
<i>Castanopsis chrysophylla</i>	WS06	43	3.1998	2.658

Table 2.3 Mean biomass increment over entire time series and inter-annual variability of model estimates (SR=no stratification, and SRQ=with stratification) at the appropriate sample size.

Age Class (# of years)	Estimate Type (# of trees sampled)	Average Biomass Increment Over Time (Mg/ha/yr)	Inter-annual Variability of average biomass increment - Standard Deviation
	Entire Population (311)	3.615	0.449
Second-growth (12)	SR (64)	3.250	0.349
	SRQ (64)	3.613	0.441
	Entire Population (159)	4.359	0.698
Mature (32)	SR (96)	4.089	0.620
	SRQ (96)	4.393	0.697
	Entire Population (71)	3.461	0.468
Old-growth (28)	SR (64)	3.428	0.449
	SRQ (64)	3.511	0.465

Figures

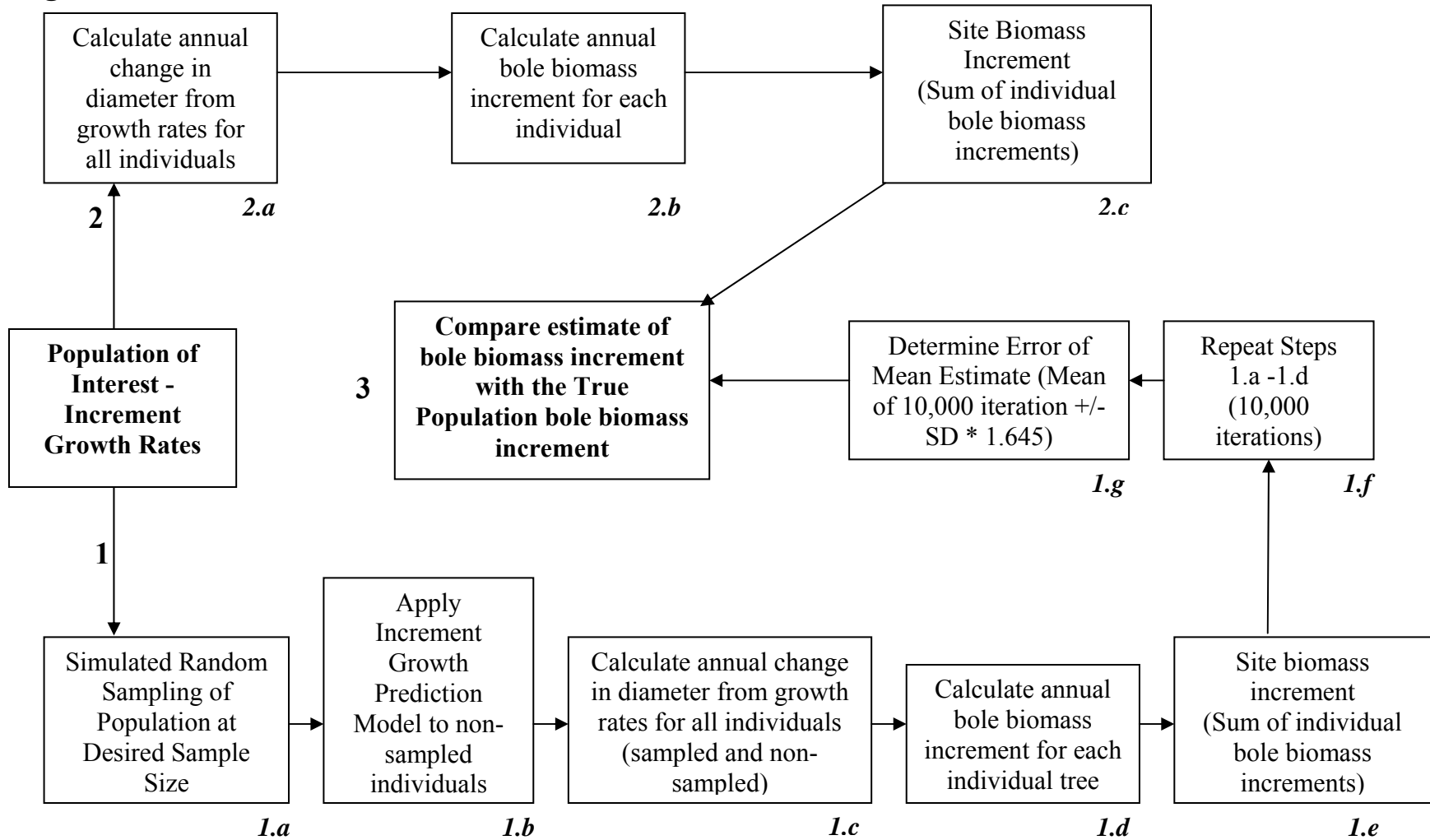


Figure 2.1 Random Sampling and Radial Increment Growth Modeling Simulation Process.

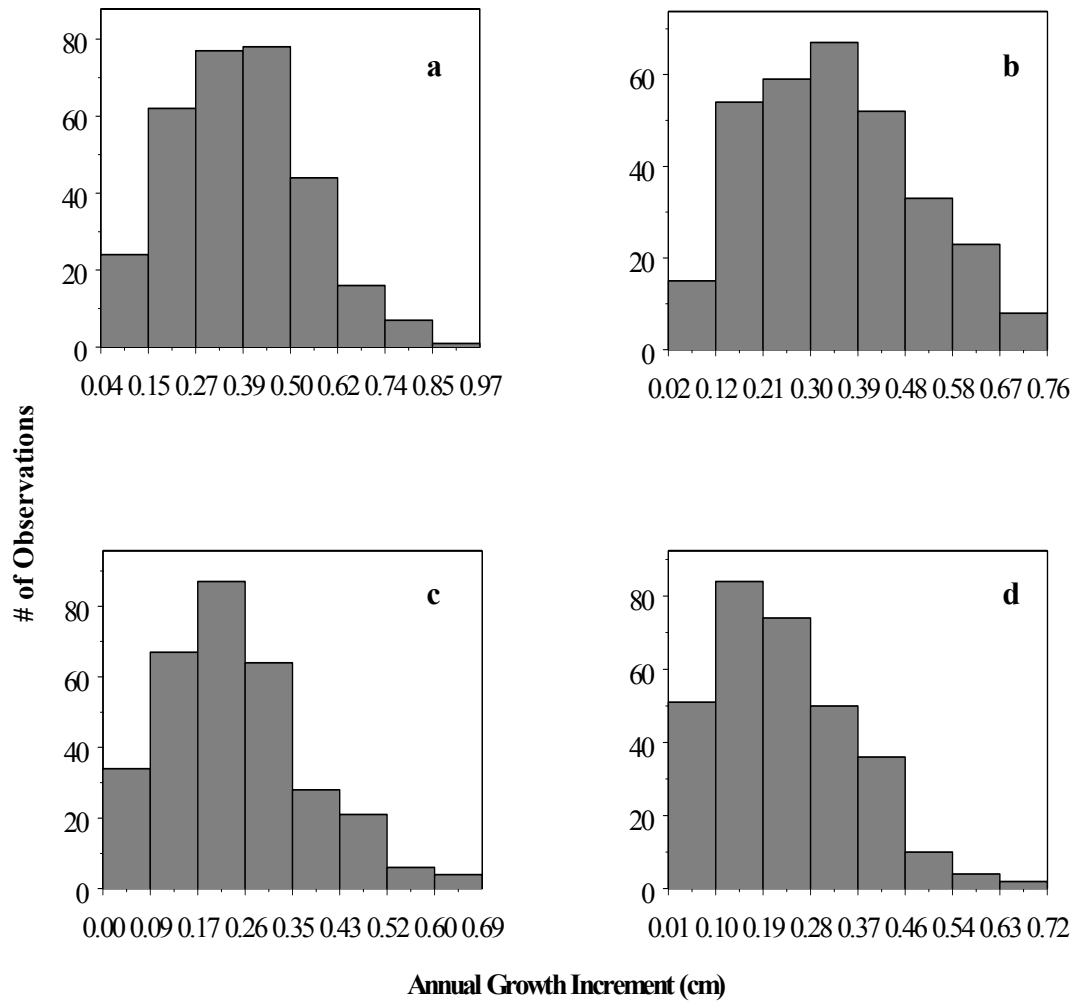


Figure 2.2 Distributions of radial growth increment of trees within the second-growth site for four different years (**a**=1991, **b**=1995, and **c**=1999, **d**=2001).

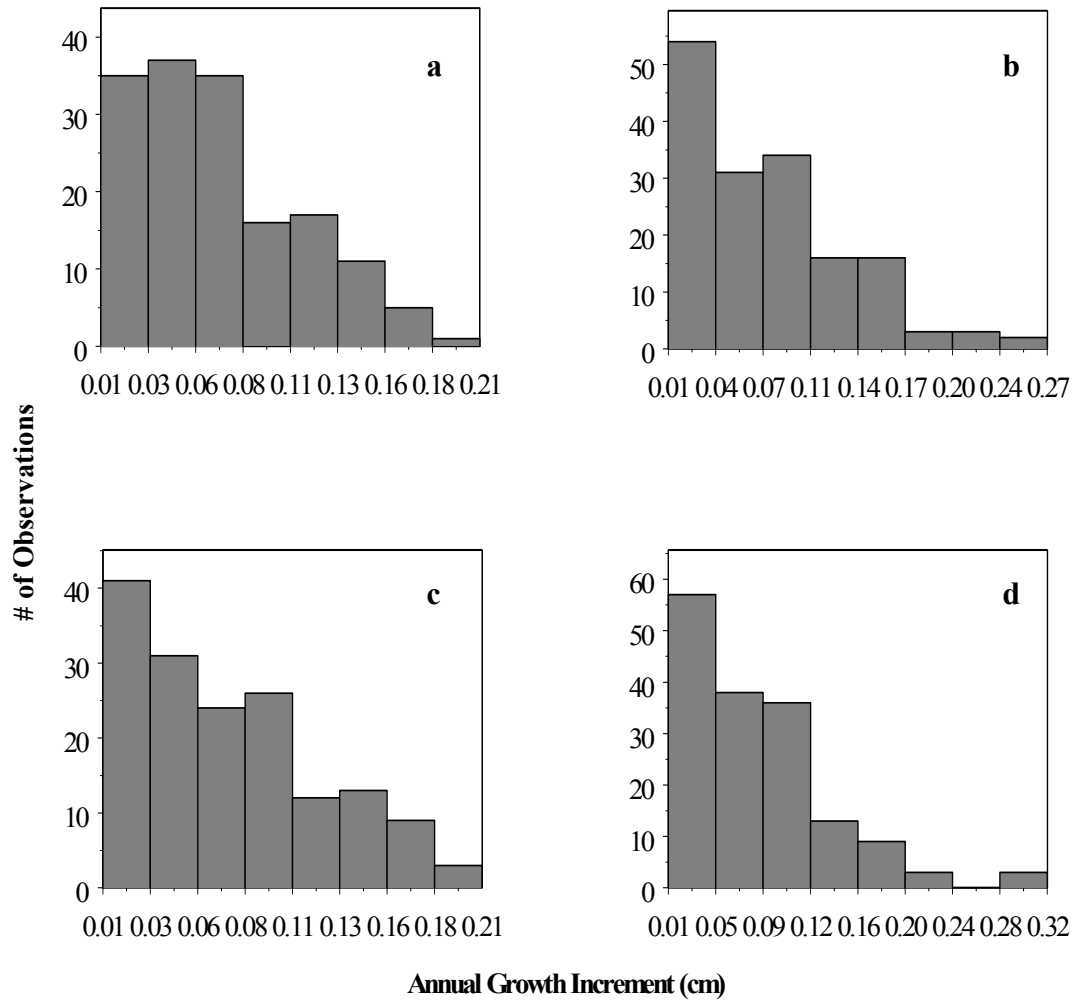


Figure 2.3 Distributions of radial growth increment of trees within the mature site for four different years (**a**=1975, **b**=1985, and **c**=1995, **d**=1999).

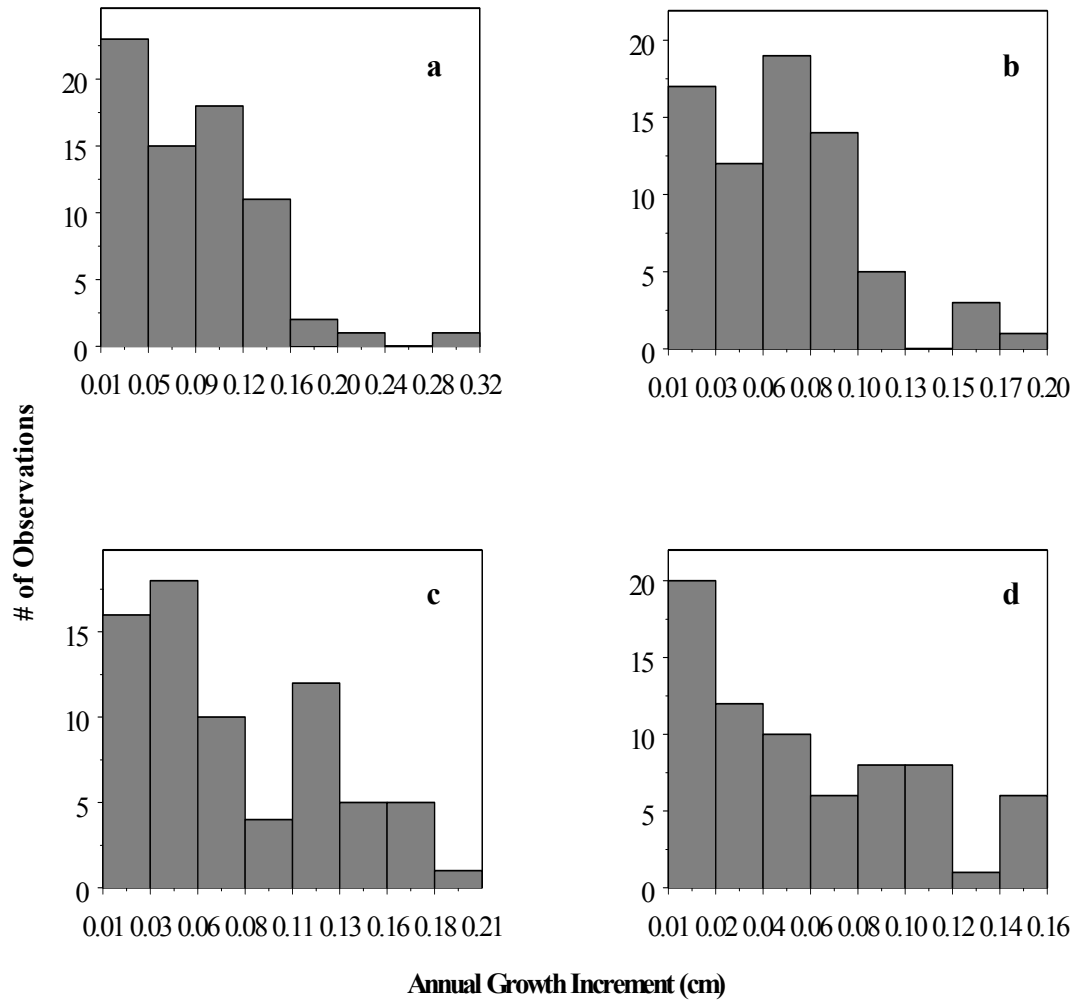


Figure 2.4 Distributions of radial growth increment of trees within the old-growth site for four different years (**a**=1975, **b**=1985, and **c**=1995, **d**=1999).

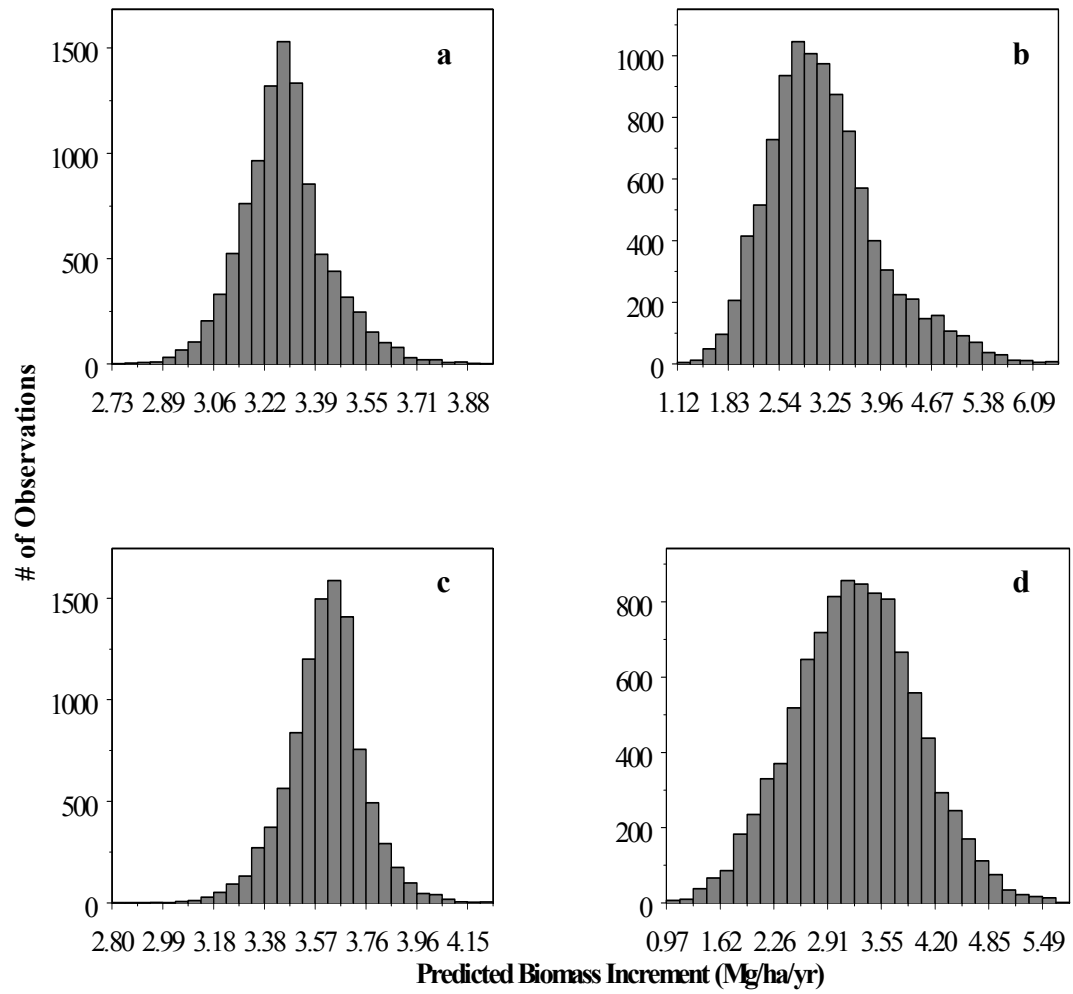


Figure 2.5 Distributions of Monte Carlo Simulation Estimates for varying sample sizes and years for the old-growth site using a simple random model (SR). Panels **a** and **b** represent year 1975, sample sizes 64 and 8, respectively. Panels **c** and **d** represent year 1995, sample sizes of 64 and 8, respectively.

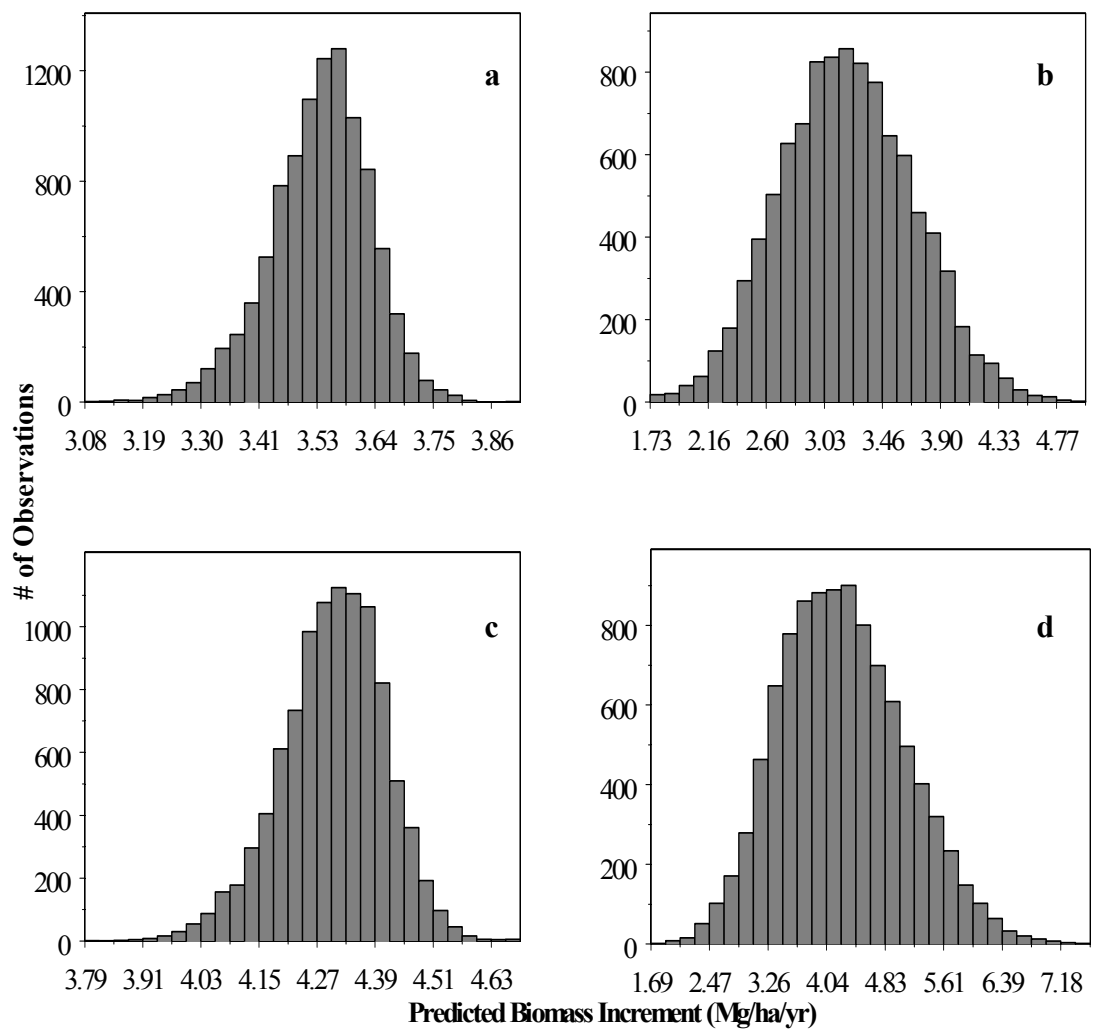


Figure 2.6 Distributions of Monte Carlo Simulation Estimates for varying sample sizes and years for the mature site using a simple random model (SR). Panels **a** and **b** represent year 1975, sample sizes 144 and 32, respectively. Panels **c** and **d** represent year 1995, sample sizes of 144 and 32, respectively.

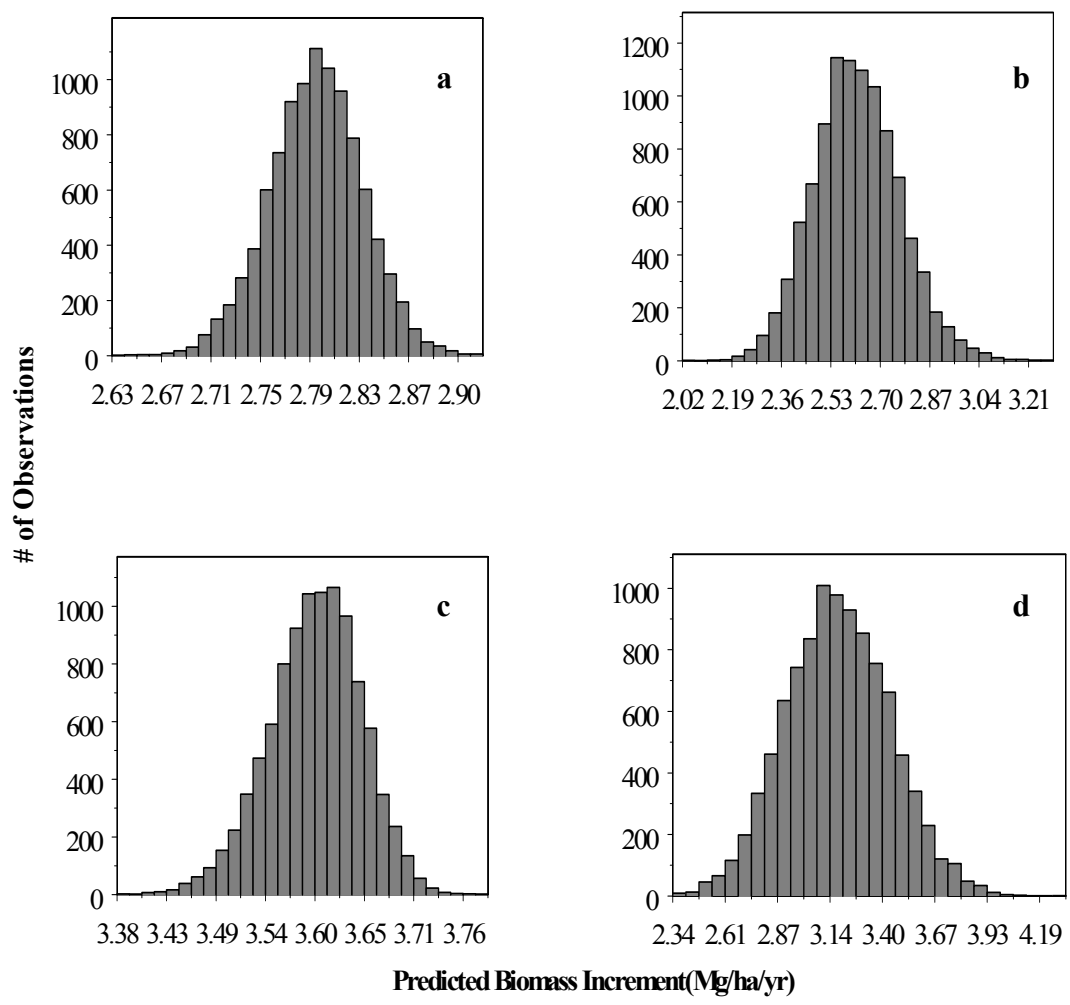


Figure 2.7 Distributions of Monte Carlo Simulation Estimates for varying sample sizes and years for the second-growth site using a simple random model (SR). Panels **a** and **b** represent year 1991, sample sizes 280 and 32, respectively. Panels **c** and **d** represent year 1999, sample sizes of 280 and 32, respectively.

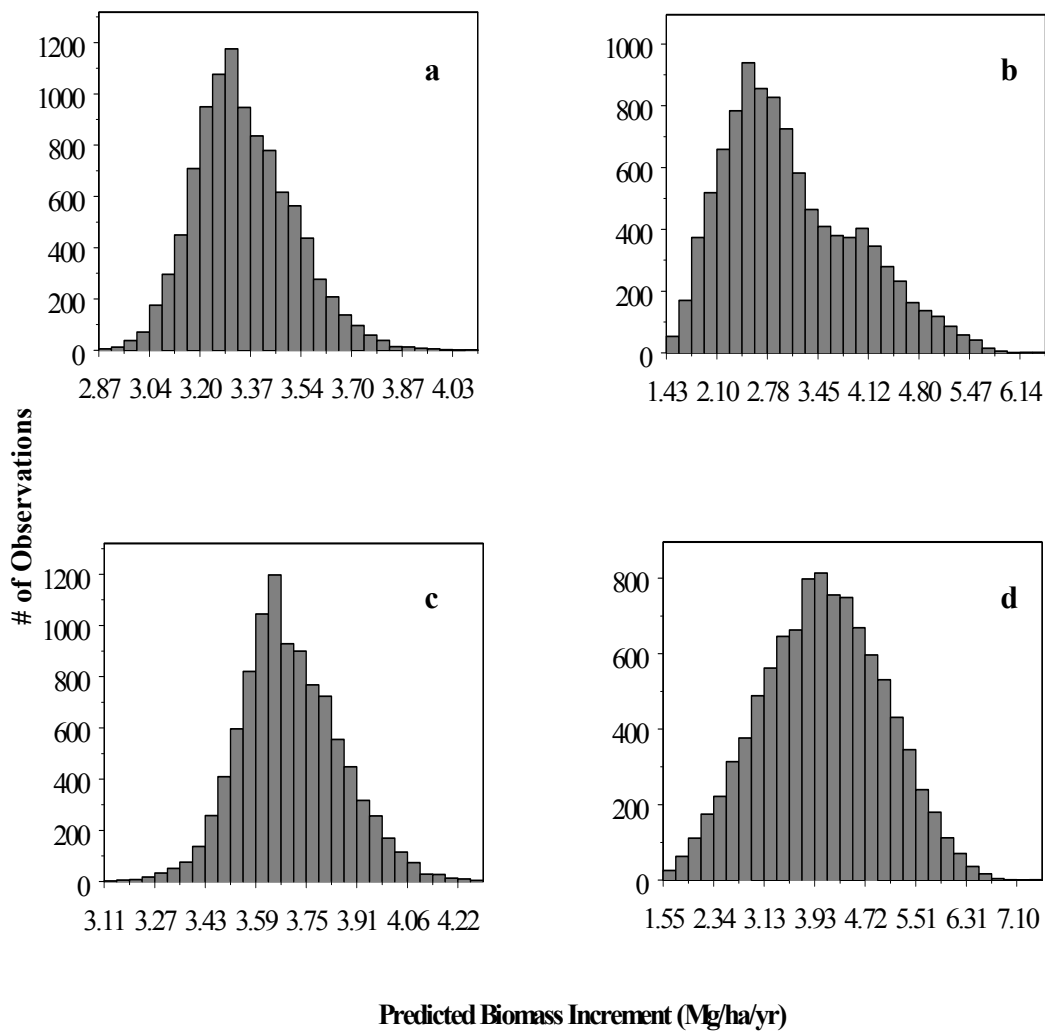


Figure 2.8 Distributions of Monte Carlo Simulation Estimates for varying sample sizes and years for the old-growth site using a simple random model with quartiles (SRQ). Panels **a** and **b** represent year 1975, sample sizes 64 and 8, respectively. Panels **c** and **d** represent year 1995, sample sizes of 64 and 8, respectively.

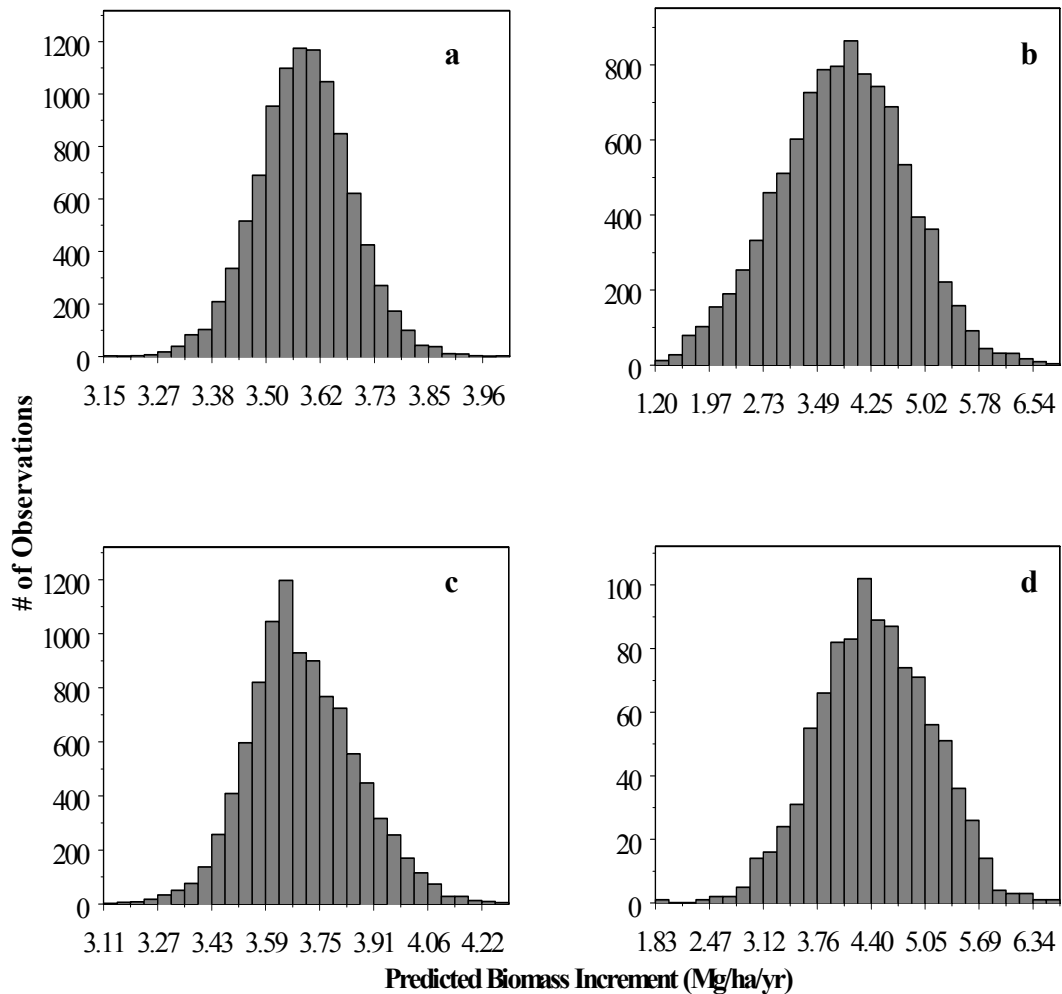


Figure 2.9 Distributions of Monte Carlo Simulation Estimates for varying sample sizes and years for the mature site using a simple random model with quartiles (SRQ). Panels **a** and **b** represent year 1975, sample sizes 144 and 32, respectively. Panels **c** and **d** represent year 1995, sample sizes of 144 and 32, respectively.

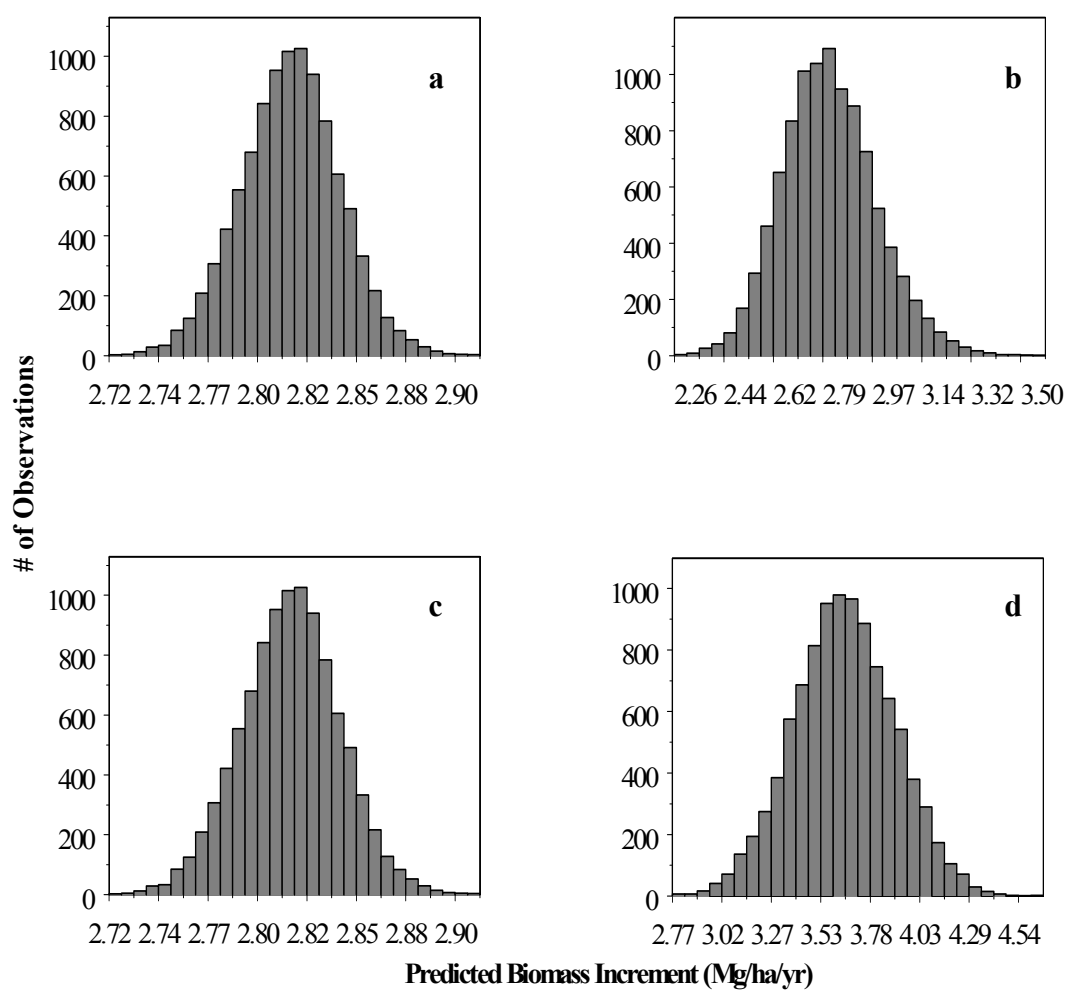


Figure 2.10 Distributions of Monte Carlo Simulation Estimates for varying sample sizes and years for the second-growth site using a simple random model with quartiles (SRQ). Panels **a** and **b** represent year 1991, sample sizes 280 and 32, respectively. Panels **c** and **d** represent year 1999, sample sizes of 280 and 32, respectively.

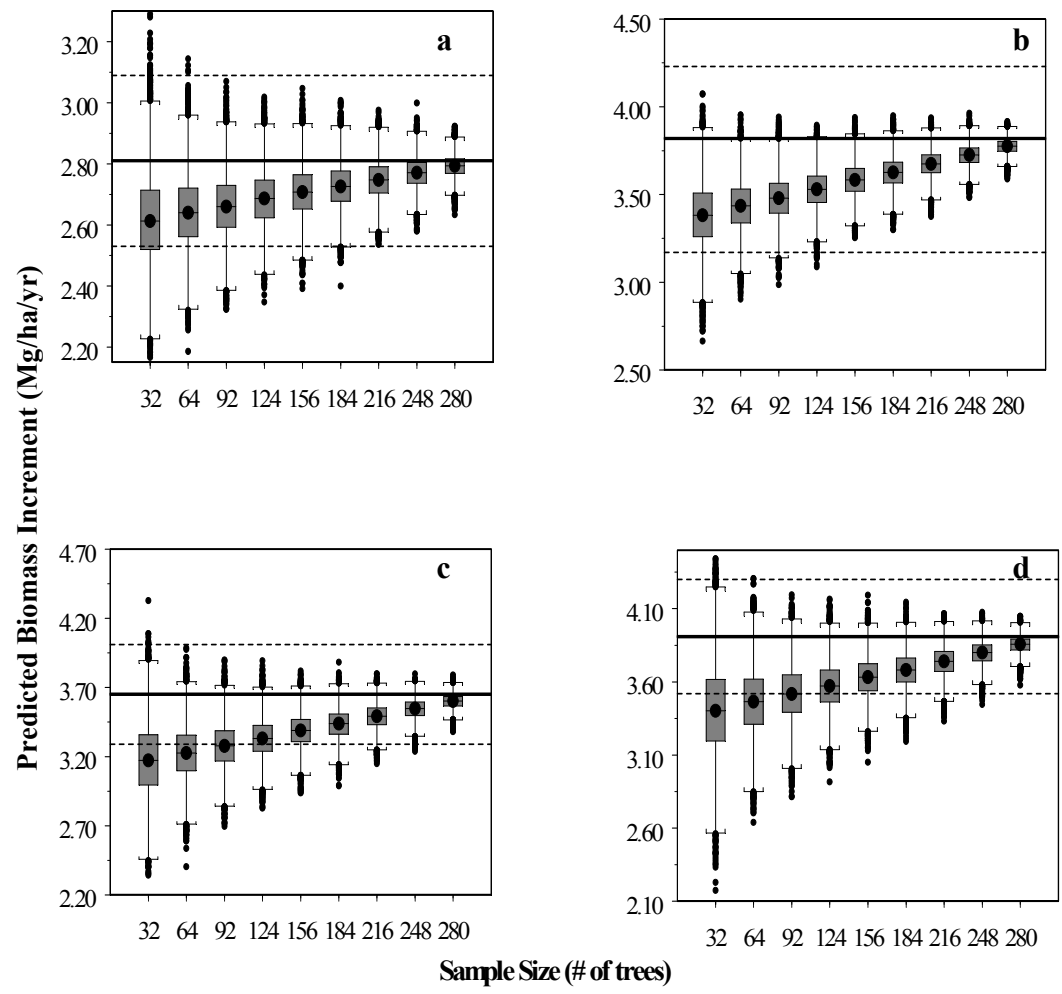


Figure 2.11 Box plots showing distributions of biomass increment estimates at varying sample levels for four different years for the second-growth site (a=1991, b=1995, and c=1999, d=2001), using a simple random model (SR). Bold line indicates true biomass increment, dashed lines are +/- 10% of true biomass increment.

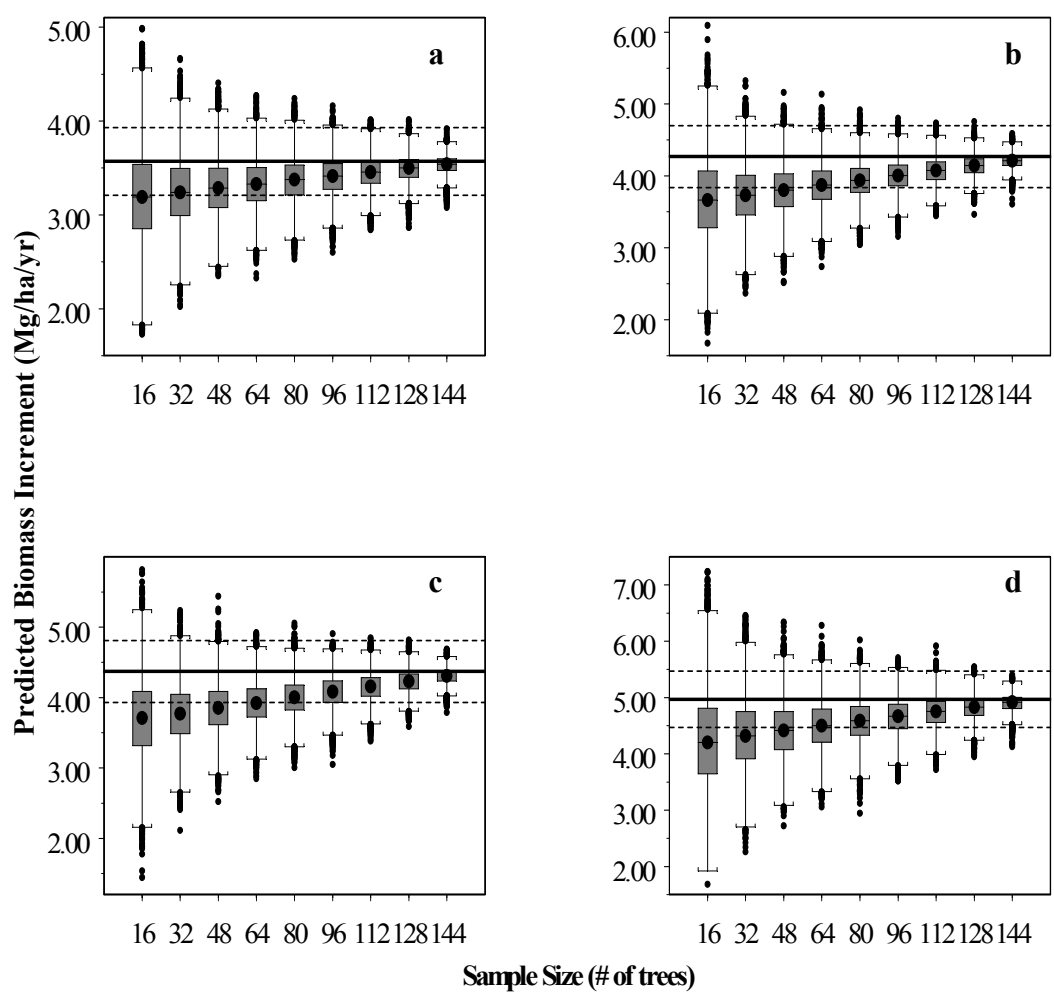


Figure 2.12 Box plots showing distributions of biomass increment estimates at varying sample levels for four different years for the mature site (a=1975, b=1985, and c=1995, d=1999), using a simple random model (SR). Bold line indicates true biomass increment, dashed lines are +/- 10% of true biomass increment.

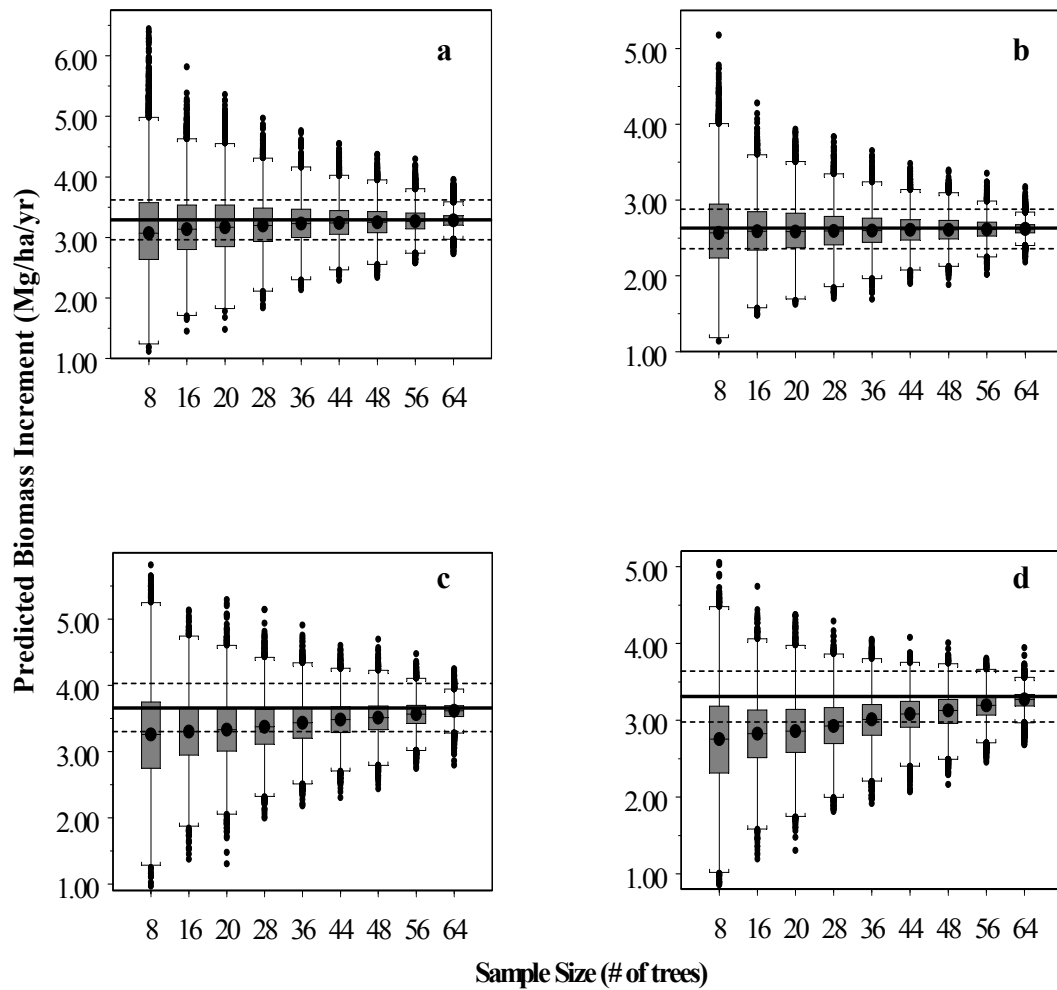


Figure 2.13 Box plots showing distributions of biomass increment estimates at varying sample levels for four different years for the old-growth site (**a**=1975, **b**=1985, and **c**=1995, **d**=1999), using a simple random model (SR). Bold line indicates true biomass increment, dashed lines are $\pm 10\%$ of true biomass increment.

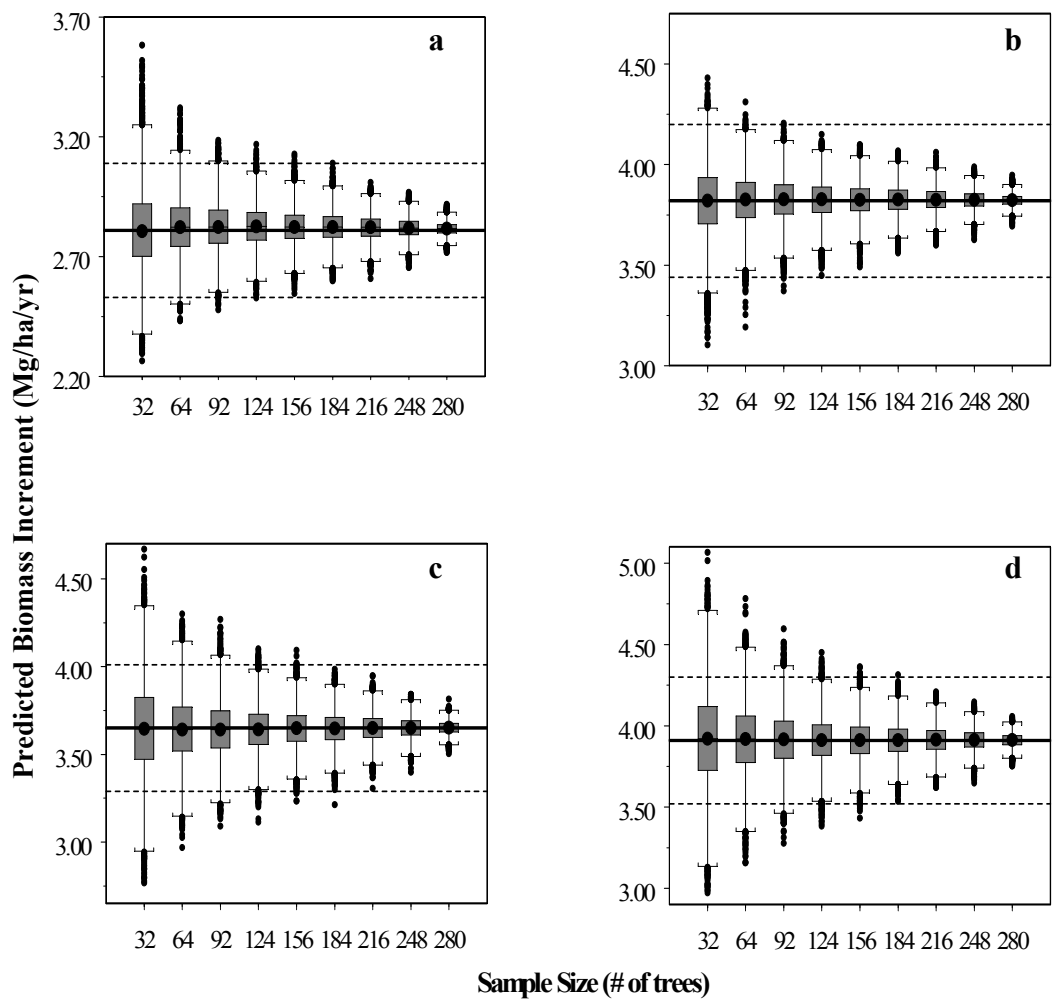


Figure 2.14 Box plots showing distributions of biomass increment estimates at varying sample levels for four different years for the second-growth site (a=1991, b=1995, and c=1999, d=2001), using a simple random model with quartiles (SRQ). Bold line indicates true biomass increment, dashed lines are +/- 10% of true biomass increment.

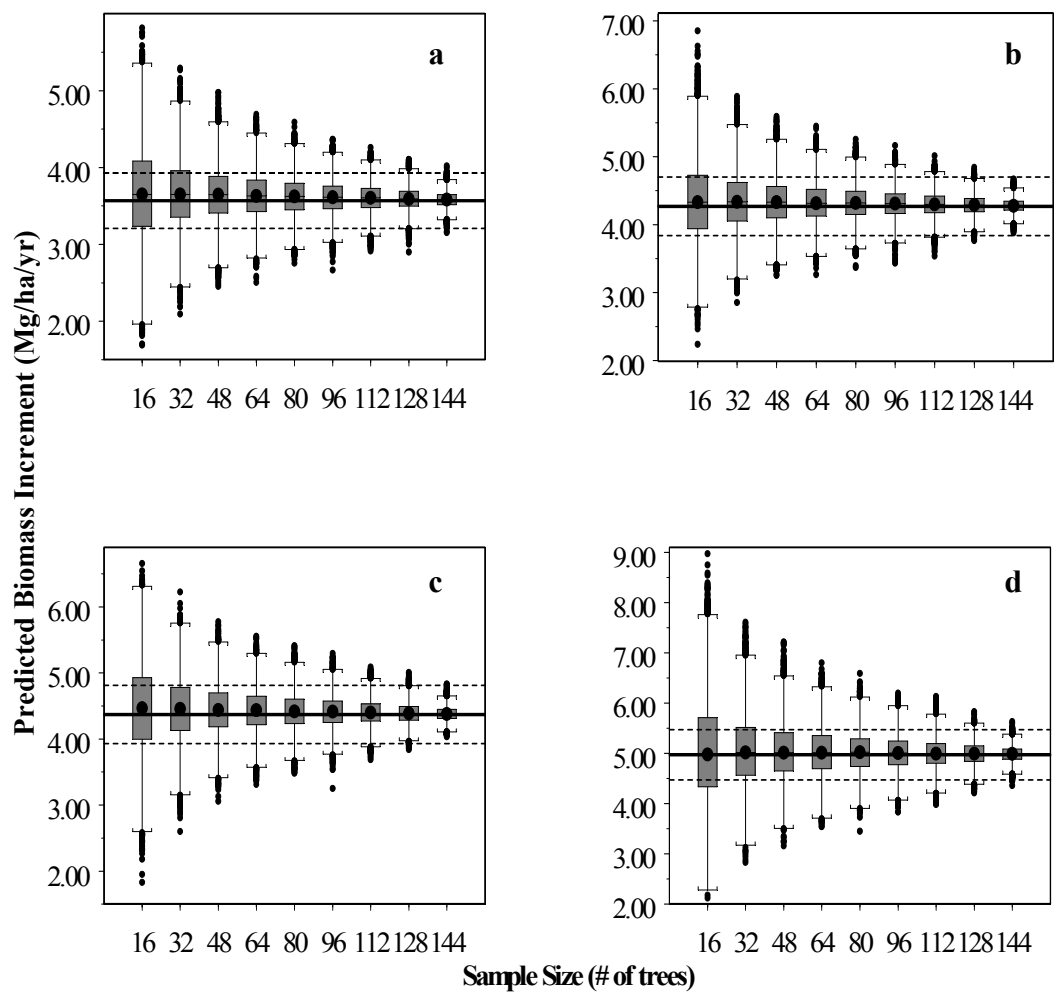


Figure 2.15 Box plots showing distributions of biomass increment estimates at varying sample levels for four different years for the mature site (**a**=1975, **b**=1985, and **c**=1995, **d**=1999), using a simple random model with quartiles (SRQ). Bold line indicates true biomass increment, dashed lines are +/- 10% of true biomass increment.

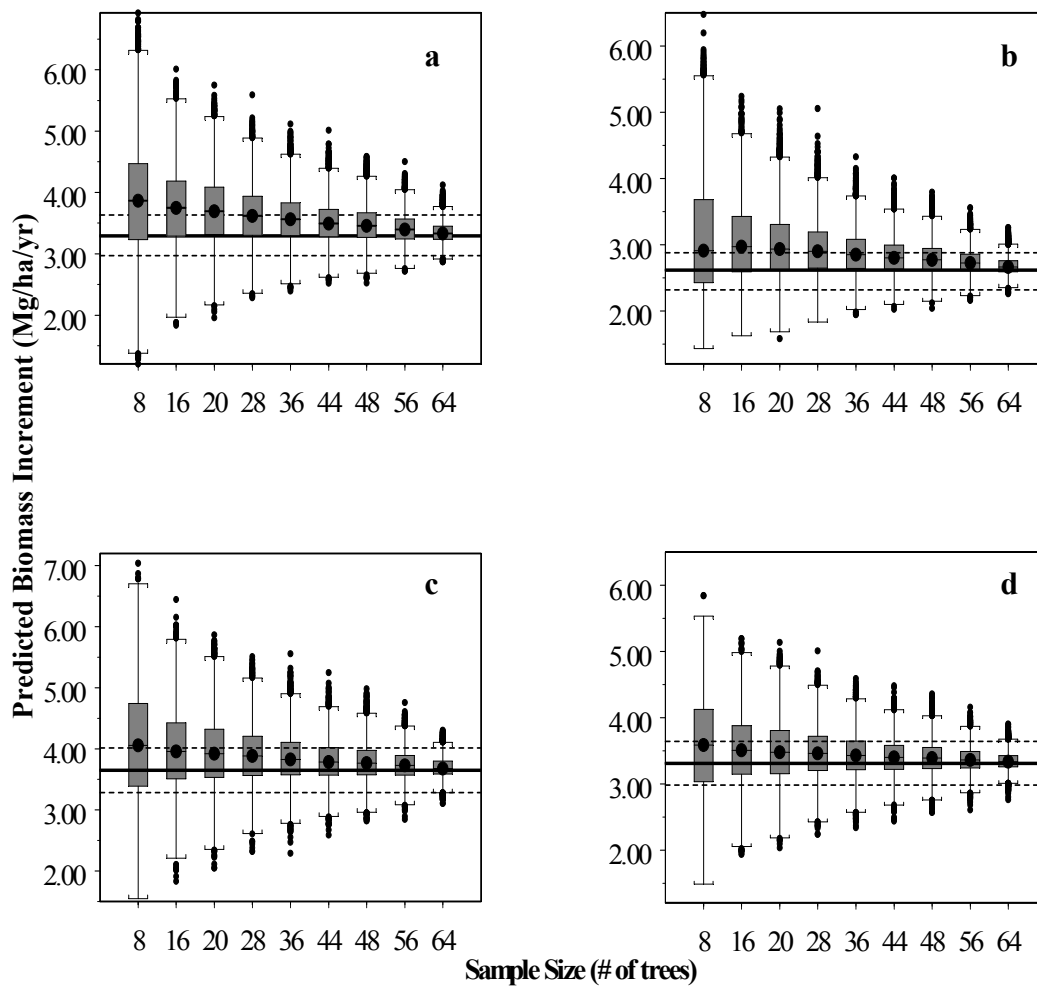


Figure 2.16 Box plots showing distributions of biomass increment estimates at varying sample levels for four different years for the old-growth site (**a**=1975, **b**=1985, and **c**=1995, **d**=1999), using a simple random model with quartiles (SRQ). Bold line indicates true biomass increment, dashed lines are +/- 10% of true biomass increment.

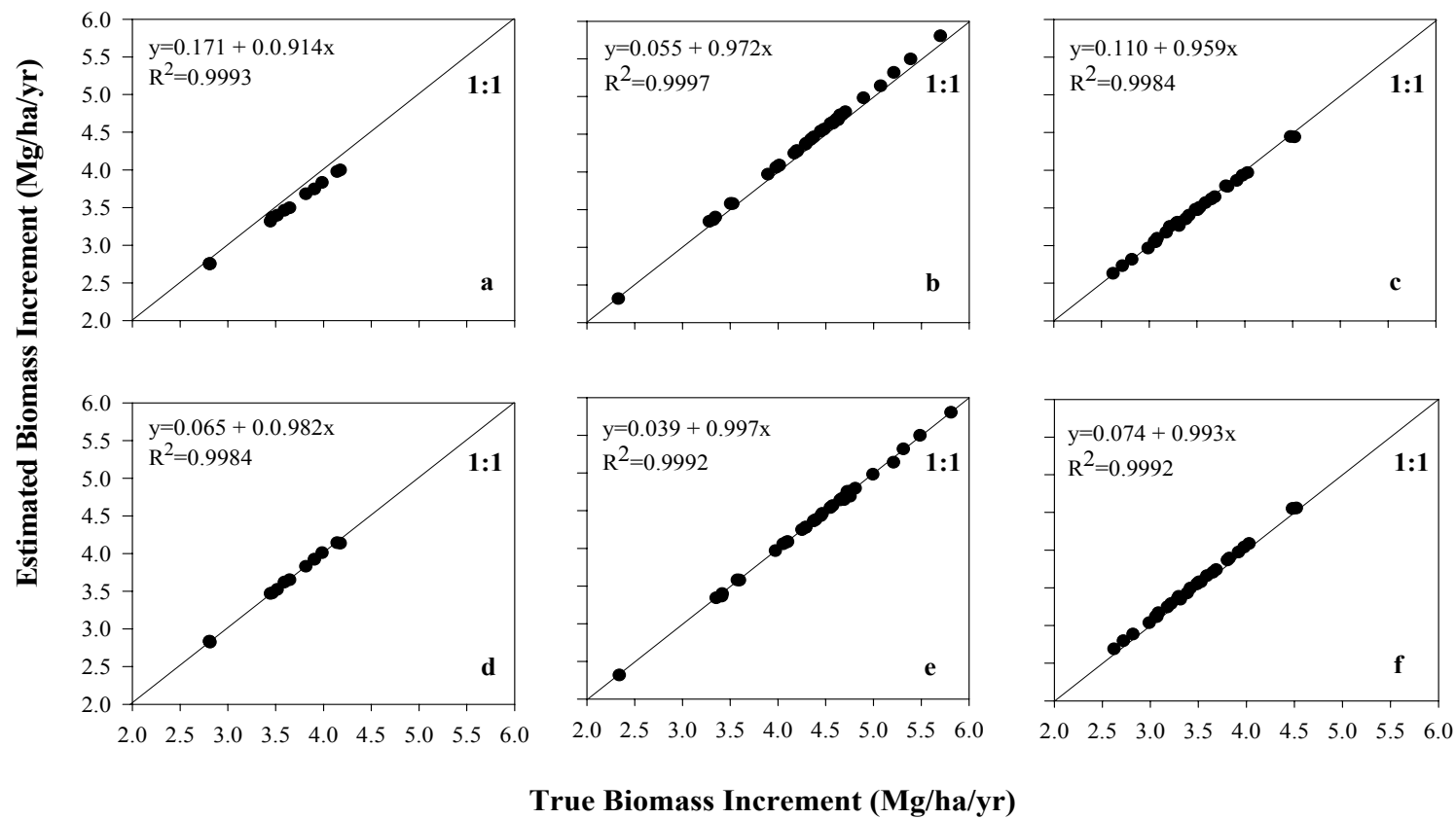


Figure 2.17 Linear regressions comparing estimated annual biomass increment and true biomass increment for both models, SR (a-c) and SRQ (d-f). Top and bottom panels are paired by age (Second-growth=a and d, mature=b and e, and old-growth=c and f). Diagonal lines represent a 1:1 relationship.

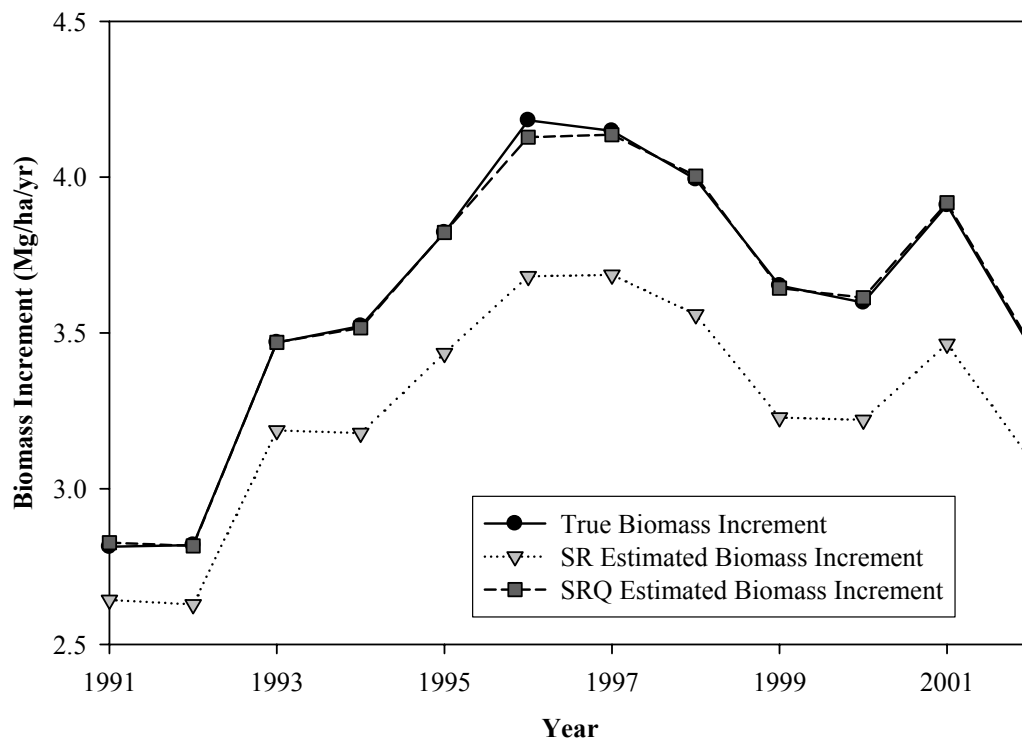


Figure 2.18 Plot of time series comparing true biomass increment and estimates from both models (SR and SRQ) for the second-growth site.

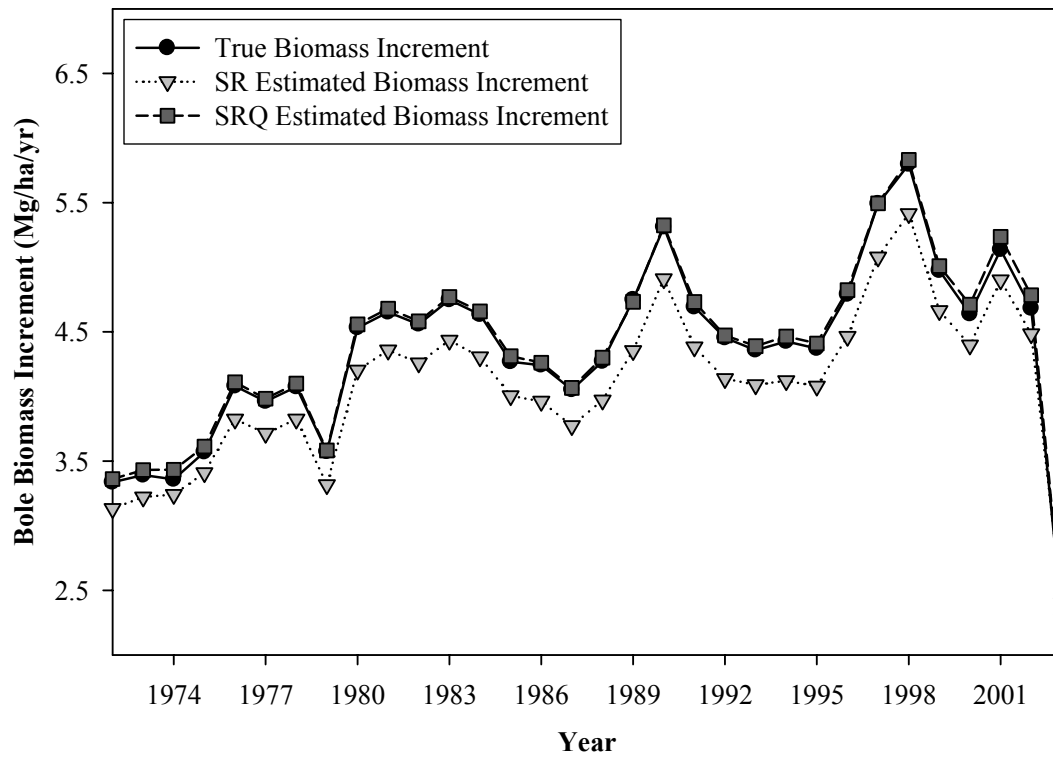


Figure 2.19 Plot of time series comparing true biomass increment and estimates from both models (SR and SRQ) for the mature site.

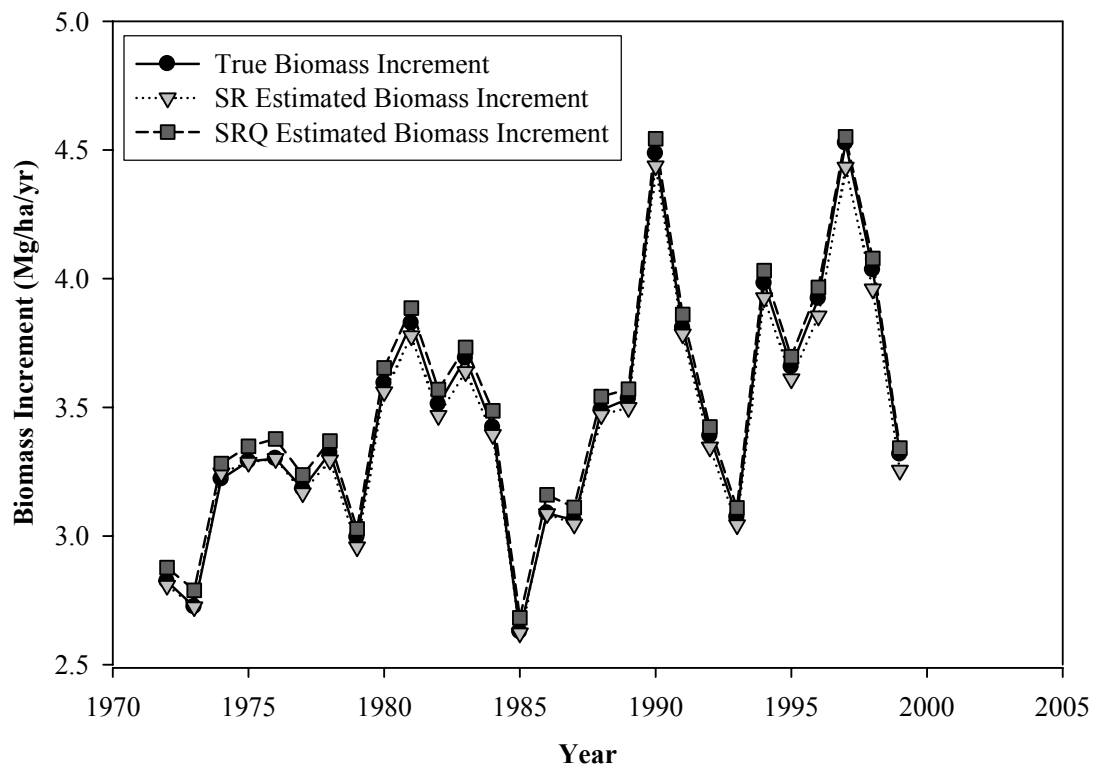


Figure 2.20 Plot of time series comparing true biomass increment and estimates from both models (SR and SRQ) for the old-growth site.

**Chapter 3: Inter-annual variation and spatial coherence of Net
Primary Productivity within and between a second-growth and an
old-growth small watershed**

Travis J. Woolley, Mark E. Harmon, and Kari E. O'Connell

Prepared for submission to the *Journal of Vegetation Science*

Abstract

Inter-annual variability of forest Net Primary Productivity (NPP) is a result of many factors (e.g., climate, local environment, physiology, and stand dynamics). Understanding this variability is critical in determining the response of ecosystem processes to global change. Productivity of tree boles (NPP_B) was determined for two adjacent small watersheds (second-growth and old-growth) in the western Cascades of Oregon. Spatial coherence (i.e., degree of synchrony between sites) of NPP_B within and between watersheds was assessed using Principle Components Analysis (PCA), Multi-response Permutation Procedures, and Cluster Analysis. NPP_B was found to be less coherent between watersheds than within watersheds indicating decreased coherence with increased spatial scale. An unexpected conclusion was that the degree of spatial coherence was not consistent and changed through time. Therefore, the coherence of sites over time is not a simple relationship, but instead exhibits complex behaviors that have implications for scaling estimates of productivity. Within a watershed, potential annual direct incident radiation and heat load were more associated with the variation of NPP_B than annual variation of climate. Climatic factors important to NPP_B varied between the two watersheds, with late growing season temperature and precipitation most correlated with NPP_B of the old-growth watershed in contrast to early season temperature, annual precipitation, prior year's monthly precipitation, and Palmer Drought Severity Index were most correlated with NPP_B in the second-growth watershed. Our results suggest that inter-annual variability and spatial coherence of forest productivity was a result of both internal (e.g., environment and stand dynamics) and external (climate) factors. Therefore, climatic

and physiological relationships used in models of NPP overestimate the coherence of NPP_B across space.

Introduction

Understanding the inter-annual variability of Net Primary Productivity (NPP) at multiple scales (i.e., watershed, landscape, region, biome) is critical in determining the response of ecosystem processes to global change (Knapp and Smith 2001; Huxman et al. 2004). A first step in this process at any scale is to determine spatial coherence of productivity through time. Spatial coherence is defined as the degree to which pairs of sites across space are synchronous (i.e., correlated) through time (definition altered from Magnuson et al. 1990; Baron and Caine 2000; Soranno et al. 1999; and Baines et al. 2000). Understanding heterogeneity of environmental influences and land use associated with spatial variation in NPP_B is important in modeling ecosystem productivity (Turner et al. 2003). Many ecosystem process models are driven by climate and physiological responses to climate, thus NPP will only be as coherent as the underlying climatic drivers used in these models. However, the degree of spatial coherence between climatic variables may differ from the spatial coherence between biological processes.

The objectives of this analysis were to examine the spatial coherence of annual tree bole productivity (NPP_B) within and between two adjacent small watersheds of contrasting ages, and understand how climate and environmental factors may be influencing spatial coherence through time. Specifically, the questions for this analysis were: 1) Which areas within each individual watershed were more correlated (i.e., spatially coherent) with one another through time in terms of NPP_B , and how do these relate to measured environmental variables of these areas?; 2) Which climatic variables were correlated with inter-annual variation of NPP_B ?; 3) Were these two

adjacent watersheds of contrasting age spatially coherent, or were they responding differently to similar environmental and climatic variables?; and 4) How do groups derived from clustering compare to topographically defined *a priori* groups?

Methods

Study Area

Data was collected in long-term permanent study plots in two small watersheds (WS01 and WS02) within the H.J. Andrews Experimental Forest, Blue River, OR (Appendix 1.1). The experimental forest covers a 6400 hectare (ha) drainage located in the western Oregon Cascades. Elevation ranges from 410 to 1630 meters (m). The maritime climate consists of cool wet winters and dry hot summers. Average annual precipitation ranges from 230 centimeters (cm) at lower elevations to 355 cm at higher elevations. Annual average daily temperatures range from 0.6° C in January, to 17.8° C in July (Bierlmaier and McKee 1989). The lower elevations are dominated by Douglas-fir (*Pseudotsuga menzeisii*), western hemlock (*Tsuga heterophylla*), and western red-cedar (*Thuja plicata*). As elevation increases, Douglas-fir and western hemlock dominance decrease, and they are replaced by noble fir (*Abies procera*), mountain hemlock (*Tsuga mertensiana*), and Pacific silver-fir (*Abies amabilis*).

Average annual precipitation through the study period (1983-2003) was 2205 mm falling mostly within fall, winter, and spring months. The topography is typical of small watersheds in the study area with steep and highly dissected slopes. Elevation in the second-growth watershed ranges from 475m to 964m and from 480m to 1,070m in the old-growth watershed.

The two adjacent sampled watersheds represent contrasting ages (second-growth and old-growth), but have similar tree species composition, topography, and experience similar climatic regimes. Both watersheds are within the *Tsuga heterophylla* forest zone (Franklin and Dyrness 1973). Table 3.1 summarizes the characteristics of each watershed. The second-growth watershed was clear-cut in the mid 1960's as part of a paired watershed study examining the effects of logging and road-building (Dyrness 1973), and is dominated by Douglas-fir. The old-growth watershed consists of primary forest dominated by Douglas-fir and western hemlock. Vegetation transects, oriented north-south, were placed at regular intervals across both watersheds prior to the harvest of the second-growth watershed, with permanent plots (0.01 and 0.1 ha, second-growth and old-growth, respectively) installed at fixed distances along each transect. These plots are also part of a long-term permanent study plot network designed to monitor changes in forest composition, structure, and function (Acker et al. 1998).

Data Collection

The two watersheds in this analysis were sampled during the summer of 2004. Trees occurring in permanent plots within each watershed (132 and 67 plots in second-growth and old-growth watersheds, respectively) were randomly selected for sampling from lists of all tagged trees ≥ 5 cm diameter at breast height (DBH).

Within the second-growth watershed, five topographic zones were delineated, and all zones were spatially contiguous. The five zones are; 1) North facing, 2) South facing, 3) Riparian, 4) North ridge, and 5) South ridge. Trees from within each zone were randomly sampled independently of the other zones. Topography within the old-

growth watershed is similar, but less spatially variable. Therefore, trees were randomly selected from plots throughout the watershed without the delineation of topographic zones.

Sampling consisted of coring a tree at breast height, and recording tag number, species, core number, DBH (cm), bark thickness (cm), core length (cm), and sapwood radius (cm) to the nearest 0.1 cm. In the old-growth watershed, trees ≥ 10 cm DBH were cored twice, at approximate right angles (preferentially side-slope and upslope). In the second-growth site, only 1 core per tree was collected due to small tree sizes. Increment cores were stored in paper straws and taken to the lab for preparation and measurement.

Increment cores were mounted on routed blocks with wood glue and then sanded with a grit of 240 using a belt sander. All cores were then scanned and measured for annual radial increment growth (cm) measured using WinDendroTM image analysis software. For the old-growth watershed, radial increment growth was calculated as an average of the two cores taken for each tree ≥ 10 cm DBH.

Tree Increment Dating Accuracy

Two methods of cross-dating ensured accurate dates of tree ring growth for the old-growth watershed. As increments were measured for individual trees, marker years (Yamaguchi et al. 1991) were recorded. All radial tree growth increment series were then loaded in COFECHA (Holmes 1983; Grissino-Mayer 2001) and output statistics were compared to marker year records. Trees with apparent discrepancies were checked visually and either remeasured or their measurements were altered, discarded, or remained unchanged if visual inspection did not detect a measurement

error. This technique was not used for the second-growth watershed because the length of each radial growth increment series was less than 50 years (Swetnam et al. 1985) and second-growth trees tend to be easily dated due to large growth rates, complacency, and lack of missing rings (Schweingruber 1988).

Calculating Annual NPP_B and Plot-level Environmental Variables

Increment data from the second-growth watershed was used within a zone to predict radial increment growth for non-sampled trees using a simple model based on average annual radial growth increment and tree size (see Chapter 1 for model details). The same model was used for increment prediction of non-sampled trees in the old-growth watershed, but on a whole watershed basis, rather than by zones. Annual stem diameter was calculated using last remeasurement DBH, combined with measured annual radial growth increment from tree cores (similar to Graumlich and Brubaker 2004). Annual bole biomass production (Mg) for individual trees was calculated using species-specific volume equations, wood/bark volume ratios, and bark and wood density values. Volume equations and density values for the second-growth watershed are from Acker (2002). Site- and species-specific bark and wood volume equations were substituted for the old-growth watershed and a similar method was used to calculate bole biomass (for coefficients for both watersheds see Appendices 1.10 – 1.14). Individual tree biomass production was summed for each year to obtain plot-level estimates of annual bole biomass production. Using long-term records of tree remeasurement and mortality, trees that died within the time frame of the study period were accounted for prior to death using the same increment growth model. Three-to six-year intervals of plot remeasurement created uncertainty in dates of annual

mortality for individual trees. This uncertainty was captured by assigning each tree an equal probability of dying within the years between remeasurements. The year of death was then randomly chosen for each individual and increments were predicted from the beginning of the study period to that date.

The modeling of radial increment growth, date of mortality, calculations of individual tree biomass production, and aggregation to plot-level estimates was repeated 1,000 times, and the average of the 1,000 estimates was used as an estimate of annual NPP_B for each plot. Plot area was slope corrected and then used to calculate annual NPP_B per hectare for each individual plot. These calculations resulted in annual NPP_B data of 23 years for 132 and 67 plots for the second-growth and old-growth watersheds, respectively.

The environmental data for this analysis consisted of five environmental variables: elevation (m), slope (degrees), heat load (index), and potential annual direct incident radiation ($\ln MJ/cm^2/yr$) for plots in each watershed. Heat load and potential annual direct incident radiation (PADIR) were calculated using the methodology of McCune and Keon (2002). Climatic data consisted of 63 variables: annual precipitation (mm), annual average temperature (C°), monthly precipitation (mm), monthly precipitation lagged one calendar year, monthly minimum, mean, and maximum temperature, and Palmer Drought Severity index (PDSI; Palmer 1965) for 23 years. All temperature and precipitation data were obtained from the Climate and Hydrology Database (<http://www.fsl.orst.edu/climdb/>). Data were used from a single meteorological station near both watersheds at the H.J. Andrews Experimental Forest. PDSI values were obtained from the PDSI grid developed by Cook and colleagues

(1999), downloaded from the National Climatic Data Center and National Oceanic and Atmospheric Administration website (<http://www.ncdc.noaa.gov/paleo/pdsidata.html>).

Data Adjustments

As second-growth sites develop they exhibit a trend of increasing biomass production over time to a theoretical asymptote (Acker et al. 2002). The questions of interest for this analysis pertain to the variation between years and not the long-term trend in NPP_B . Therefore, a transformation to remove this trend was necessary. A smoothing function was applied to the NPP_B data for both watersheds using a local mean with a rectangular kernel, and a smoothing parameter of five years. This calculation resulted in data sets of unstandardized residuals of NPP_B . A decrease in years from the original data set resulted from the removal of two years from each end of the data set that was not averaged with five years of data (i.e., not enough preceding or succeeding years to obtain a five year average). Three years (instead of 2) were removed from the beginning of the data set because sampling that may not have captured tree growth for the first three years in some plots in the second-growth watershed. The climatic matrix was adjusted accordingly. Relativization was not performed because the residuals from smoothing were scaled similarly for all plots, and variables were automatically standardized in subsequent analysis. Figure 3.1 suggests that this procedure effectively removed the long term temporal pattern of NPP_B , although some adjacent years were similar.

Outlier analysis using the Euclidean distance measure (a geometric measure of distance between points in ordination space) was performed on the residuals (Table 3.2). Two extreme outliers (plots 416R, 507R) were found in the data for the second-

growth watershed. Further inspection of these plots revealed higher inter-annual variability compared to other riparian plots and these plots were responding quite differently from one another in certain years (Figure 3.2). They also had little effect on the group (riparian plots) average (Figure 3.3). The plots were of biological interest due to their proximity to the stream, so they were included in all subsequent analyses. Only one year (1999) was more than two standard deviations from the mean NPP_B for all years and no rationale for exclusion could be made. However, two years (1995 and 1997) had large kurtosis values, which influenced the mean kurtosis (Table 3.3).

One extreme outlier was detected in the old-growth watershed (plot 806), and one year (1997) was more than two standard deviations from the mean NPP_B of all years. Because no evidence existed to warrant exclusion of these outliers they were included in the analysis.

Data Analysis

Data were analyzed with PC-ORD version 4 (McCune and Mefford 1999). The Euclidean distance measure was used to accommodate negative values (residuals). Principal Components Analysis (PCA) was performed using all three data sets. PCA is an ideal technique for data with approximately linear relationships among variables (McCune and Grace 2002). The data met the assumptions necessary for use of PCA. All eigenvalues for axes reported have exceeded the broken-stick model criterion, a heuristic criterion that distributes variance randomly among the components (McCune and Grace 2002). If the axis eigenvalue is greater than the broken-stick eigenvalue then that axis contains more information than expected by chance. However, this is a rule of thumb rather than a criterion for interpretation of an axis.

Group differences within a watershed and between watersheds were addressed using hierarchical cluster analysis and Multi-response Permutation Procedures (MRPP). Cluster analysis was performed using Ward's method with Euclidean distance. The A-statistic from MRPP, the within group agreement, was used to assess the strength of *a priori* groupings of plots and of groups derived from cluster analysis. Groupings were compared at the 5 group level for consistency.

Results

Climate

A PCA ordination of the years of NPP_B over all plots in the second-growth watershed shows a distinct pattern of low productivity to high productivity years (Figure 3.4). The first two axes in this ordination account for 88% of the total variation (Table 3.4). An overlay of climatic variables (Figure 3.5) indicates that previous year's May precipitation was most strongly correlated with axis 1 ($r=0.606$). June maximum temperature and previous year's November precipitation also had strong correlations ($r=0.474$ and 0.523 , respectively) with axis 1 (Table 3.5). PDSI showed the strongest correlation with axis 2 ($r=-0.558$), but annual precipitation was also correlated with this axis as well ($r=-0.482$). Axis 3 was most strongly correlated with April minimum temperature, May maximum and mean temperature, April mean temperature, and February precipitation. For correlations of annual NPP_B and climatic variables with principal components of growth see Table 3.5.

Years of NPP_B across all old-growth plots (Figure 3.6) display a similar relationship as compared to the second-growth watershed. However, the years in which NPP_B was low or high varied between watersheds. The first axis of the

ordination accounted for 91.9% of the variation between plots and subsequent axes contribute minimally to explanation of variance (Table 3.4). An overlay of climatic variables (Figure 3.7) indicates that the pattern of low to high NPP_B years in the old-growth watershed was most correlated with August mean temperature ($r = -0.618$) and October precipitation ($r = -0.577$), while July, August, and September minimum temperature also had high ($r > 0.50$) correlations with axis 1.

Environment and Topography

Analysis using MRPP indicated the five *a priori* topographic groups differed significantly in patterns of NPP_B ($A = 0.22$, $p < 0.0001$). The low p-value reflects a large sample size and not necessarily the effect size of group differences. The A-statistic represents the chance corrected within group agreement compared to a randomization test, and better represents the differences between groups. Results from pair wise comparisons between all combinations of groups are shown in Table 3.6. South and north facing groups were the most different from one another ($A = 0.195$). The most similar groups were south facing ridge and south facing plots ($A = 0.017$). Riparian plots had the greatest within group variability, similar to both north and south facing groups, and they were considerably different from north facing ridge plots ($A = 0.142$). South facing ridge plots were the least variable of all *a priori* groups.

Groups formed by cluster analysis for the second-growth watershed and *a priori* groups were similar, with group membership differing most for ridge and riparian plots. Groups were cut off at the five group level for comparison to *a priori* groups using MRPP. At the five group level approximately 65 % information remained, and the clustering resulted in only 2% chaining. According to MRPP cluster

groups were stronger ($A=0.36$) than *a priori* groups. Average Euclidean distance within each cluster group ranged from 0.528 to 1.115, compared to 0.522 to 1.391 range of average distance within each *a priori* group.

Groups for the old-growth watershed were also formed using cluster analysis at the five group level (4 % chaining, 60 % information remaining). Within group distances of cluster groups for the old-growth watershed were much smaller than cluster or *a priori* groups for the second-growth watershed. Average distance within each group ranged from 0.177 to 0.307. MRPP indicated differences among all cluster groups ($A=0.32$) were similar to results for cluster groups from the second-growth watershed ($A=0.36$). Annual NPP_B also differed between the second-growth and old-growth watersheds ($A=0.177$, $p<0.0001$). Average Euclidean distance between plots within each watershed varied considerably (0.953 and 0.361 second-growth and old-growth, respectively), indicative of differences in spatial variation of NPP_B within adjacent watersheds.

The first two axes in an ordination of plots in the second-growth watershed in annual NPP_B space explained 55% of the variance and little explanation of variance was gained with additional axes (Table 3.7). Overlays of environmental variables indicate that plots separated according to topographic characteristics used in the formation of *a priori* groups (Figure 3.8). North facing and south facing plots were the two most distinct groups with the other 3 groups (riparian and south/north ridge groups) falling between all other plots on the ordination. However, the two apparent riparian outliers fell on opposite ends of the ordination forcing all other points in the ordination closer together. Axis 1 represents a gradient of heat load and PADIR

($r=0.519$ and 0.442 , respectively). None of the measured environmental variables had considerable correlations with Axis 2 (Table 3.8).

The first two axes in an ordination of plots in the old-growth watershed in annual NPP_B space explained 58% of the variance and additional axes contributed very little to variance explained (Table 3.7). Overlays of environmental variables reveal similar but less distinct patterns than the second-growth watershed (Figure 3.9) with plots arranged according to topography. Groups formed by cluster analysis separated according to heat load and potential solar radiation along axis 1. Correlations for environmental variables with axes 1 and 2 (Table 3.8) were much lower for potential solar radiation and heat load ($r=0.245$ and 0.282 , respectively) than the correlations for the second-growth watershed.

An ordination of plots from both second-growth and old-growth watersheds corresponding to years of NPP_B (Figure 3.10) explained 66% of the variance in the first three axes. Most of this variance (42%) can be explained by the first axis (Table 3.9), which again was most strongly correlated with potential solar radiation and heat load (Table 3.10). This ordination shows that NPP_B in the old-growth watershed was much less variable compared to the second-growth watershed. Tighter grouping of plots for the old-growth watershed along the axes indicates less response of NPP_B to potential solar radiation and heat load across the entire watershed.

Figure 3.11 displays second-growth watershed plots ordinated according to their environment (topographic variables). The first axis accounts for 59% of the variation and the second axis accounts for an additional 27% of the overall variation between plots (Table 3.11). Plots fell into north and south facing groups, with axis 1

representing potential solar radiation ($r=-0.905$) and heat load ($r=-0.888$), and axis 2 corresponding to slope ($r=-0.448$) and elevation ($r=-0.759$). Table 3.12 summarizes environmental correlations with the first two axes. A differing response of NPP_B exists for at least 4 of the 18 years for the north and south facing groups. In the years 1984 and 2000, the south facing plots had higher NPP_B in than the north facing plots. In the years 1987 and 2001, the north facing plots responding more positively than the south facing plots (see Table 3.17 for correlations of all years). This pattern of high coherence in some years and low coherence in others is summarized in Table 3.14.

Unlike the second-growth watershed, when old-growth plots were ordinated according to their topographic variables (Figure 3.12) there were no distinct grouping(s) of plots (i.e., north and south facing plots). Although axes were correlated to the same variables as the second-growth watershed, the variance was distributed along three axes rather than two. PADIR and heat load were highly correlated with axis 1 ($r=-0.961$ and -0.960 , respectively), slope was most strongly correlated with axis 2 ($r=0.737$), while elevation and slope were strongly correlated with axis 3 ($r=0.697$ and -0.676 , respectively). The first three axes in this ordination accounted for 80.0% of the variation (Table 3.11). Overlaying years of NPP_B indicates that there were no years in which plots in the watershed had a notable difference in response of annual NPP_B along gradients of heat load PADIR. The correlations of years with axis 1 (Table 3.13) were much lower than the correlations of years for the second-growth watershed.

Examining an ordination of plots from both watersheds according to their environmental measures (Figure 3.13) reveals that most of the old-growth plots are

environmentally similar to south facing plots in the second-growth watershed. There were a number of years in which the north facing plots in the second-growth watershed responded differently from south facing second-growth and all old-growth plots with respect to annual NPP_B . Table 3.16 gives correlations of axes with all years of NPP_B . This indicates that plots between watersheds were much less coherent than plots within either watershed, but that the lack of coherence was more related to dissimilarity in environment than the age of the watershed per se. In three of the years that lacked coherence (1987, 1993, and 1998), average NPP_B of the two watersheds was actually out of synch and responding opposite one another (Figure 3.14). The lack of coherence in the other years was a result of differing amplitudes of response between watersheds (Figure 3.14).

Discussion

Annual NPP_B within a small second-growth watershed, within an adjacent small old-growth watershed, and between these two watersheds was examined in relation to environment and climate. Inter-annual climate variability appears to have differing relationships with inter-annual variability of NPP_B in the second-growth and old-growth watersheds. Late growing season temperature and precipitation were the predominant climatic factors correlated to variation of annual NPP_B of the old-growth forest, indicating that annual NPP_B may be driven by late season radial tree growth and thus late season climate variation. NPP_B in the second-growth watershed was more correlated with early summer climatic variables, temperature in particular, and PDSI. A study examining tree water use in these two watersheds (Moore et al. 2004) reported higher water use by younger trees compared to old-growth trees, with age and

species composition being important factors. Therefore, the second-growth watershed may have depleted water sources earlier in the growing season, and thus NPP_B in this watershed was more influenced by early season climatic variation. Productivity in the old-growth watershed may be more dependent on climate patterns later in the growing season when water becomes more limiting.

Annual precipitation was also potentially an important factor for year to year variation of NPP_B in the second-growth watershed, but not for the old-growth watershed. Graumlich and others (1989) reported that long-term records of NPP_B in high elevation forests of western Washington were significantly correlated with summer temperature and less so with annual precipitation.

An interesting relationship was that of previous year's May precipitation and NPP_B for the second-growth watershed, where increased precipitation in the previous May resulted in lower NPP_B in the following year. This may be an artifact of using a large number of climatic variables, or it may be that previous May precipitation was related to another variable that may better explain inter-annual variation in NPP_B . The amount of precipitation in the previous November also had an affect on annual NPP_B , likely by changing soil water storage and availability the following growing season.

There were distinct differences in annual NPP_B between different topographic zones in the second-growth watershed; the most distinct difference was between the north facing and south facing plots. This difference could be attributed to the large variation in both heat load and PADIR between these two groups. Closer inspection of individual plots reveals consistent negative correlations between south facing, and north and south facing ridge plots, and PDSI. North facing plots exhibit positive

relationships with PDSI, where as there was no consistent pattern between riparian plots and PDSI. Hotter, drier areas appear to be much more affected by drought conditions than cooler, moister plots. A caveat to this would be that PDSI did not become extremely negative during the study period, and one would expect all plots to be less productive when PDSI becomes highly negative.

The old-growth watershed exhibited similar relationships of NPP_B with heat load and PADIR, but NPP_B was much less variable between old-growth plots than for the second-growth watershed. A non-subjective method of grouping plots by annual NPP_B formed much tighter groups for the old-growth watershed, also indicating lower spatial variation of NPP_B for that watershed. This pattern may be partly attributed to the lower degree of heterogeneity in environment (i.e., smaller degree of variability of heat load and PADIR across plots) in the old-growth watershed.

Many forest productivity models rely on incoming radiation and/or photosynthetically active radiation coupled with physiological and climatic constraints to model productivity at varying scales (e.g., Landsberg and Waring 1997; Runyon et al. 1994). The topographic position of a site is important in determining the amount of PADIR a site receives as well as the effect of this radiation on site temperatures (McCune and Keon 2002). Therefore, to better understand the variation within a site and between sites the heterogeneity of the landscape becomes an important factor, especially at an annual time step. Gradients of soil moisture, soil characteristics, and species composition, may help explain more variation among plots within and between watersheds. Using direct measurements of PAR, monthly values of PDSI (e.g., Watson and Huckman 2002) and seasonal climatic variables (e.g., Graumlich et

al. 1989) may result in stronger relationships than those found in this study. It is evident that the variation of temperature and precipitation can have an influence on the productivity, but other environmental factors affect this relationship as well. Climatic variables can have a lagged effect on NPP_B and prior year's precipitation (monthly) and/or temperature can significantly influence current year productivity. A longer time series of NPP_B may strengthen or even alter NPP_B climate relationships found in this study.

Within watersheds, patterns of spatial coherence of NPP_B vary from watershed to watershed, but were related to similar environmental features of each watershed (i.e., heat load and potential annual incident radiation). When watersheds were examined together spatial coherence decreased. The two watersheds were less spatially coherent more frequently than results indicated between plots within either watershed. Within the second-growth watershed patterns of spatial coherence were driven by the lack of coherence in a few years, where as in the old-growth watershed high spatial coherence occurred in all years as. Results across watersheds indicate a larger number of years in which annual NPP_B was less coherent between watersheds, but NPP_B was still related to environmental factors. This analysis has shown that spatial coherence can be high in some years, and low in others, suggesting this behavior was more complex than sites either being in synch or out of synch consistently over time.

Conclusions

A multivariate analysis of two small adjacent watersheds of contrasting ages showed different responses of NPP_B within and between watersheds to environmental

variables. However, the amplitude of response differed between watersheds. Even at the small spatial scale of a watershed, tree bole NPP_B was not as spatially coherent as would be assumed based solely on physiological and climatic relationships. Results within the two watersheds indicated that response of NPP_B to differing climatic drivers and differing responses to climatic variability over time, i.e., low spatial coherence. NPP_B in the old-growth watershed responded more to late growing season climate variability, while NPP_B of the second-growth watershed was related more to early growing season climate variability. Lack of coherence in some years in the second-growth watershed indicates that climate may be less of an influence on productivity in some years, when other stand-level dynamics and other environmental variability may be contributing to lower coherence within and between watersheds. We did not find the same relationship in the old-growth watershed which we hypothesize is due to lower environmental variability (i.e., heat load and annual direct incident radiation) across plots. When we compared watersheds together, NPP_B of old-growth plots responded similarly to south facing plots in the second-growth watershed (i.e., coherence), but exhibited differences in NPP_B compared to north facing plots in the second-growth watershed (i.e., lack of coherence). As spatial scale increases, spatial coherence may also be decreasing. Time since disturbance (i.e., age class) may also be contributing to decreased coherence of NPP_B between watersheds given correlation to different climatic variables.

We also concluded that spatial coherence was not consistent and changed through time. Therefore, the coherence of sites over time is not a simple and strict relationship, instead exhibiting complex behaviors that have implications for scaling

estimates of productivity. This pattern has implications for the temporal scale at which coherence is examined, i.e., time step dependency. As researchers begin to answer these same questions at larger spatial scales (landscape, region, biome) we speculate that a decrease of spatial coherence between biological variables such as NPP_B will be seen, although abiotic factors may still be highly correlated. Now it will be important to begin to think of how to apply this understanding to better comprehend effects of climate change and anthropogenic influences on these biological variables.

Literature Cited

- Acker, S. A., Halpern, C.B., Harmon, M.E., and Dyrness, C.T. 2002. Trends in Biomass accumulation, net primary production, and tree mortality in *Psuedotsuga menziesii* forest of contrasting age. *Tree Physiology* **22**:213-217.
- Acker, S. A., W. A. McKee, M. E. Harmon, and J. F. Franklin. 1998. Long-term research on forest dynamics in the Pacific Northwest: a network of permanent forest plots. *in* F. Dallmeier and J. A. Comiskey, editors. *Forest biodiversity in North, Central, and South America and the Caribbean: Research and Monitoring*. The Parthenon Publishing Group, Washington, DC.
- Baines, S. B., K. E. Webster, T. K. Kratz, S. R. Carpenter, and J. J. Magnuson. 2000. Synchronous behavior of temperature, calcium, and chlorophyll in lakes of northern Wisconsin. *Ecology* **81**:815-825.
- Baron, J. S., and N. Caine. 2000. Temporal coherence of two alpine lake basins of the Colorado Front Range, U.S.A. *Freshwater Biology* **43**:463-476.
- Bierlmaier, F. A., and A. McKee. 1989. Climatic Summaries and Documentation for the Primary Meteorological Station, H.J. Andrews Experimental Forest, 1972 to 1984. Gen. Tech. Rep. PNW-GTR-242. General Technical Report PNW-GTR-242, Department of Agriculture, Forest Service, Pacific Northwest Research Station, Portland, OR.
- Cook, E. R., D. M. Meko, D. W. Stahle, and M. K. Cleaveland. 1999. Drought reconstructions for the continental United States. *Journal of Climate* **12**:1145-1162.
- Dyrness, C. T. 1973. Early stages of plant succession following logging and burning in the western Cascades of Oregon. *Ecology* **54**:57-69.
- Franklin, J. F., and C. T. Dyrness. 1973. Natural vegetation of Oregon and Washington. USDA Forest Service General Technical Report PNW 8. Pacific Northwest Forest and Range Experiment Station.
- Graumlich, L. J., L. B. Brubaker, and C. C. Grier. 1989. Long-term trends in forest Net primary productivity: Cascade Mountains, Washington. *Ecology* **70**:405-410.
- Grissino-Mayer, H. D. 2001. Evaluating Crossdating accuracy: A manual and tutorial for the computer program COFECHA. *Tree-Ring Research* **57**:205-221.
- Holmes, R. L. 1983. Computer-assisted quality control in tree-ring dating and measurement. *Tree Ring Bulletin* **43**:69-78.

- Huxman, T. E., M. D. Smith, P. A. Fay, A. K. Knapp, R. M. Shaw, M. E. Lolk, S. D. Smith, D. T. Tissue, J. C. Zak, J. F. Weltzin, W. T. Pockman, O. E. Sala, B. M. Haddad, J. Harte, G. W. Koch, S. Schwinning, E. E. Small, and D. G. Williams. 2004. Convergence across biomes to a common rain use efficiency. *Nature* **429**:651-654.
- Knapp, K. A., and Smith, M.D. 2001. Variation among biomes in temporal dynamics of aboveground primary production. *Science* **291**:481-484.
- Landsberg, J. J., and R. H. Waring. 1997. A generalised model of forest productivity using simplified concepts of radiation-use efficiency, carbon balance and partitioning. *Forest Ecology and Management* **95**:209-228.
- Magnuson, J. J., B. J. Benson, and T. K. Kratz. 1990. Temporal coherence in the limnology of a suite of lakes in Wisconsin, USA. *Freshwater Biology* **23**:145-159.
- McCune, B., and J. B. Grace. 2002. *Analysis of Ecological Communities*. MJM Software, Gleneden Beach, Oregon.
- McCune, B., and D. Keon. 2002. Equations for potential annual direct incident radiation and heat load. *Journal of Vegetation Science* **13**:603-606.
- McCune B., and M. J. Mefford. 1999. *PC-ORD. Multivariate Analysis of Ecological Data*. V.4. MJM Software, Gleneden Beach, Oregon.
- Moore, G. W., B. J. Bond, J. A. Jones, N. Phillips, and F. C. Meinzer. 2004. Structural and compositional controls on transpirations in 40- and 450-year old riparian forests in western Oregon, USA. *Tree Physiology* **24**:481-491.
- Palmer, W. C. 1965. *Meteorological Drought*. U.S. Department of Commerce, Washington, D.C.
- Schweingruber, F. H. 1988. *Tree Rings: Basics and Application of Dendrochronology*. D. Reidel Pub. Company, Dordrecht, Holland.
- Soranno, P. A., K. E. Webster, J. L. Riera, T. K. Kratz, J. S. Baron, P. A. Bukaveckas, G. W. Kling, D. S. White, N. Caine, R. C. Lathrop, and P. R. Leavitt. 1999. Spatial Variation among Lakes within Landscapes: Ecological Organization along Lake Chains. *Ecosystems* **2**:395-410.
- Swetnam, T. W., M. A. Thompson, and E. K. Sutherland. 1985. Using dendrochronology to measure radial growth of defoliated trees. USDA Forest Service Cooperative State Research Service.

Turner, D. P., M. Guxy, M. A. Lefsky, S. Van Tuyl, O. Sun, C. Daly, and B. E. Law. 2003. Effects of land use and fine scale environmental heterogeneity on net ecosystem production over a temperate coniferous forest landscape. *Tellus* **55**:657-668.

Watson, E., and B. H. Luckman. 2001. Dendroclimatic reconstruction of precipitation for sites in the southern Canadian Rockies. *The Holocene* **11**:203-213.

Tables

Table 3.1 Site Characteristics for second-growth and old-growth watersheds.

Site	Age Class (yrs)	Elevation range (m)	Dominant Tree Species	# of Plots
WS01	Second-growth (40)	480-965	<i>Pseudotsuga menziesii</i>	132
WS02	Old-growth (450)	475-1070	<i>Pseudotsuga menziesii</i> / <i>Tsuga heterophylla</i>	67

Table 3.2 Outlier Statistics for both watersheds showing average distances of sample units from other plots and standard deviations from the grand mean of distances between plots. Letter next to plot number indicates zone.

Watershed	Rank	Plot	Average Distance	Standard Deviations
Second-growth	1	416R	2.164	5.403
	2	507R	2.117	5.193
	3	405N	1.498	2.432
	4	105R	1.452	2.229
	5	211N	1.446	2.200
	6	404N	1.440	2.173
Old-growth	1	806	0.701	4.073
	2	202	0.571	2.503
	3	606	0.545	2.201
	4	903	0.530	2.012

Table 3.3 Summary Statistics for plots and years including outliers for both the second-growth and old-growth watersheds.

Watershed	Attribute	Average Skewness	Average Kurtosis
Second-growth	Plots	0.028	0.867
	Years	0.216	5.298
Old-growth	Plots	0.540	0.003
	Years	0.114	2.502

*CV (%) = (Standard Deviation/Mean)*100

Table 3.4 PCA statistics for the first 4 axes corresponding to Figures 3.4 and 3.5. Ordination transposed matrix - years in plot space for the second-growth and old-growth watersheds.

Watershed	Axis	Eigenvalue	% of Variance Extracted	Cum. % Variance Extracted	Broken-stick Eigenvalue
Second-growth	1	101.25	76.70	76.70	5.46
	2	14.99	11.36	88.06	4.46
	3	4.47	5.21	91.45	3.96
	4	2.69	2.04	93.49	3.63
Old-growth	1	61.59	91.926	91.926	4.789
	2	1.262	1.883	93.809	3.789
	3	0.965	1.441	95.250	3.289
	4	0.650	0.971	96.220	2.956

Table 3.5 Correlation coefficients for climatic variables and associated axes for the second-growth and old-growth watersheds corresponding to Figures 3.5 and 3.6 - annual NPP_B ordinated in plot space. (r) > 0.30

Variable	Second-growth Watershed		Old-growth Watershed	
	Axis 1	Axis 2	Axis 1	Axis 2
	r	r	r	r
Average Annual Temperature	-	-	-0.390	-0.538
Annual Precipitation	-0.157	-0.482	-	-
March precipitation	-	-	0.047	0.491
April Precipitation	-0.314	-0.334	-	-
May Precipitation	-0.322	-0.345	-	-
October Precipitation	-	-	-0.577	-0.113
November Precipitation	-	-	0.021	-0.431
Previous year's May Precipitation	0.606	0.184		
Previous year's August Precipitation	-0.238	-0.432	-0.441	-0.304
Previous year's November Precipitation	0.523	-0.469	0.435	-0.215
May Minimum Temperature	-0.385	0.076	-0.202	0.419
July Minimum Temperature	-	-	-0.524	-0.353
August Minimum Temperature	-	-	-0.540	-0.293
September Minimum Temperature	-	-	-0.518	0.034
November Minimum Temperature	-	-	-0.307	-0.538
December Minimum Temperature	-	-	0.273	-0.539
February Mean Temperature	-	-	-0.190	-0.602
May Mean Temperature	0.040	0.411	-	-
June Mean Temperature	0.462	-0.139	-	-

Table 3.5 (continued)

Variable	Second-growth Watershed		Old-growth Watershed	
	Axis 1	Axis 2	Axis 1	Axis 2
	r	r	r	r
July Mean Temperature	-	-	-0.437	-0.463
August Mean Temperature	-	-	-0.618	-0.396
September Mean Temperature	-	-	-0.415	-0.102
January Maximum Temperature	-	-	-0.505	-0.299
February Maximum Temperature	-	-	-0.126	-0.561
May Maximum Temperature	0.129	0.454	-	-
June Maximum Temperature	0.474	-0.259	-	-
September Maximum Temperature	-0.230	0.301	-0.390	-0.538
December Maximum Temperature	-	-	0.047	0.491
PDSI	-0.248	-0.558	-	-

Table 3.6 A-statistics from MRPP of pair-wise comparisons of *a priori* groups in the second-growth watershed. Values above 0.1 are in bold.

Group	1	2	3	4	5	Average within group distance
North Facing Ridge	1	-	-	-	-	0.856
North Facing Slope	0.123	1	-	-	-	0.666
Riparian	0.142	0.080	1	-	-	1.391
South Facing Slope	0.066	0.195	0.100	1	-	0.731
South Facing Ridge	0.121	0.069	0.094	0.017	1	0.522

Table 3.7 PCA statistics with outliers for the first 4 axis corresponding to Figures 3.8 and 3.9. Ordination of main matrix - plots in NPP_B space for both the second-growth and old-growth watersheds individually.

Watershed	Axis	Eigenvalue	% of Variance Extracted	Cum. % Variance Extracted	Broken-stick Eigenvalue
Second-growth	1	7.369	40.94	40.94	3.49
	2	2.569	14.27	55.216	2.49
	3	2.26	12.57	67.78	1.99
	4	2.03	11.26	79.04	1.66
Old-growth	1	7.929	44.049	44.049	3.495
	2	2.546	14.145	58.194	2.495
	3	1.35	7.503	65.696	1.995
	4	1.235	6.861	72.558	1.662

Table 3.8 Correlation coefficients for measured environmental variables and associated axis for the second-growth and old-growth watersheds corresponding to Figures 3.8 and 3.9, plots ordinated in annual NPP_B space.

Variable	Second-growth Watershed		Old-growth Watershed	
	Axis 1	Axis 2	Axis 1	Axis 2
	r	r	r	r
Elevation	0.081	0.006	0.112	-0.085
Slope	-0.028	0.041	-0.164	0.198
Direct Incident Radiation	0.442	0.022	0.245	-0.169
Heat Load	0.519	0.019	0.282	-0.070

Table 3.9 PCA statistics with outliers for the first 4 axis corresponding to Figure 3.10. Ordination of main matrix - plots in year space for comparison of old-growth and second-growth watersheds.

Axis	Eigenvalue	% of Variance Extracted	Cum. % Variance Extracted	Broken-stick Eigenvalue
1	7.606	42.258	42.258	3.495
2	2.503	13.907	56.166	2.495
3	1.919	10.662	66.828	1.995
4	1.809	10.047	76.875	1.662

Table 3.10 Correlation coefficients for measured environmental variables and associated axis for the comparison of old-growth and second-growth watersheds corresponding to Figure 3.10, plots ordinated in annual NPP_B space.

Variable	Axis 1		Axis 2		Axis 3	
	r	r ²	r	r ²	r	r ²
Elevation	0.089	0.008	0.141	0.02	-0.038	0.001
Slope	-0.105	0.011	-0.155	0.024	0.153	0.023
Direct Incident	-0.571	0.326	-0.087	0.008	-0.114	0.013
Heat Load	-0.55	0.302	0.051	0.003	-0.146	0.021

Table 3.11 PCA statistics for the first 4 axes corresponding to Figures 3.11 and 3.12. Plots were ordinated along environmental gradients for both watersheds individually.

Watershed	Axis	Eigenvalue	% of Variance Extracted	Cum. % Variance Extracted	Broken-stick Eigenvalue
Second-growth	1	2.358	58.947	58.947	2.083
	2	1.077	26.921	85.868	1.083
	3	0.507	12.669	98.536	0.583
	4	0.059	1.464	100	0.250
Old-growth	1	1.848	46.194	46.194	2.083
	2	1.055	26.375	72.569	1.083
	3	0.946	23.654	96.223	0.583
	4	0.151	3.777	100	0.250

Table 3.12 Correlation coefficients for measured environmental variables and associated axis for the second-growth and old-growth watersheds corresponding to Figures 3.11 and 3.12, plots ordinated in environmental space.

Variable	Second-growth		Old-growth		
	Axis 1	Axis 2	Axis 1	Axis 2	Axis 3
	r	r	r	r	r
Elevation	-0.496	-0.759	0.052	0.715	0.697
Slope	0.71	0.448	-0.02	0.737	-0.676
Direct	-0.905	0.388	-0.961	0.031	-0.009
Heat Load	-0.888	0.387	-0.96	-0.007	0.061

Table 3.13 Correlation coefficients for years of NPP_B and associated axis for the second-growth and old-growth watersheds corresponding to Figures 3.11 and 3.12, plots ordinated in environmental space.

Year	Second-growth	Old-growth
	Axis 1	Axis 1
	r	r
1984	-0.471	-0.247
1985	-0.433	0.120
1986	-0.284	-0.289
1987	0.514	0.230
1988	0.208	0.209
1989	-0.272	0.264
1990	0.068	-0.172
1991	0.244	-0.230
1992	0.076	0.020
1993	0.228	0.211
1994	0.249	0.182
1995	-0.256	0.191
1996	-0.192	-0.070
1997	0.074	-0.198
1998	0.377	-0.266
1999	-0.221	0.208
2000	-0.509	0.076
2001	0.535	-0.104

Table 3.14 Response (+/-) of north and south facing zones in the second-growth watershed for different years, indicating spatial coherence between topographic zones changes through time.

Years	South Facing	North Facing	Spatially Coherent?
1984 and 2000	+	-	No
1987 and 2001	-	+	No
All other Years	+	+	Yes
	-	-	Yes

Table 3.15 Correlation coefficients for years of NPP_B and associated axis for the comparison of second-growth and old-growth watersheds corresponding to Figure 3.13, plots ordinated in environmental space.

Year	Axis 1	Axis 2	Axis 3
	r	r	r
1984	-0.403	0.082	0.026
1985	-0.493	-0.249	0.14
1986	-0.315	-0.07	0.133
1987	0.538	0.358	-0.151
1988	0.327	0.388	-0.168
1989	-0.322	-0.254	0.088
1990	0.098	0.102	-0.193
1991	0.285	0.204	-0.125
1992	-0.13	-0.396	0.116
1993	0.361	0.464	-0.16
1994	0.292	0.094	-0.044
1995	-0.186	0.004	0.068
1996	-0.077	0.13	-0.071
1997	-0.047	-0.039	0.004
1998	0.443	0.282	-0.14
1999	-0.306	-0.29	0.185
2000	-0.57	-0.253	0.201
2001	0.589	0.228	-0.184

Table 3.16 PCA statistics for the first 4 axes corresponding to Figure 3.13. Plots ordinated along environmental gradients for both watersheds together.

Axis	Eigenvalue	% of Variance Extracted	Cum. % Variance Extracted	Broken-stick Eigenvalue
1	2.062	51.538	51.538	2.083
2	1.218	30.452	81.99	1.083
3	0.645	16.117	98.107	0.583
4	0.076	1.893	100	0.250

Table 3.17 Correlation coefficients for measured environmental variables and associated axis for old-growth and second-growth watersheds together corresponding to Figure 3.13, plots ordinated in environmental space.

Variable	Axis 1		Axis 2		Axis 3	
	r	r ²	r	r ²	r	r ²
Elevation	-0.238	0.056	0.825	0.681	0.512	0.262
Slope	0.503	0.253	-0.622	0.387	0.600	0.360
Direct Incident Radiation	-0.932	0.868	-0.303	0.092	0.047	0.002
Heat Load	-0.940	0.883	-0.242	0.058	0.145	0.021

Figures

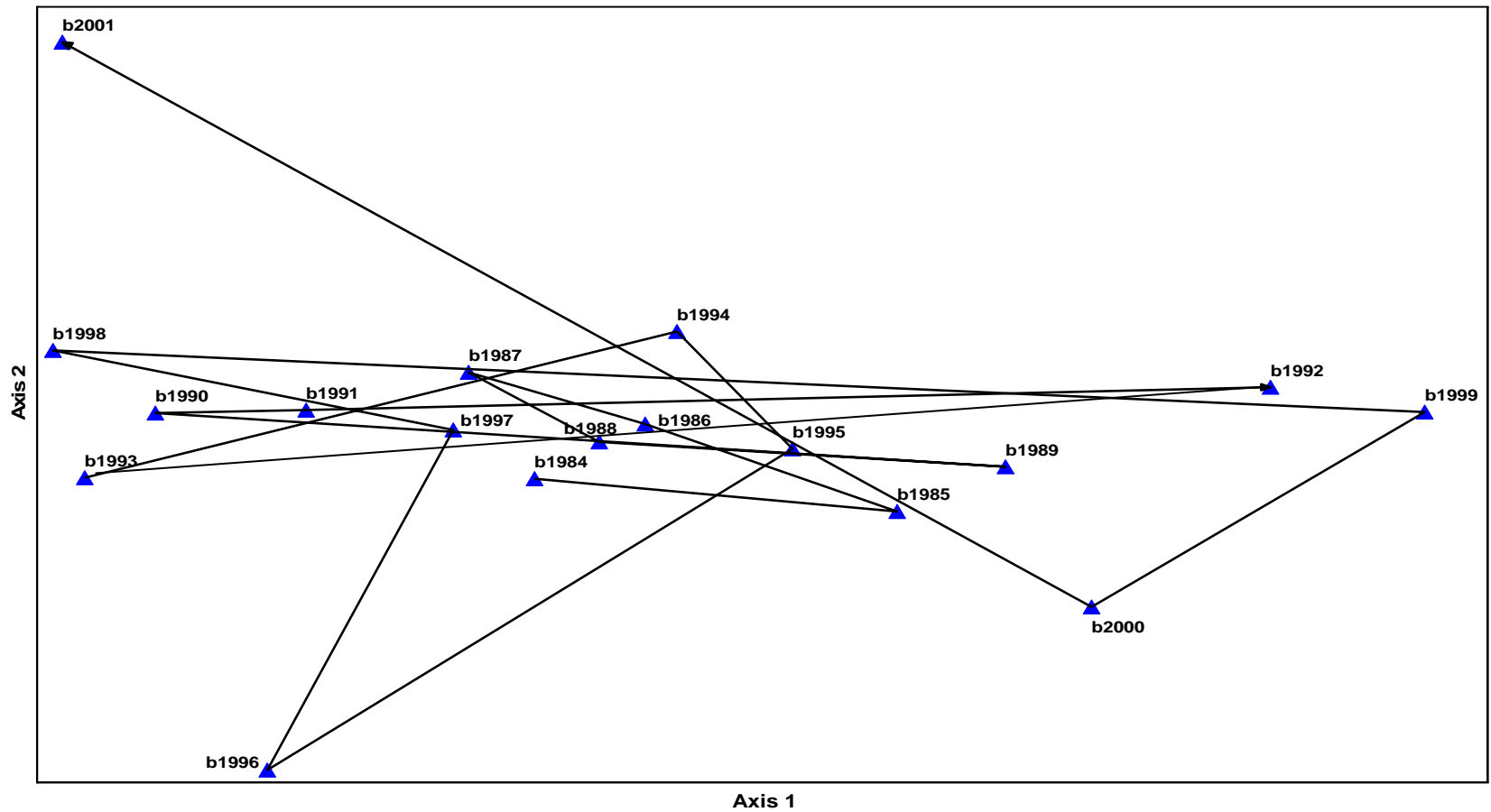


Figure 3.1 Ordination of years of NPP_B across all plots for the second-growth watershed with vectors connecting successive years showing no consistent long-term temporal trend in annual NPP_B .

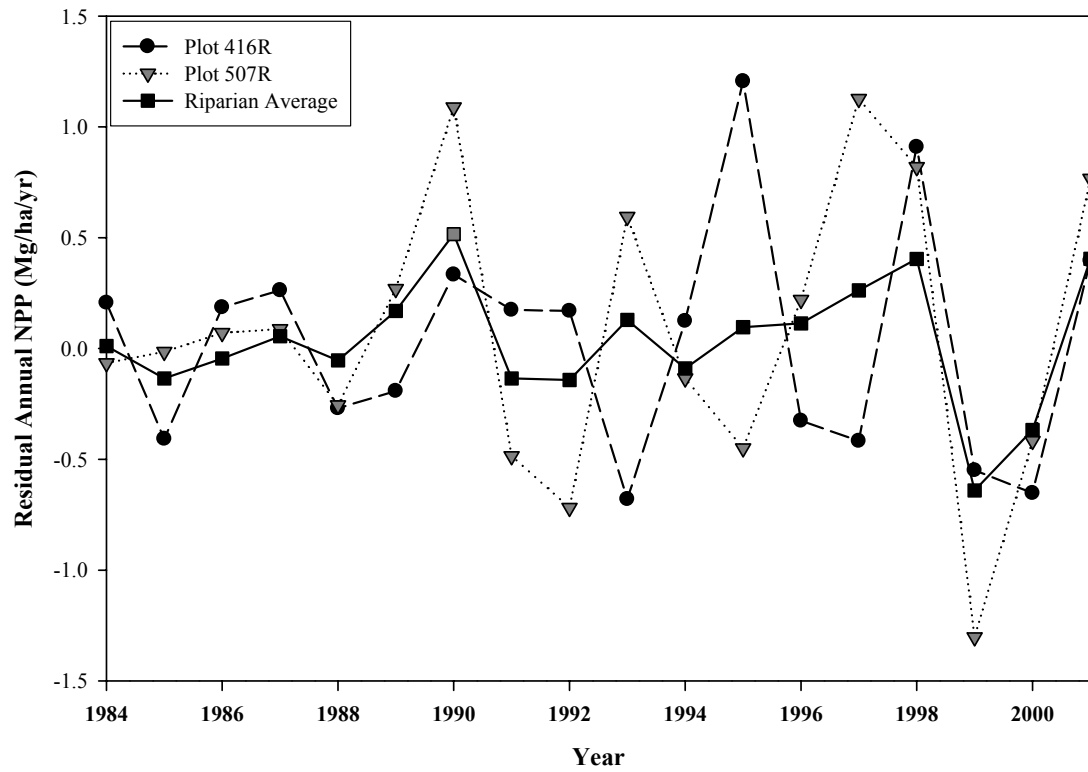


Figure 3.2 Residual NPP_B (Mg/ha/yr) for two outlier plots (dotted and dashed lines) and the average residual NPP_B of all riparian plots (solid line).

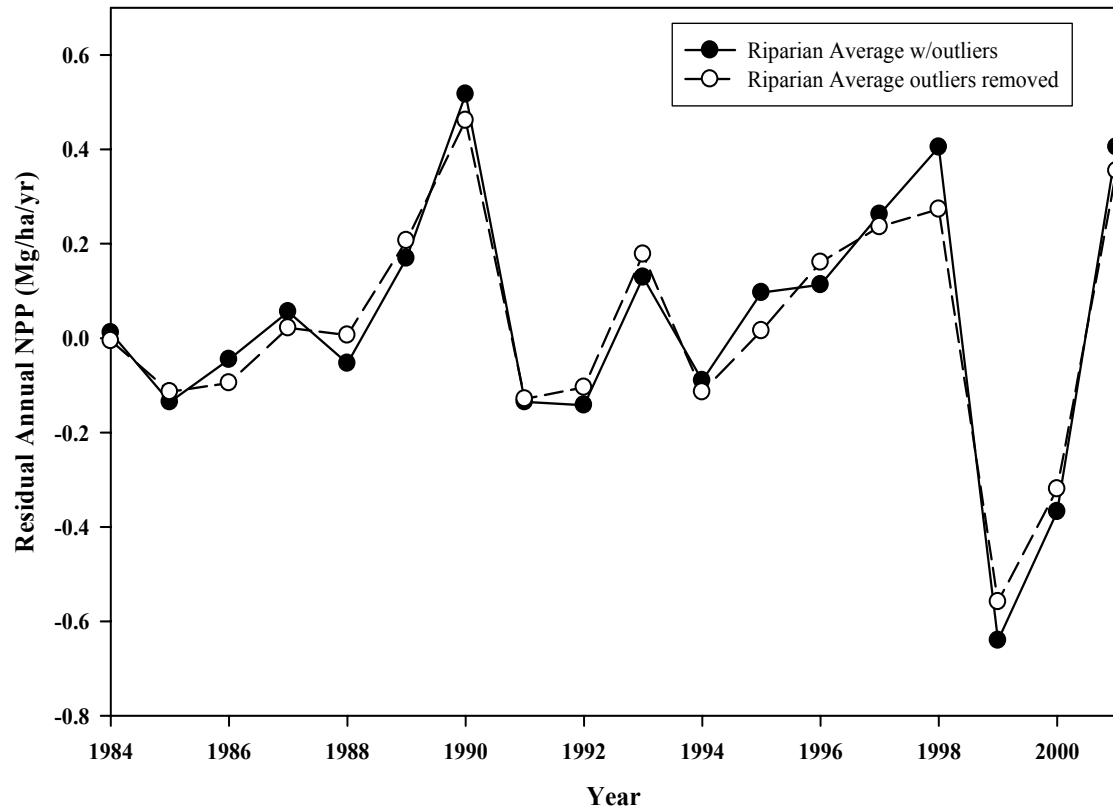


Figure 3.3 Average residual NPP_B (Mg/ha/yr) for riparian plots with and without outliers illustrating the lack of influence by outliers.

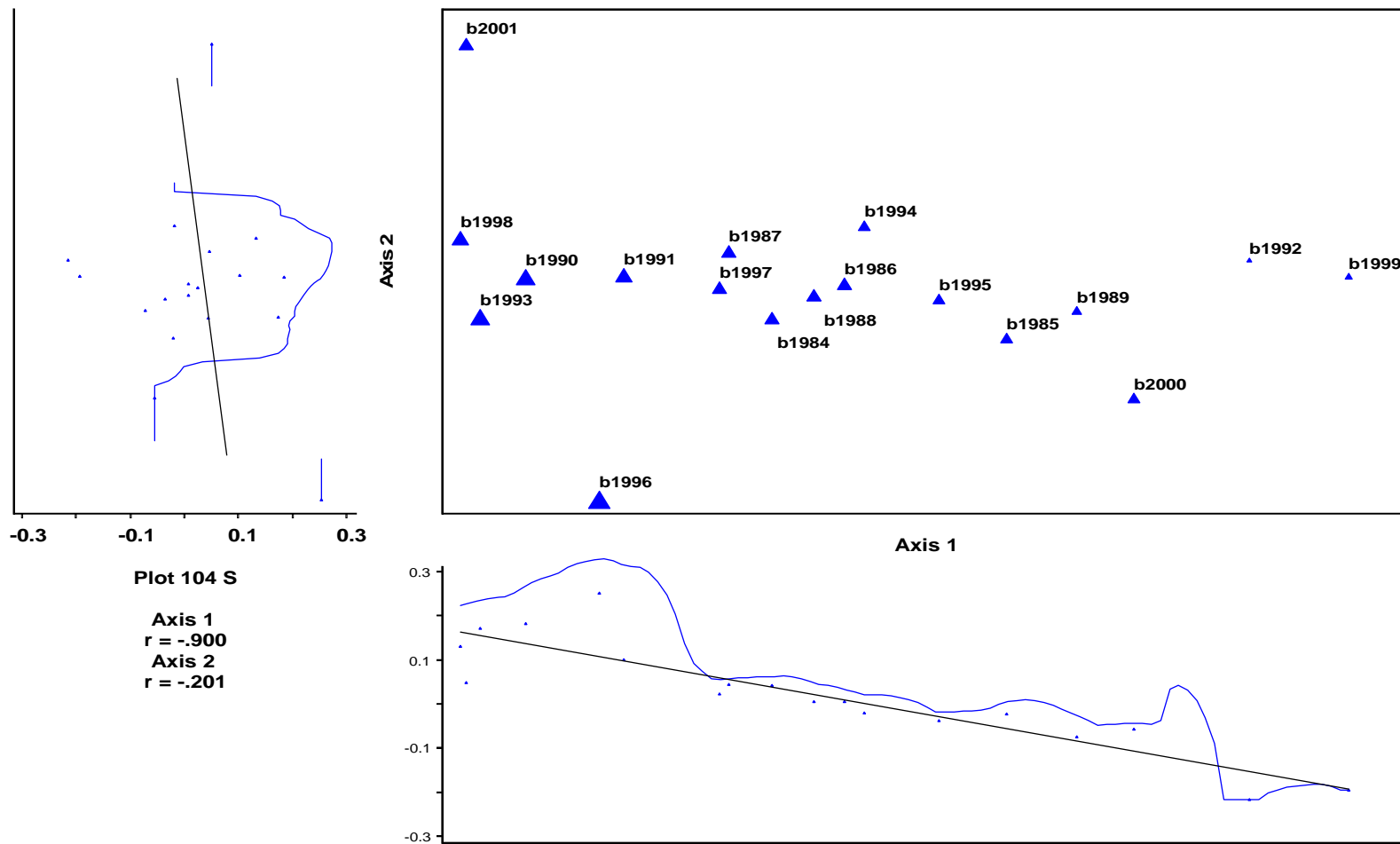


Figure 3.4 Years of NPP_B across all plots for the second-growth watershed. Annual NPP_B is increasing from right to left indicated by size of symbol. Left and lower panels display the correlation of a single plot characterizing the general pattern of all plots.

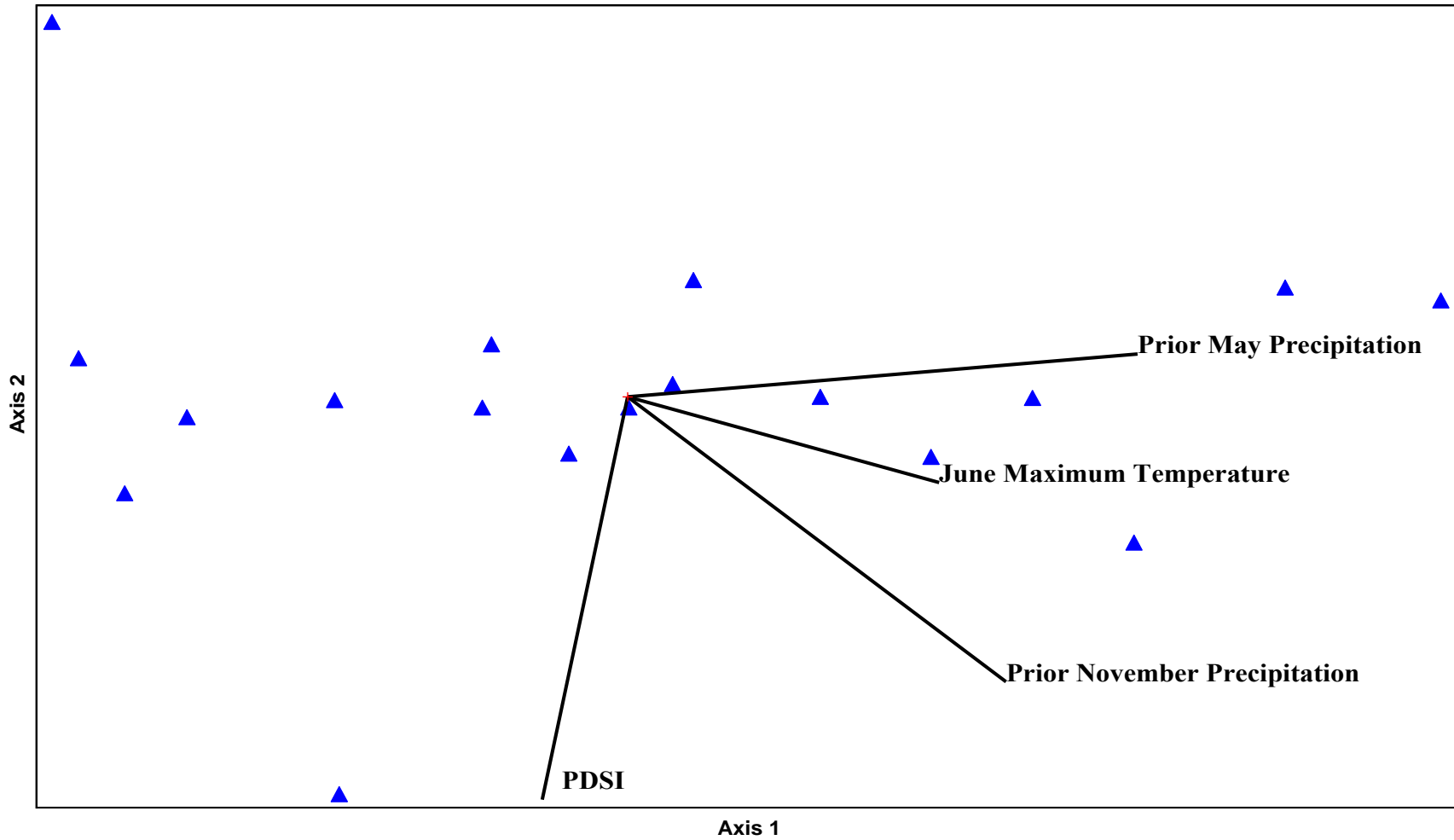


Figure 3.5 Years of NPP_B across all plots for the second-growth watershed with an overlay of climatic variables correlated with axis 1 and 2. Vector length indicates strength of correlation for that variable.

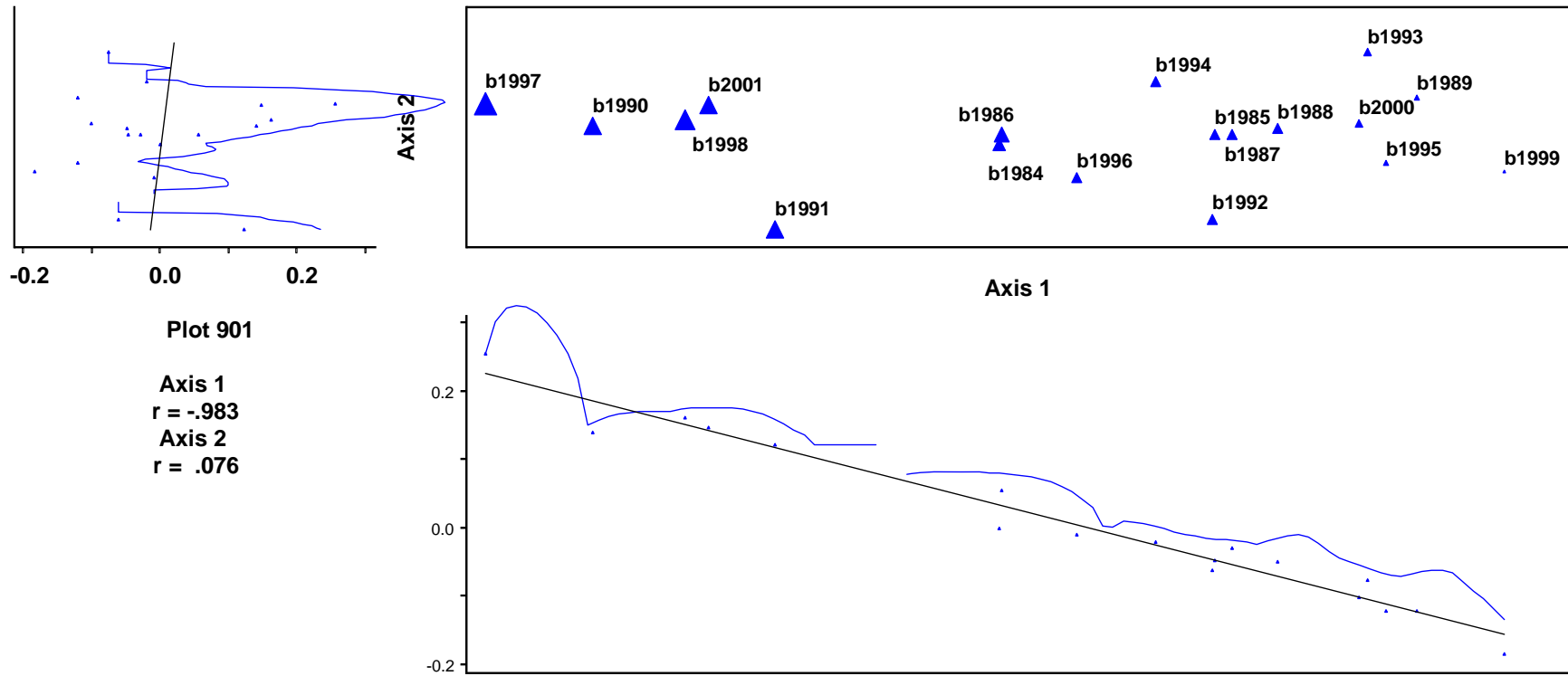


Figure 3.6 Years of NPP_B across all plots for the old-growth watershed. Annual NPP_B is increasing from left to right indicated by size of symbol. Left and lower panels display the relationship of a single plot characterizing the general pattern of all plots.

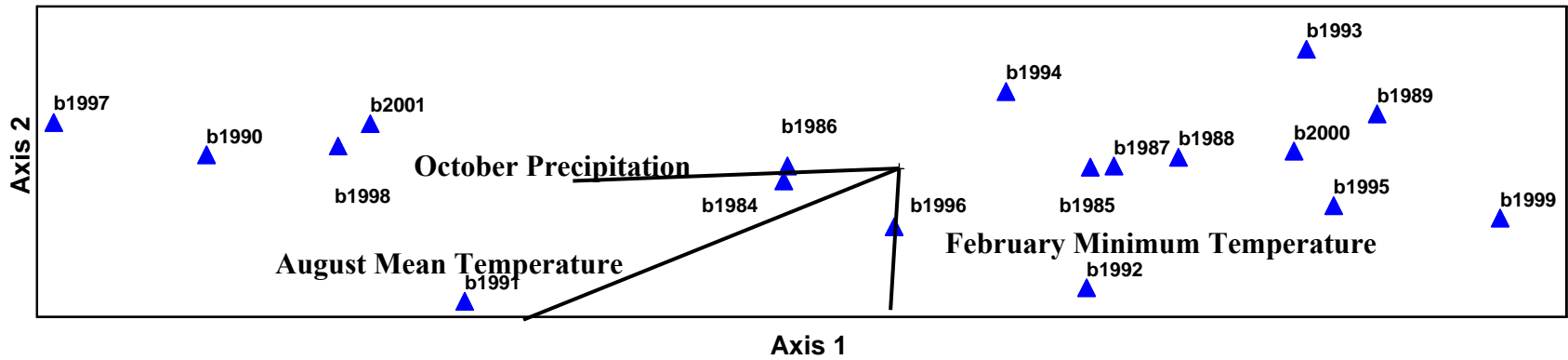


Figure 3.7 Years of NPP_B across all plots for the old-growth watershed with an overlay of climatic variables correlated with axis 1 and 2. Vector length indicates strength of correlation for that variable.

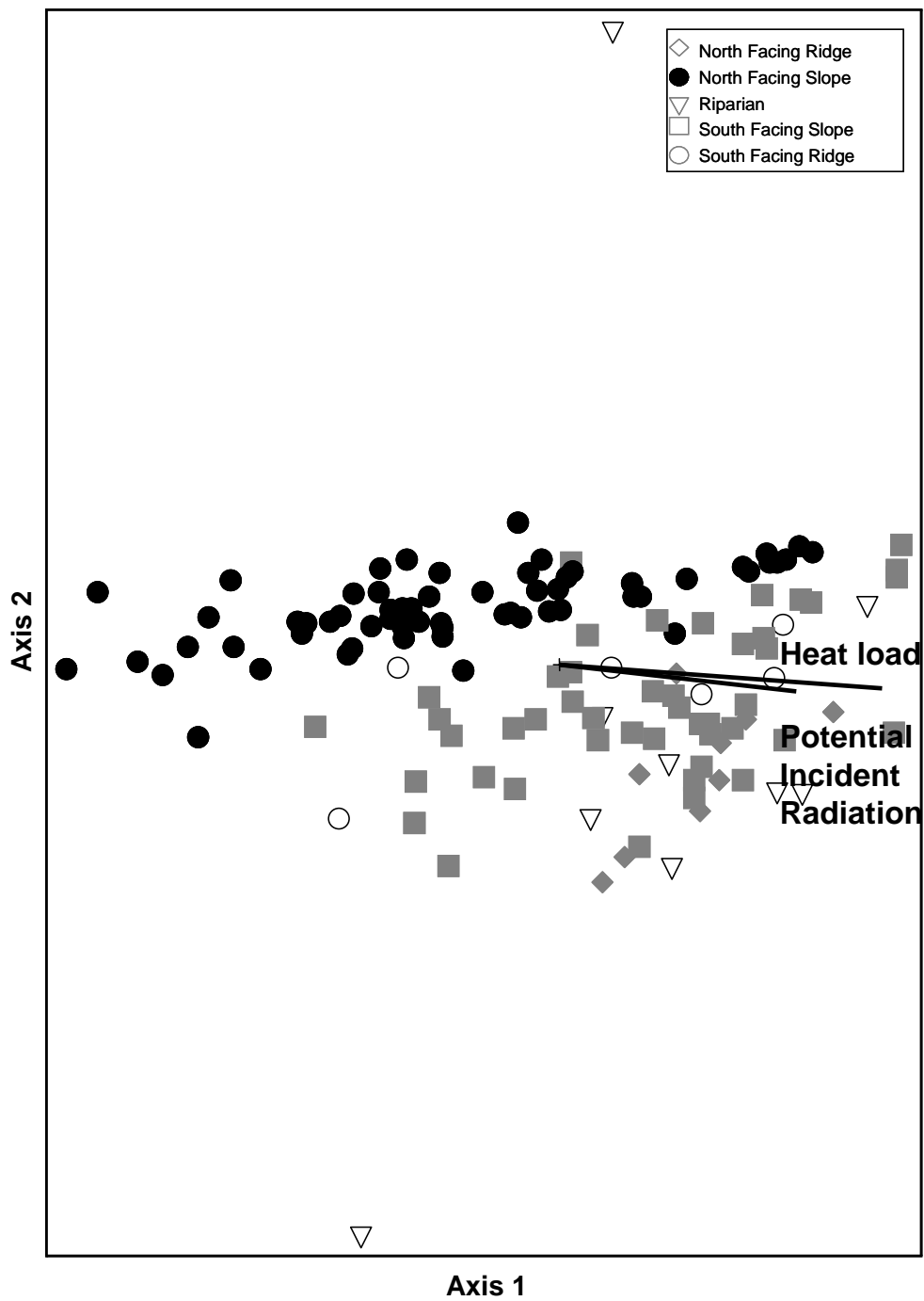


Figure 3.8 Ordination of plots in the second-growth watershed in annual NPP_B space with an overlay of heat load and annual potential incident radiation correlated with axis 1. Plots are coded by *a priori* topographic position.

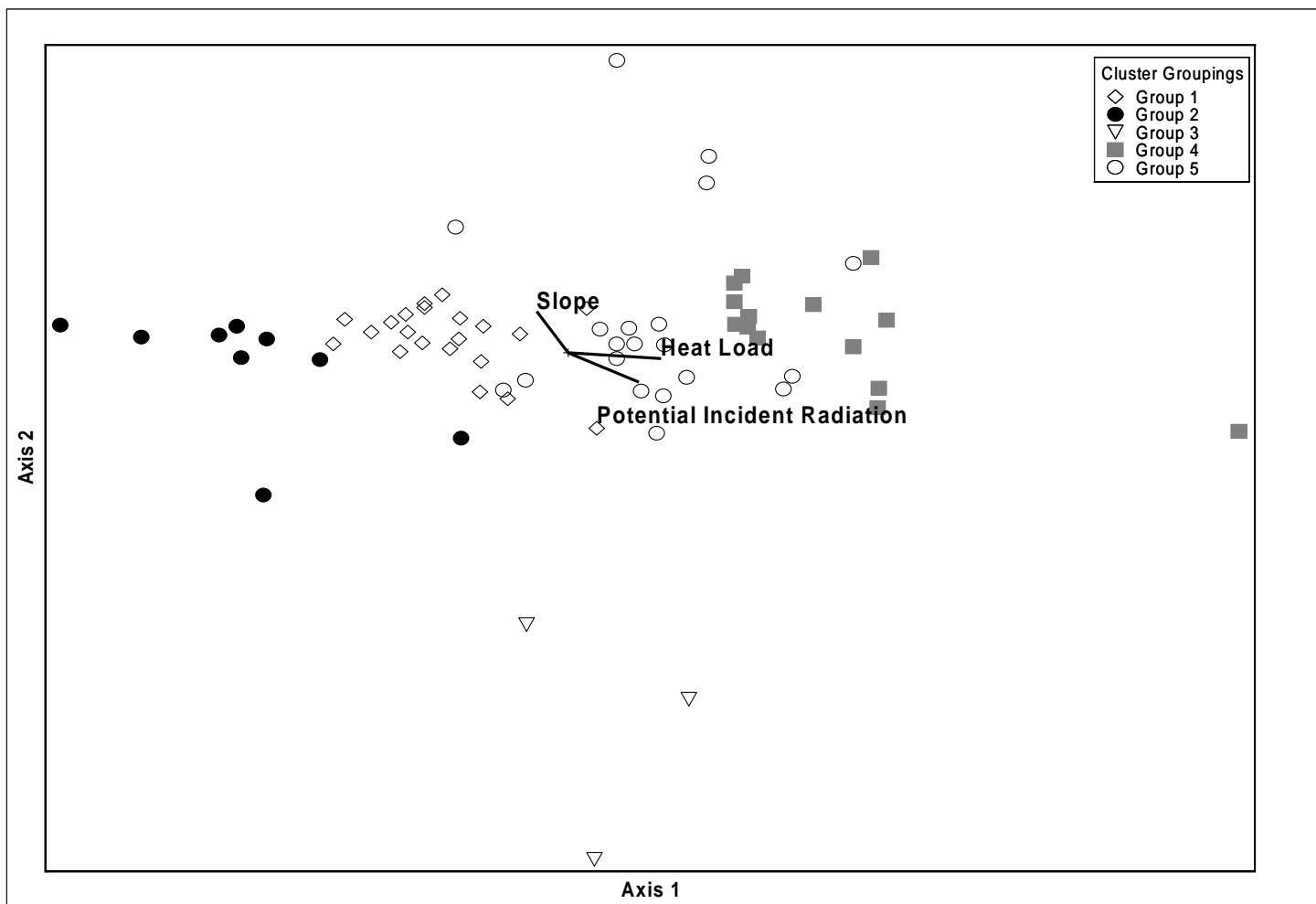


Figure 3.9 Ordination of plots in the old-growth watershed, in annual NPP_B space with an overlay of heat load and annual potential incident radiation correlated with axis 1. Plots are coded by groups determined by cluster analysis.

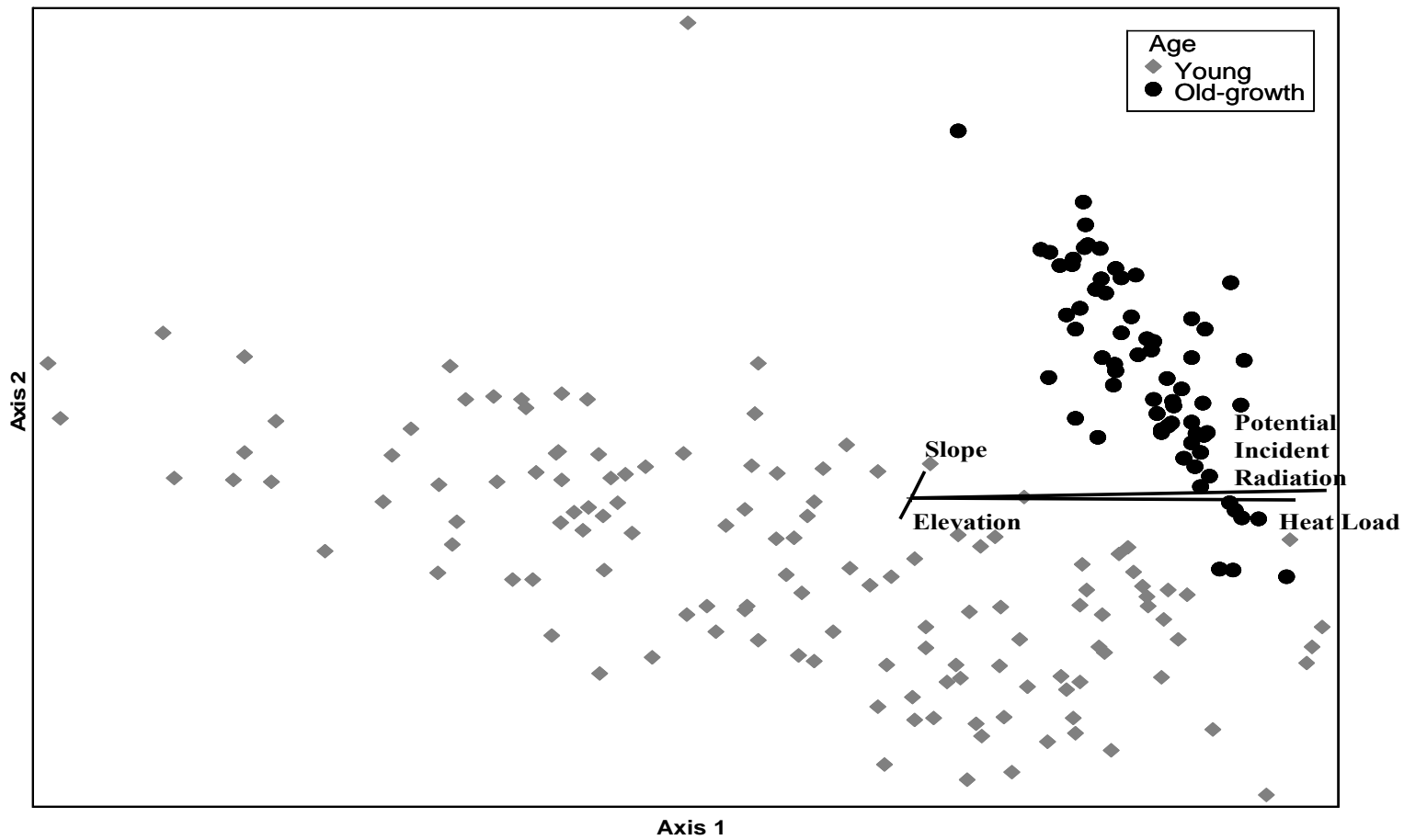


Figure 3.10 Ordination of plots in both watersheds, in annual NPP_B space with an overlay of heat load and annual potential incident radiation correlated with axis 1 and slope and elevation correlated with axis 3. Plots are coded according to watershed age.

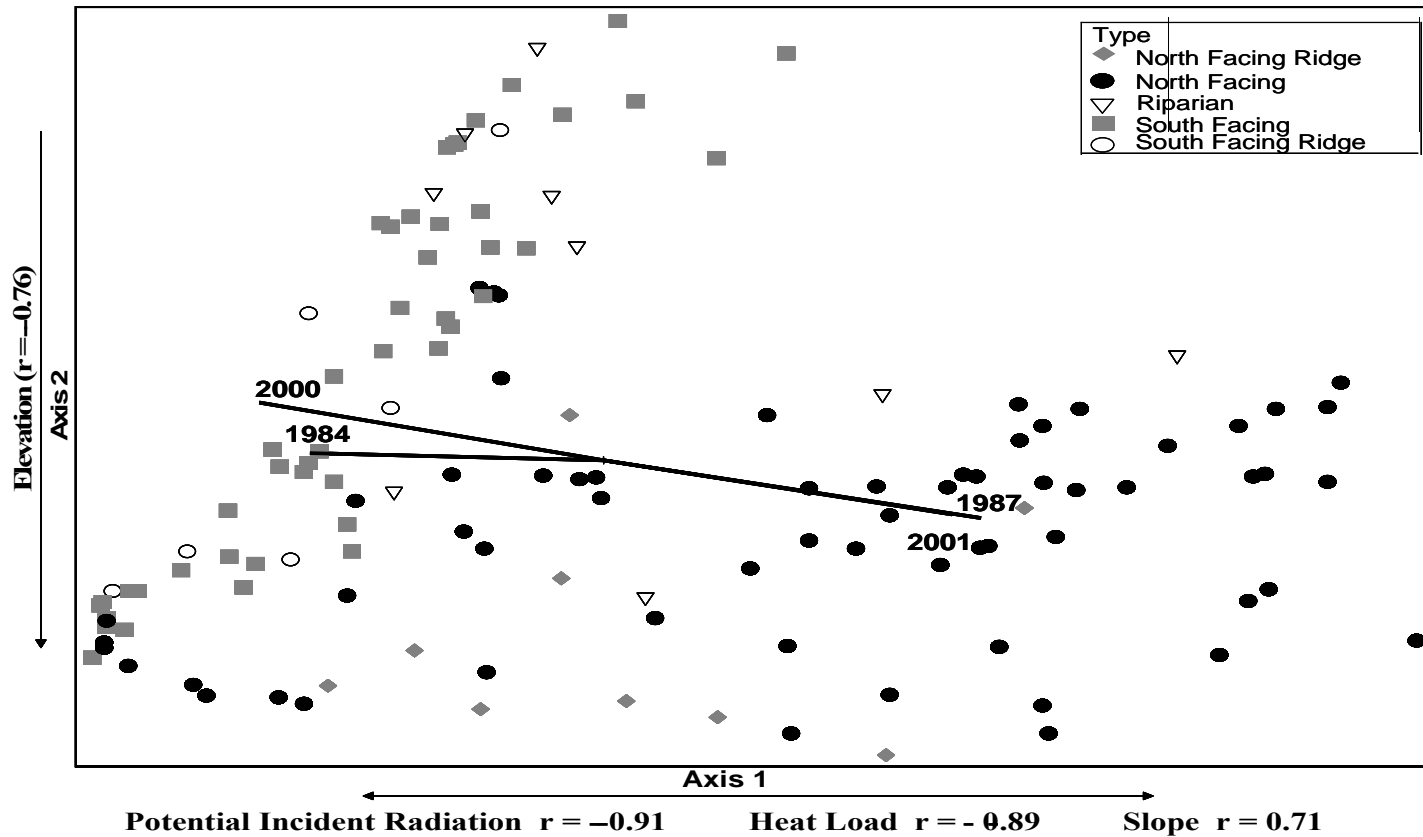


Figure 3.11 Ordination of plots in the second-growth watershed in environmental space. North and south facing plots are grouped along axis 1 and 2. Overlay of years of NPP_B indicate that these two groups are responding differently in the years shown (vector direction indicates positive correlation).

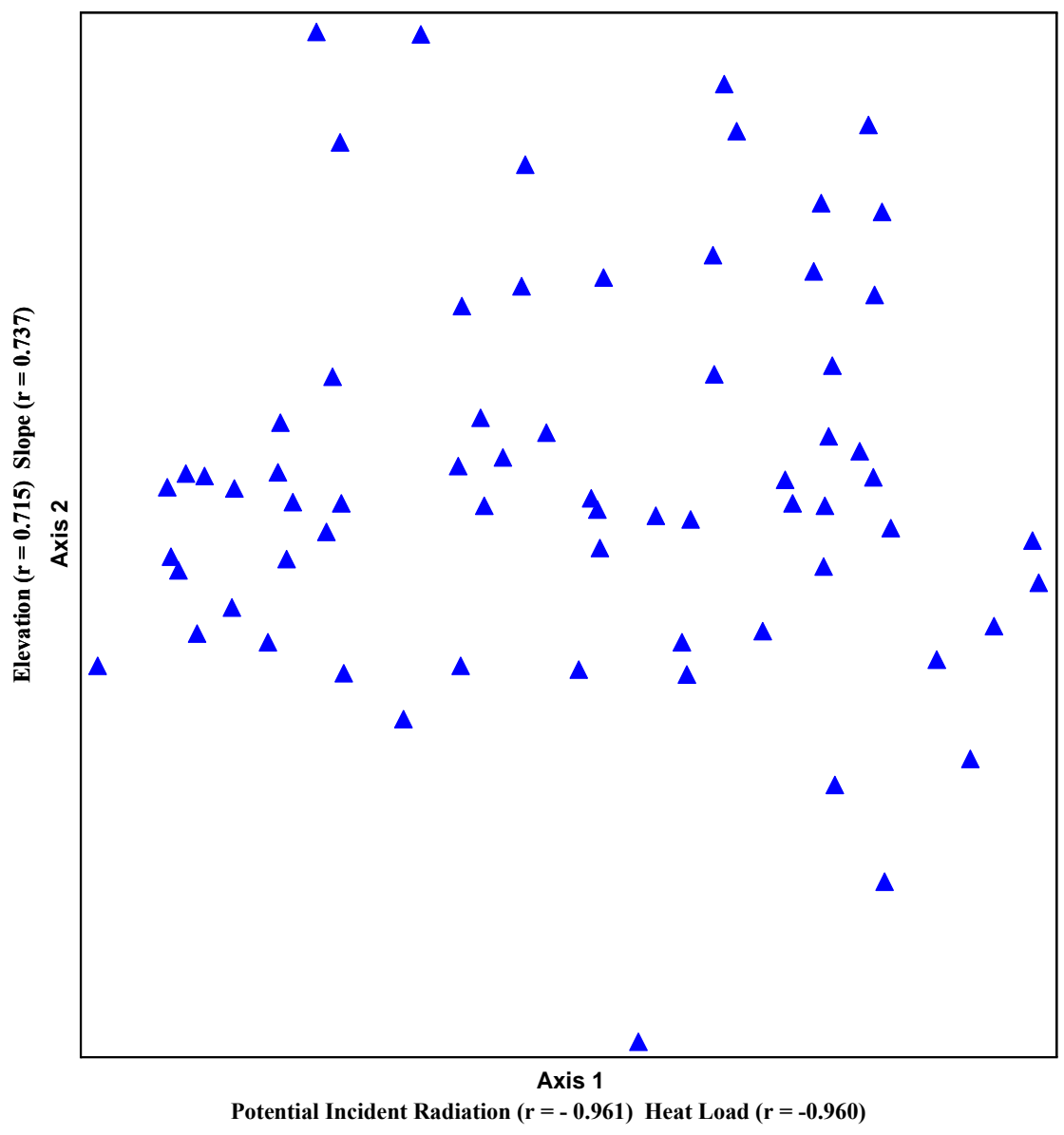


Figure 3.12 Ordination of plots in the old-growth watershed in environmental space. Plots tend to be spread out and not grouped along axis 1 and 2. Overlay of years of NPP_B indicate that these two groups were responding differently in the years shown (vector direction indicates positive correlation).

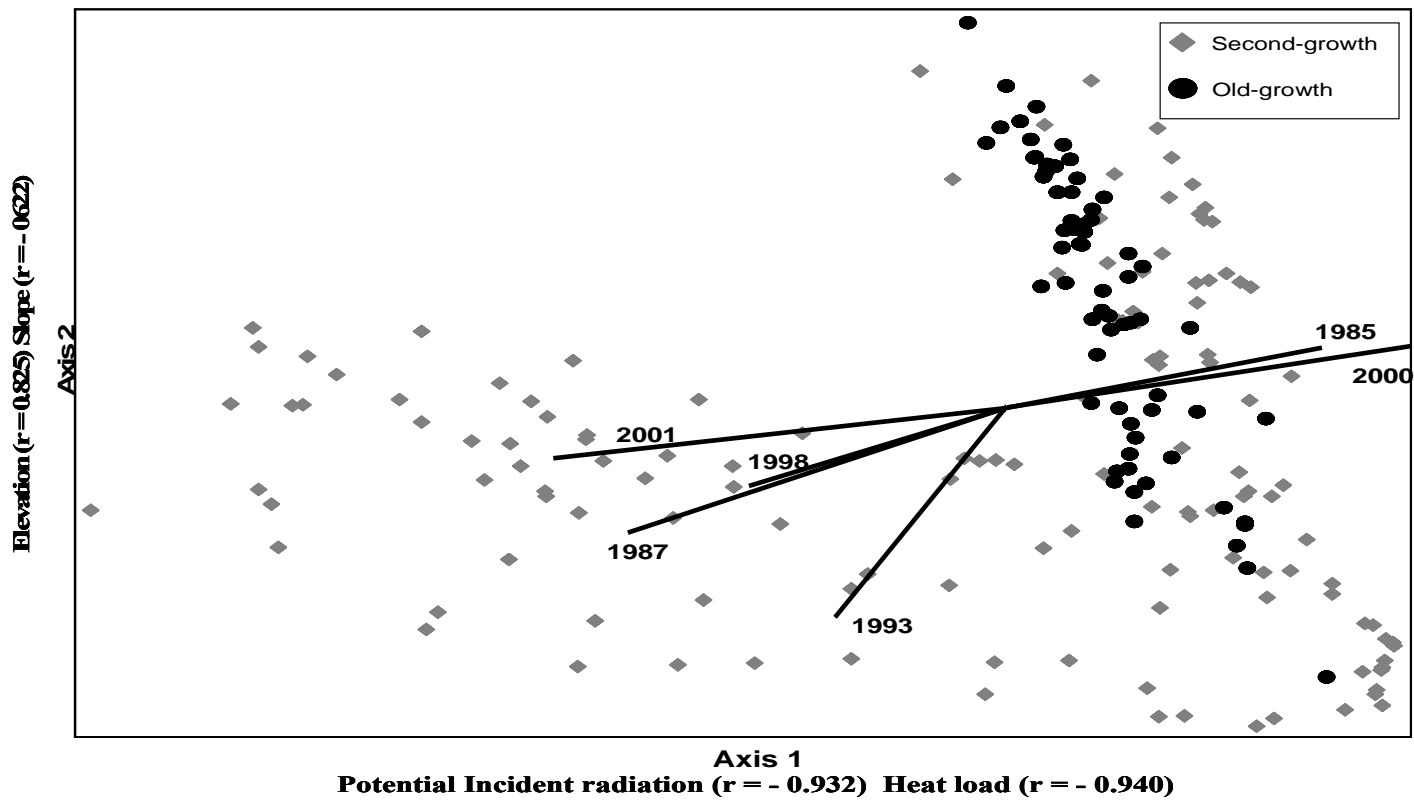


Figure 3.13 Ordination of plots in both watersheds in environmental space. Plots are grouped according to age and environmental variables along axis 1 and 2. Overlay of years of NPP_B indicate that these two watersheds were responding differently in the years shown (vector direction indicates positive correlation).

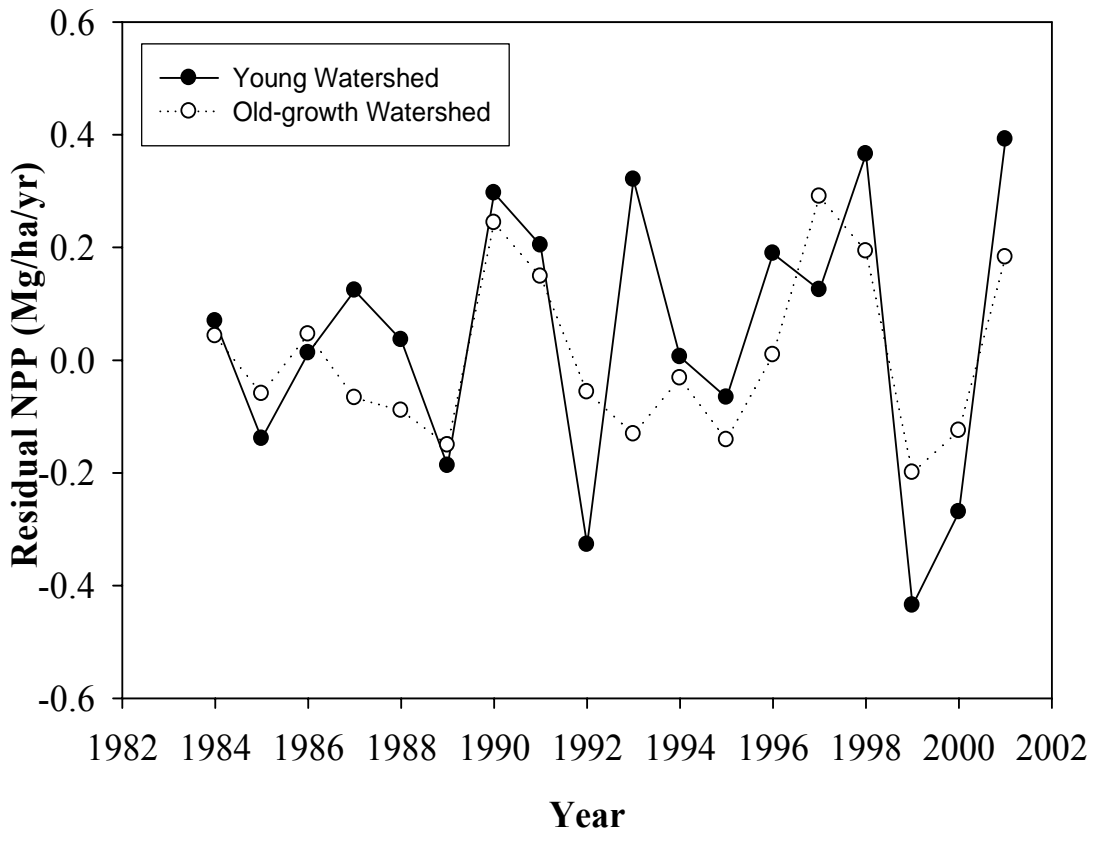


Figure 3.14 Average annual residual NPP_B for both the second-growth and old-growth watersheds. Lack of coherence and differing degree of response in particular years, drives overall spatial coherence between watersheds.

Chapter 4: Inter-annual variation and spatial coherence of Net Primary Productivity within and between sites across a Western Oregon Cascades landscape

Travis J. Woolley, Mark E. Harmon, and Kari E. O'Connell

Prepared for submission to *Global Change Biology*

Abstract

Quantifying and modeling processes involved in the global carbon cycle will be important to evaluate the temporal and spatial variability of these processes and understand the effect of this variability on future response to changing climate and land use patterns. Net Primary Productivity (NPP) is an integral piece of ecosystem carbon balance in terrestrial ecosystems, and therefore garners much attention by ecologists. The inter-annual variability of NPP of forests is a function of both extrinsic (i.e., climate) and intrinsic (e.g., disturbance and competition) factors. Determining the spatial coherence (i.e., the degree of synchrony of a variable between sites) is a way in which the relative importance of these factors can be determined. As we scale estimates of NPP from trees to sites to the landscape the effects of these factors become important on how NPP behaves spatially and temporally. If spatial coherence is low then we can use this measure as a means to improve future predictions as estimates are scaled up spatially. Here I examine the spatial coherence of annual tree bole productivity (NPP_B) in sites of varying age, elevation, moisture, and species composition across a forested landscape in the western Cascade Range of Oregon. Tree growth within a site was investigated and the consequences of that variability in growth have on site level NPP_B . Comparisons of site variation and landscape variation in NPP_B were also made. Similar behaviors of increasing inter-annual variability with increased rates of growth and NPP_B emerged for trees within a site and for sites across the landscape. Second-growth sites were the most spatially coherent ($r= 0.92$) while older sites and comparisons between ages showed a much larger range in coherence ($r= -0.18$ to 0.85). Climate was a more important factor between sites that had a high

degree of coherence and it appears that intrinsic factors (i.e., stand dynamics) within a site and spatial proximity between sites across the landscape also had a significant affect on the level of coherence.

Introduction

The inter-annual variability of Net Primary Productivity (NPP) of forests is a function of both extrinsic (i.e., climate) and intrinsic (e.g., disturbance and competition) factors. Many studies have shown that climate plays a role in determining tree growth patterns (Brubaker 1980 and Fritts et al. 1976), while others have reported that stand dynamics caused by disturbance and competition to be important as well (Piutti and Cescatii 1997; Fritts and Swetnam 1989; Cook and Kairiukstis 1990). Heterogeneity of environmental influences and land use associated with this spatial variation can also play an important role in ecosystem productivity across the landscape (Turner et al. 2003).

The balance between NPP and losses of carbon through heterotrophic respiration determines whether an ecosystem is a net source or sink of carbon from the atmosphere (Net Ecosystem Productivity). The production of woody tissue by trees (NPP_B) is a large component of NPP of forests, thus contributing considerably to overall ecosystem productivity. Within site variability in annual tree growth and the factors affecting this variability, will determine the overall pattern of NPP within a site. Thus, the temporal variability and spatial correlation of NPP between sites will in part shape ecosystem carbon balance across the landscape. Specifically, the spatial coherence of NPP between sites will affect the capacity of a landscape to act as a net source or a net sink of carbon. Spatial coherence can be defined as the degree to which pairs of sites across space are synchronous (i.e., correlated) through time (definition altered from Magnuson et al. 1990; Baron and Caine 2000; Soranno et al. 1999; and Baines et al. 2000). Whether the response of NPP is amplified or modulated over time

with respect to land use and climate change could also determine the magnitude of ecosystem productivity.

Biogeochemical (BGC) models (Running and Gower 1991, Running and Hunt 1993, Running 1994, White et al. 2000) of NPP are based on physiological processes interacting with climate at very fine temporal resolutions. Therefore, the inter-annual variation of NPP between sites is likely to be perfectly correlated from year to year, at least to the degree that underlying climatic drivers are correlated. Furthermore comparisons of annual estimates and patterns of inter-annual variability from BGC models do not always match estimates derived from field measurements (Turner pers. comm. 2005). Predicting ecological change for ecosystems presents a challenge because site history and spatial location on the landscape affect the response to identical system drivers (Kratz et al. 2003) such as climate. As model estimates are scaled up spatially from square meters to stands, landscapes, regions, and biomes, and temporally from days to months to annual estimates, the correlation or coherence of processes such as NPP may decrease. Other factors and processes that are not apparent at smaller spatial or temporal scales may need to be accounted for.

Using a new methodology to sub-sample trees from long-term permanent plots and calculate annual tree bole productivity (NPP_B), the following questions were asked: 1) Within a site, what were the general patterns of annual radial increment growth within and between trees? 2) What is the degree of spatial coherence of annual bole NPP_B between sites across the landscape? and 3) What influence does inter-annual climatic variability have on the inter-annual variability of NPP_B ?

Methods

Study Area

Data was collected in long-term permanent study plots within the H.J. Andrews Experimental Forest, Blue River, OR (Appendix 1.1). The experimental forest covers a 6400 hectare (ha) drainage located in the western Oregon Cascades. Elevation ranges from 410 to 1630 meters (m). The maritime climate consists of cool wet winters and dry hot summers. Average annual precipitation ranges from 230 centimeters (cm) at lower elevations to 355 cm at higher elevations. Annual average daily temperatures range from 0.6° C in January to 17.8° C in July (Bierlmaier and McKee 1989). The lower elevations are dominated by Douglas-fir (*Pseudotsuga menzeisii*), western hemlock (*Tsuga heterophylla*), and western red-cedar (*Thuja plicata*). As elevation increases, Douglas-fir and western hemlock dominance decrease, and they are replaced by noble fir (*Abies procera*), mountain hemlock (*Tsuga mertensiana*), and Pacific silver-fir (*Abies amabilis*).

Average annual precipitation through the study period (1983-2003) was 2205 mm falling mostly within fall, winter, and spring months. Each site sampled is one of three age classes (second-growth, mature, and old-growth) and low, medium, or high elevation (Table 4.1). Ten of the eleven sites are within the *Tsuga heterophylla* forest zone (Franklin and Dyrness 1973), the exception falling within the *Abies amabilis* zone. All sites are part of a long-term permanent study plot network designed to monitor changes in forest composition, structure, and function (Acker et al. 1998). Most sites are characterized as square reference stands ranging from 0.25 to 2.00 ha divided into equal-sized plots. The second-growth sites and one old-growth site are small watershed study areas that contains transects with small sampling plots (0.01

and 0.1 ha, second-growth and old-growth, respectively) spaced at regular intervals. Although these sites were not randomly selected, they represent gradients of age, moisture, and elevation present in this forested landscape.

Data Collection

Trees within each permanent plot were randomly selected for sampling from lists of all tagged trees ≥ 5 cm diameter at breast height (DBH). Sampling consisted of coring a tree at breast height, and recording tag number, species, core number, DBH (cm), bark thickness (cm), core length (cm), and sapwood radius (cm) to the nearest 0.1 cm. In the old-growth sites, trees ≥ 10 cm DBH were cored twice, at approximate right angles (preferentially side-slope and upslope). In the second-growth sites, only 1 core per tree was collected due to small tree sizes. Increment cores were stored in paper straws and taken to the lab for preparation and measurement.

Increment cores were mounted on routed blocks with wood glue and then sanded with a grit of 240 using a belt sander. All cores were then scanned and measured for annual radial increment growth (cm) measured using WinDendroTM image analysis software. For old-growth and mature sites, radial increment growth of each tree used for analysis was the average growth of the two cores taken.

Tree Increment Dating Accuracy

To ensure dating accuracy of tree ring growth for mature and old-growth sites a system was used combining two methods of cross-dating. As increments were measured for individual trees marker years (Yamaguchi et al. 1991) was recorded. All radial tree growth increment series were then loaded in COFECHA (Holmes 1983; Grissino-Mayer 2001) and output statistics were compared to marker year records.

Trees with apparent discrepancies were checked visually and either remeasured or their measurements were altered, discarded, or remained unchanged due to visual inspection not detecting measurement error. This technique was not used for the second-growth watersheds because the length of each radial growth increment series was less than 50 years (Swetnam et al. 1985) and second-growth trees tend to be easily dated due to large growth rates, complacency, and lack of missing rings (Schweingruber 1988).

Calculating Annual Net Primary Productivity (NPP_B)

Increment data from within a site was used to predict annual radial increment growth for non-sampled trees in that site using a simple model based on average annual radial growth increment and tree size (see Chapter 1 for model details). Annual stem diameter was calculated using last remeasurement DBH, combined with measured annual radial growth increment from tree cores (similar to Graumlich et al. 1989). Annual bole biomass production (Mg) for individual trees was calculated using species-specific volume equations, wood/bark volume ratios, and bark and wood density values. Volume equations and density values for the 2 second-growth watersheds were from Acker (2002). Site and species-specific bark and wood volume equations were substituted for the mature and old-growth sites and a similar method was used to calculate bole biomass (for coefficients see Appendices 1.10-1.14). Individual tree biomass production was summed for each year to obtain site-level estimates of annual bole biomass production. Watershed plots were summed to the plot level. Using long-term records of tree remeasurement and mortality, trees that died in the past were accounted for previous to death using the same increment growth

model. Three to six year remeasurement intervals created uncertainty in dates of annual mortality for individual trees. This uncertainty was captured by assigning each tree an equal probability of dying within the years between remeasurements. The year of death was then randomly chosen for each individual and increments were predicted from the beginning of the time series to that date.

The modeling of radial increment growth, date of mortality, calculations of individual tree biomass production, and aggregation to site and plot-level estimates was repeated 10,000 times, and the average of the 10,000 estimates was used as an estimate of annual NPP_B for each plot. Plot area in watersheds was slope corrected and then used to calculate annual NPP_B per hectare for each individual plot, then averaged for the entire watershed.

Statistical Analysis

At the individual site level radial growth patterns of individual trees were visually examined, and simple linear regression was used to examine the relationship between mean radial tree growth over time and the inter-annual variability of that growth. At the landscape level spatial coherence of annual NPP_B was estimated over time between sites and between annual NPP_B and climatic variables using Pearson's product-moment correlation coefficient (r).

Annual site level NPP_B (Mg/ha/yr) was compared with annual precipitation (mm), annual average temperature (C°), monthly precipitation (mm), monthly mean temperature, Palmer Drought Severity index (PDSI; Palmer 1965), and average monthly snow depth from January through April. All temperature and precipitation data was obtained from the Climate and Hydrology Database

(<http://www.fsl.orst.edu/climdb/>). Data was used from the primary meteorological station at the H.J. Andrews Experimental Forest (430 m elevation), with the exception of snow depth which was collected from the central meteorological station (1018 m elevation). PDSI values were obtained from the PDSI grid developed by Cook and colleagues (1999), downloaded from the National Climatic Data Center and National Oceanic and Atmospheric Administration website (<http://www.ncdc.noaa.gov/paleo/pdsidata.html>).

Second-growth watersheds exhibited a trend of increasing NPP_B over time to an asymptote and some mature and old-growth sites displayed a slight increase or decrease of NPP_B over time. Therefore, to solely evaluate inter-annual variability between sites and not long-term trends, a smoothing function was applied to the NPP_B data for all sites using a local mean with a rectangular kernel and a smoothing parameter of five years. This technique resulted in unstandardized residuals of NPP_B for which was used for analysis of coherence between sites.

Results

Average radial increment growth ranged from 0.27 to 0.31, 0.08 to 0.09, and 0.07 to 0.11 cm/yr for second-growth, mature, and old-growth sites, respectively over the study period. The inter-annual variability of radial tree growth (standard deviation of mean radial increment growth) was highest for second-growth sites (0.09-0.12 cm/yr) and was similar for old-growth and mature sites (0.02 to 0.04 cm/yr). Figure 4.1 displays residual radial growth increment (mean of radial growth increment for each year subtracted from the mean radial growth increment of all trees in that year) over time for a single old-growth site. Trees that were growing slower than the overall

mean in a site tended to be much less variable and more coherent through time than trees that were growing faster than the overall mean. Comparisons between slow growing trees generally yielded r values of greater than 0.5, as compared to fast growing trees that exhibited a large range of correlations, r values from -0.60 to as high as 0.90. These patterns were consistent across all sites.

The pattern observed between annual radial growth increment within and among trees and the variability of that growth through time indicates increased variability with increased rate of growth. Linear regressions (Figure 4.2) of three sites (second-growth, mature, and old-growth) showed a significant ($p < 0.001$) positive relationship between mean radial growth increment and the standard deviation of mean radial growth increment for individual trees in all three age classes. This relationship became stronger as age class increased as indicated by increased r^2 values ($r^2 = 0.441, 0.481, 0.586$ young, mature, and old-growth, respectively).

Values of annual NPP_B (Mg/ha/yr) for all sites are reported in Table 4.1. Across all sites the highest mean annual NPP_B was for a mature site (6.052 Mg/ha/yr), and a second-growth site had the highest inter-annual variability of NPP_B (1.572 Mg/h/yr) due to the increase in live biomass from stand initiation (Table 4.1; Figures 4.3 and 4.4). The greatest inter-annual variability of NPP_B between all other sites was exhibited by an old-growth site (0.780 Mg/ha/yr). Old-growth sites exhibited the largest range of NPP_B within an age class (3.948 to 5.845 Mg/ha/yr). Mean annual NPP_B of all sites over the study period was 4.88 Mg/ha/yr, with inter-annual variability of 0.39 Mg/ha/yr. The resulting coefficient of variation for NPP_B is only

8% compared to the coefficient of variation for individual sites ranging from 11-33% (Table 4.1).

A similar relationship to that of individual trees was found between sites across the landscape (Figure 4.4). As annual NPP_B increased, the inter-annual variability in NPP_B became larger ($p=0.019$). This relationship was not as robust as that of individual trees within old-growth sites (based on r^2 values), but was stronger than trees within mature and second-growth sites.

Analysis of coherence of residual NPP_B between sites resulted in a wide range of correlations ($r= -0.18$ to 0.92) and 12 of the 55 comparisons between sites were not significant ($p>0.05$) indicating no correlation between these sites. All but one of the comparisons between sites was positive. The negative correlation ($r= -0.18$), between an old-growth and second-growth site, was not significant ($p=0.7663$) and thus the correlation was essentially zero. Contrasting second-growth and old-growth sites comprised the greatest degree of variability in coherence, with r values ranging from -0.18 to 0.64 . The range of coherence between sites of similar ages was markedly different. Old-growth sites had the largest range in coherence ($r=0.57$ to 0.85) of any within age class comparison. Xeric and mesic site comparisons fell at the lower end of this range ($r=0.57$) and sites with similar site moisture characteristics had higher correlations ($r=0.60$ to 0.80). Comparisons of sites at extremes of the elevation gradient (high and low) also had lower degrees of coherence than sites similar in elevation ($r=0.85$). The highest degree of coherence between sites were for the two second-growth sites ($r= 0.92$ $p=0.0013$). This was the only comparison of second-growth sites in this analysis; although the high degree of correlation and its

significance suggests that other second-growth sites across the landscape were likely to be highly coherent as well. Furthermore, these sites are of contrasting elevations.

Annual bole productivity appears to exhibit complex temporal patterns across the landscape in which some years NPP_B is in synchrony across the landscape, while in other years there was a complete lack of coherence, lags between sites, or complete lack of coherence between some sites. For example, in 1990 all sites (Figure 4.5) show a significant increase in NPP_B , and in other years some sites were synchronous while others were not.

Relationships between annual NPP_B and climate varied between sites. NPP_B of individual sites was correlated with either temperature or precipitation variables, but not both. A number of sites responded positively to early season precipitation (June precipitation $r= 0.44$ to 0.47), others responded positively to late growing season precipitation (October precipitation $r= 0.39$ - to 0.59) and others to mean temperature (September and August mean temperature $r= 0.42$ to 0.63). Dry sites also responded positively to PDSI ($r= 0.47$), indicating drought as an important factor affecting NPP_B of drier sites. High elevation sites were negatively correlated with early spring snow depth (March and April snow depth $r= -0.82$ and -0.65 , respectively) presumably due to a prolonged growing season with decreased snow depth in late spring. Regardless of age, sites exhibiting the highest spatial coherence ($r > 0.50$) were either responding to similar climatic parameters such as PDSI, monthly and annual precipitation, or were in close proximity on the landscape. The exception being the two second-growth sites that were not in close spatial proximity, but exhibited a high degree of coherence.

Discussion

We sub-sampled trees for radial increment growth and modeled radial increment growth for non-sampled trees and trees that died previously using long-term permanent plots and mortality records to estimate annual NPP_B . Our estimates of annual NPP_B are comparable to those found in other studies of productivity in the area (Campbell et al. 2004, Acker 2002, Gholz 1982) and forests in the Pacific Northwest (Graumlich et al. 1989). However, our estimates for old-growth are higher than reported by Grier and Logan (1977) and estimates of NPP_B for all age classes are lower than reported by Van Tuyl and others (2005). Old-growth sites did have the largest range of NPP_B between sites of the three age classes.

Inspection of inter-annual variability and spatial coherence of tree growth within sites and NPP_B among sites across the landscape resulted in the emergence of similar behaviors across spatial scales. Individual radial tree growth within a site and the coherence between those trees will determine whether annual variation of NPP_B of the site is amplified or modulated. This behavior has direct effects on the inter-annual variability of site level NPP_B because amplification of the annual response of NPP_B of individual trees will increase inter-annual variability at the site level, while modulation caused by a lack of coherence of individual trees will decrease this variability. Slowly growing trees were highly coherent, but as mean growth rates increased this coherence broke down and variability of growth increased. This pattern should result in modulation of NPP_B and decreased inter-annual variability within each site. Although the level of modulation would depend on the ratio of slow growing to fast growing trees. A similar relationship was found with increased variability of site level NPP_B as

the mean rate of NPP_B increased across sites (Figure 4.4). This correlation has implications for future response to climate. If NPP_B is steadily increasing in response to climate change (Graumlich et al. 1989, Lamarche 1984) then the variability of NPP_B is also likely to increase. However, from some patterns observed in this study it is possible that increased variability and amplification of annual NPP_B may lead to increased coherence between sites across the landscape.

A large range exists in the degree of coherence between places across the landscape. This finding conflicts with the high coherence of NPP ($r= 0.46-0.83$) found by Graumlich and colleagues (1989) of forests in the Cascades of Washington. Our study had a larger number of sites for comparison as compared to Graumlich et al. (1989), but these comparisons were made over a much shorter time period. It is possible that if the study period was extended to similar time periods of one to two hundred years coherence may increase, but it is likely a wide spectrum of coherence across sites will still persist. The inclusion of mortality in our estimates of NPP_B is more reasonable for most forests across the landscape and likely decreases the level of coherence between sites as temporal variability of annual mortality patterns are likely to be site specific (Franklin et al. 1987). The sites used for this analysis also better represented extremes of age, elevation, and site moisture than the study by Graumlich and others (1989). However, this analysis would benefit from having more comparisons of second-growth sites to determine if the high degree of correlation found in this analysis is consistent across the landscape. In particular because second-growth forests are a predominant part of the present landscape, and will continue to be in the near future.

Climate variability seems to be in part driving inter-annual variability of NPP_B , particularly between sites that were highly coherent. The positive relationship of some sites with mean temperature and precipitation later in the growing season was somewhat surprising, although Graumlich et al. (1989) found summer temperature as a significant factor in annual NPP and annual precipitation less so. Furthermore, correlations of some sites with early growing season precipitation indicate that timing of precipitation is important, but the timing and what climatic feature is important varies from place to place. The relationship between snow pack and NPP_B at higher elevations is also evidence of the importance of the timing of climatic factors.

The amplified response and high degree of spatial coherence of all sites in individual years may also be driven by climatic forces. One year in particular (1990) had one of the wetter and warmer spring months (April) of the study period. This may have increased early season growth of lower elevations sites and induced a longer growing season for higher elevations sites through early snow melt. This indicates that when speculations about future climate change scenarios are made, the focus should be less on the average changes in climate (e.g., precipitation) and focus more on changes in the variability and timing of increased annual precipitation and other factors such as increased temperature.

The lack of coherence between sites in some years and coherence in others results in complex behaviors over time. Places that are generally out of synchrony may become more synchronous when certain factors such as climate influence the landscape as a whole. These patterns of spatial coherence between sites have implications for landscape level annual NPP_B . Over time landscape level NPP_B was

modulated in most years due to lack of coherence among sites, but in some years response between sites was spatially coherent and caused larger fluctuations in average NPP_B of the landscape (Figure 4.6). Overall landscape inter-annual variability of NPP_B was dampened compared to site level variability by the lack of coherence between sites throughout the study period.

The high degree of coherence between second-growth sites combined with the variability of coherence that older forests display indicates that heterogeneity of the landscape with respect to forest age class may be important in modulating future response to disturbance and climate change. Overall ecosystem carbon balance across the landscape will in part reflect the coherence of NPP_B and thus the heterogeneity or lack thereof across the landscape. As there are other factors that affect ecosystem carbon balance such as heterotrophic respiration.

A deeper understanding of the specific mechanisms that control coherence of NPP_B rather than the broader generalizations raised by this study, would benefit the modeling of NPP_B immensely. It is imperative to have field measurements to help evaluate the performance of process models (Jenkins et al. 2001) and improve predictions of ecosystem processes such as NPP_B . This study was an attempt to begin to attain those measurements in the Pacific Northwest to compare with models of forest productivity for the region. Incorporation of spatial coherence would improve our ability to scale productivity both spatially and temporally. Future studies would benefit from measuring differences of site characteristics such as spatial proximity, annual rate of mortality, and species composition and using these to determine what characteristics most influence coherence (Baines et al. 2000). Since sites were not

randomly selected it would also be beneficial to test coherence estimates using a randomization test for the null hypothesis that $r=1.0$.

Conclusions

As the rate of growth for individual trees and site NPP_B increased, these rates exhibit increased inter-annual variability over time. Coherence between slower growing trees was higher than that of faster growing trees and was much less variable. This pattern has implications for the modulation of site level NPP_B . Spatial coherence of annual NPP_B between sites was much more variable than expected, which resulted in complex behaviors over time. This resulted in a modulation of inter-annual variability of NPP_B at the landscape scale. Climate does play a role in the variability of productivity and spatial coherence between sites, as indicated by correlation with climate combined with the high coherence of NPP_B between some sites. However, local intrinsic factors (i.e., stand dynamics) and spatial proximity were also important factors indicated by the lack of coherence over the study period between some sites. Our results suggest that heterogeneity of the landscape with respect to age class can possibly modulate effects of future climate change possibilities. Spatial coherence of NPP_B across the landscape was much lower than is assumed by current biogeochemical models. The year to year variability of productivity at the landscape scale is more modulated than these models predict. As rates of productivity are predicted and responses of ecosystem processes are forecasted, accounting for changes in coherence as we scale spatially and temporally should result in more realistic and accurate representations of future NPP_B .

Literature Cited

- Acker, S. A., Halpern, C.B., Harmon, M.E., and Dyrness, C.T. 2002. Trends in Biomass accumulation, net primary production, and tree mortality in *Psuedotsuga menziesii* forest of contrasting age. *Tree Physiology* **22**:213-217.
- Acker, S. A., W. A. McKee, M. E. Harmon, and J. F. Franklin. 1998. Long-term research on forest dynamics in the Pacific Northwest: a network of permanent forest plots. *in* F. Dallmeier and J. A. Comiskey, editors. *Forest biodiversity in North, Central, and South America and the Caribbean: Research and Monitoring*. The Parthenon Publishing Group, Washington, DC.
- Baines, S. B., K. E. Webster, T. K. Kratz, S. R. Carpenter, and J. J. Magnuson. 2000. Synchronous behavior of temperature, calcium, and chlorophyll in lakes of northern Wisconsin. *Ecology* **81**:815-825.
- Baron, J. S., and N. Caine. 2000. Temporal coherence of two alpine lake basins of the Colorado Front Range, U.S.A. *Freshwater Biology* **43**:463-476.
- Bierlmaier, F. A., and A. McKee. 1989. Climatic Summaries and Documentation for the Primary Meteorological Station, H.J. Andrews Experimental Forest, 1972 to 1984. Gen. Tech. Rep. PNW-GTR-242. General Technical Report PNW-GTR-242, Department of Agriculture, Forest Service, Pacific Northwest Research Station, Portland, OR.
- Brubaker, L. B. 1980. Spatial patterns of tree growth anomalies in the pacific northwest. *Ecology* **61**:798-807.
- Campbell, J., O. Sun, and B. E. Law. 2004. Disturbance and net ecosystem production across three climatically distinct forest landscapes. *Global Biogeochemical Cycles* **18**:1-11.
- Cook, E. R., et al. 2004. North American Summer PDSI Reconstructions. *in* I. P. W. D. C. f. Paleoclimatology, editor. *Data Contribution Series # 2004-045*, NOAA/NGDC Paleoclimatology Program, Boulder CO, USA.
- Cook, E. R., and L. A. Kairiukstis. 1990. *Methods of Dendroecology. Applications in the Environmental Sciences*. Kluwer Academic Publishers, Dordrecht, Netherlands.
- Franklin, J. F., H. H. Shugart, and M. E. Harmon. 1987. Tree Death as an Ecological Process. *BioScience* **37**:550-556.
- Franklin, J. F., and C. T. Dyrness. 1973. *Natural vegetation of Oregon and Washington*. USDA Forest Service General Technical Report PNW 8. Pacific Northwest Forest and Range Experiment Station.

- Fritts, H. C. 1976. Tree rings and climate. Academic Press, London, England.
- Fritts, H. C., and T. W. Swetnam. 1989. Dendroecology: a Tool for Evaluating Variations in Past and Present Forest Environments. *Advances in Ecological Research* **19**:111-188.
- Gholz, H. L. 1982. Environmental limits on aboveground net primary production, leaf area and biomass production in vegetation zones of the pacific northwest. *Ecology* **63**:469-481.
- Grier, C. C., and Logan, R.S. 1977. Old-growth *Pseudotsuga menziesii* communities of a western Oregon watershed: Biomass distribution and production budgets. *Ecological Monographs* **47**:373-400.
- Grissino-Mayer, H. D. 2001. Evaluating Crossdating accuracy: A manual and tutorial for the computer program COFECHA. *Tree-Ring Research* **57**:205-221.
- Holmes, R. L. 1983. Computer-assisted quality control in tree-ring dating and measurement. *Tree Ring Bulletin* **43**:69-78.
- Jenkins, J. C., R. A. Birdsey, and Y. Pan. 2001. Biomass and NPP estimation for the mid-atlantic region (USA) using plot-level forest inventory data. *Ecological Applications* **11**:1174-1193.
- Kratz, T. K., Deegan, L.A., Harmon, M.E., Lauenroth, W.K. 2003. Ecological Variability in space and time: Insights gained from the US LTER program. *BioScience* **53**:57-67.
- Lamarche, V. C. 1984. Increasing Atmospheric Carbon Dioxide: Tree Ring Evidence for Growth Enhancement in Natural vegetation. *Science* **225**:1019-1021.
- Magnuson, J. J., B. J. Benson, and T. K. Kratz. 1990. Temporal coherence in the limnology of a suite of lakes in Wisconsin, USA. *Freshwater Biology* **23**:145-159.
- Palmer, W. C. 1965. Meteorological Drought. U.S. Department of Commerce, Washington, D.C.
- Piutti, E., and A. Cescatti. 1997. A quantitative analysis of the interactions between climate response and intraspecific competition in European beech. *Canadian Journal of Forest Research* **27**:277-284.
- Running, S. W. 1994. Testing Forest-BGC ecosystem process simulations across a climatic gradient in Oregon. *Ecological Applications* **4**:238-247.

- Running, S. W., and J. C. Coughlan. 1988. FOREST BGC, A general model of forest ecosystem processes for regional applications I. Hydrologic balance canopy gas exchange and primary production. *Ecological Modeling* **42**:125-154.
- Running, S. W., and E. R. J. Hunt. 1993. Generalisation of a forest ecosystem process model for other biomes, BIOME-BGC, and an application for global scale models. Academic Press, San Diego.
- Schweingruber, F. H. 1988. *Tree Rings: Basics and Application of Dendrochronology*. D. Reidel Pub. Company, Dordrecht, Holland.
- Soranno, P. A., K. E. Webster, J. L. Riera, T. K. Kratz, J. S. Baron, P. A. Bukaveckas, G. W. Kling, D. S. White, N. Caine, R. C. Lathrop, and P. R. Leavitt. 1999. Spatial Variation among Lakes within Landscapes: Ecological Organization along Lake Chains. *Ecosystems* **2**:395-410.
- Swetnam, T. W., M. A. Thompson, and E. K. Sutherland. 1985. Using dendrochronology to measure radial growth of defoliated trees. USDA Forest Service Cooperative State Research Service.
- Turner, D. P. 2005. Personal Communication. *in*.
- Turner, D. P., M. Guxy, M. A. Lefsky, S. Van Tuyl, O. Sun, C. Daly, and B. E. Law. 2003. Effects of land use and fine scale environmental heterogeneity on net ecosystem production over a temperate coniferous forest landscape. *Tellus* **55**:657-668.
- Van Tuyl, S., Law, B.E., Turner, D.P., Gitelman, A.I. 2005. Variability in net primary production and carbon storage in biomass across Oregon forests-an assessment integrating data from forest inventories, intensive sites, and remote sensing. *Forest Ecology and Management* **209**:273-291.
- White, M. A., P. E. Thornton, S. W. Running, and R. R. Nemani. 2000. Parameterization and sensitivity analysis of the BIOME _BGC terrestrial ecosystem model: Net Primary Production controls. *Earth Interactions* **4**:1-85.
- Yamaguchi, D. K. 1991. A simple method for cross-dating increment cores from living trees. *Canadian Journal of Forest Research* **21**:414-416.

Tables

Table 4.1 Values of NPP_B for 11 sites sampled in the western Cascades, H.J. Andrews Experimental Forest, Oregon. CV% is the coefficient of variation. Inter-annual variability is the standard deviation of mean annual NPP_B.

Site	Age Class (yrs.)	Elevation (m)	Dominant Tree Species	Mean Annual NPP _B (Mg/ha/yr)	Inter-annual Variability	CV%
RS01	Old-growth (460)	510	<i>Pseudotsuga menseizii</i> / <i>Acer macrophyllum</i>	3.948	0.721	18.3
RS07	Old-growth (460)	520	<i>Pseudotsuga menseizii</i> / <i>Tsuga heterophylla</i>	3.628	0.413	11.4
RS12	Old-growth (460)	950	<i>Pseudotsuga menseizii</i> / <i>Tsuga heterophylla</i>	3.858	0.426	11.1
RS22	Old-growth (450)	1440	<i>Abies procera</i> / <i>Pseudotsuga menseizii</i>	5.105	0.604	11.8
RS26	Mature (150)	920	<i>Pseudotsuga menseizii</i> / <i>Tsuga heterophylla</i>	6.052	0.749	12.4
RS32	Mature (145)	460	<i>Pseudotsuga menseizii</i> / <i>Tsuga heterophylla</i>	5.015	0.697	13.9
RS33	Mature (145)	500	<i>Tsuga heterophylla</i> / <i>Thuja plicata</i>	4.062	0.660	16.2
RS34	Old-growth (450)	610	<i>Thuja plicata</i> / <i>Pseudotsuga menseizii</i>	5.598	0.710	12.7
WS01	Second-growth (40)	480-965	<i>Pseudotsuga menseizii</i>	4.690	1.572	33.5
WS02	Old-growth (460)	475-1070	<i>Pseudotsuga menseizii</i> / <i>Tsuga heterophylla</i>	5.845	0.780	13.3
WS06	Second-growth (25)	900-1020	<i>Pseudotsuga menseizii</i>	4.837	0.643	13.3

Figures

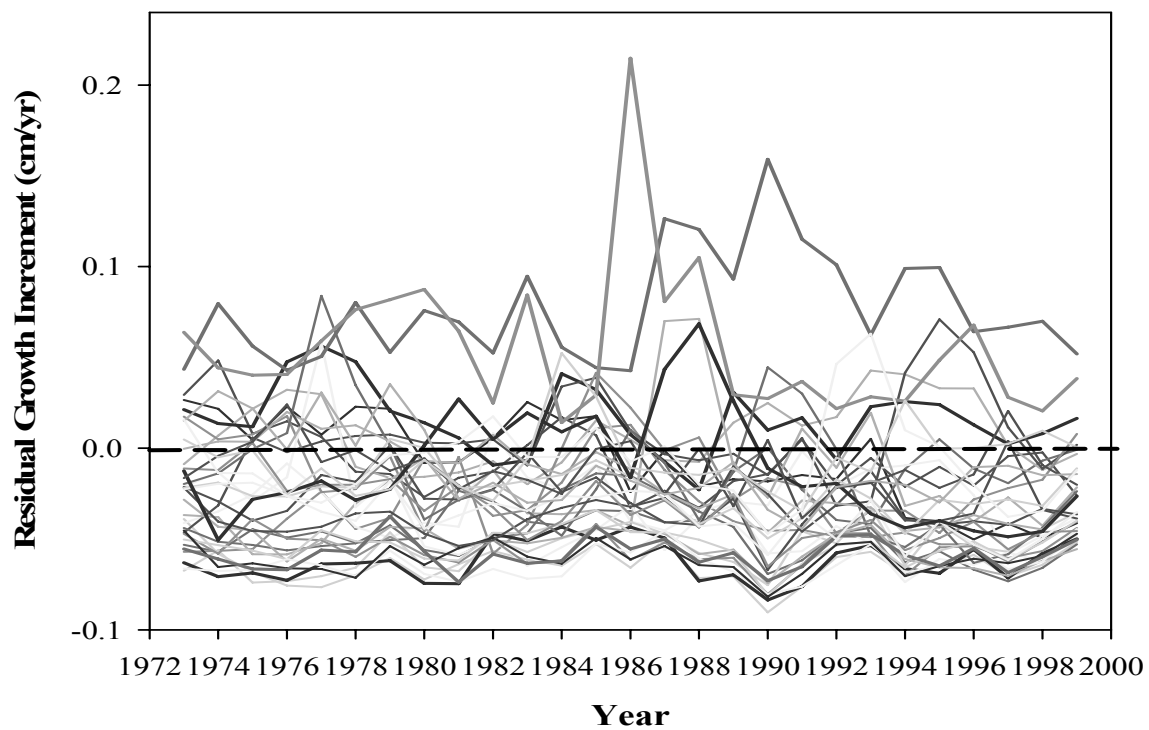


Figure 4.1 Residual annual radial growth increments (annual growth increment – average annual growth increment) for 56 trees in an old-growth site. Dashed line (0.0) indicates the mean growth rate of all trees over time. As growth rate increases coherence decreases and inter-annual variability increases.

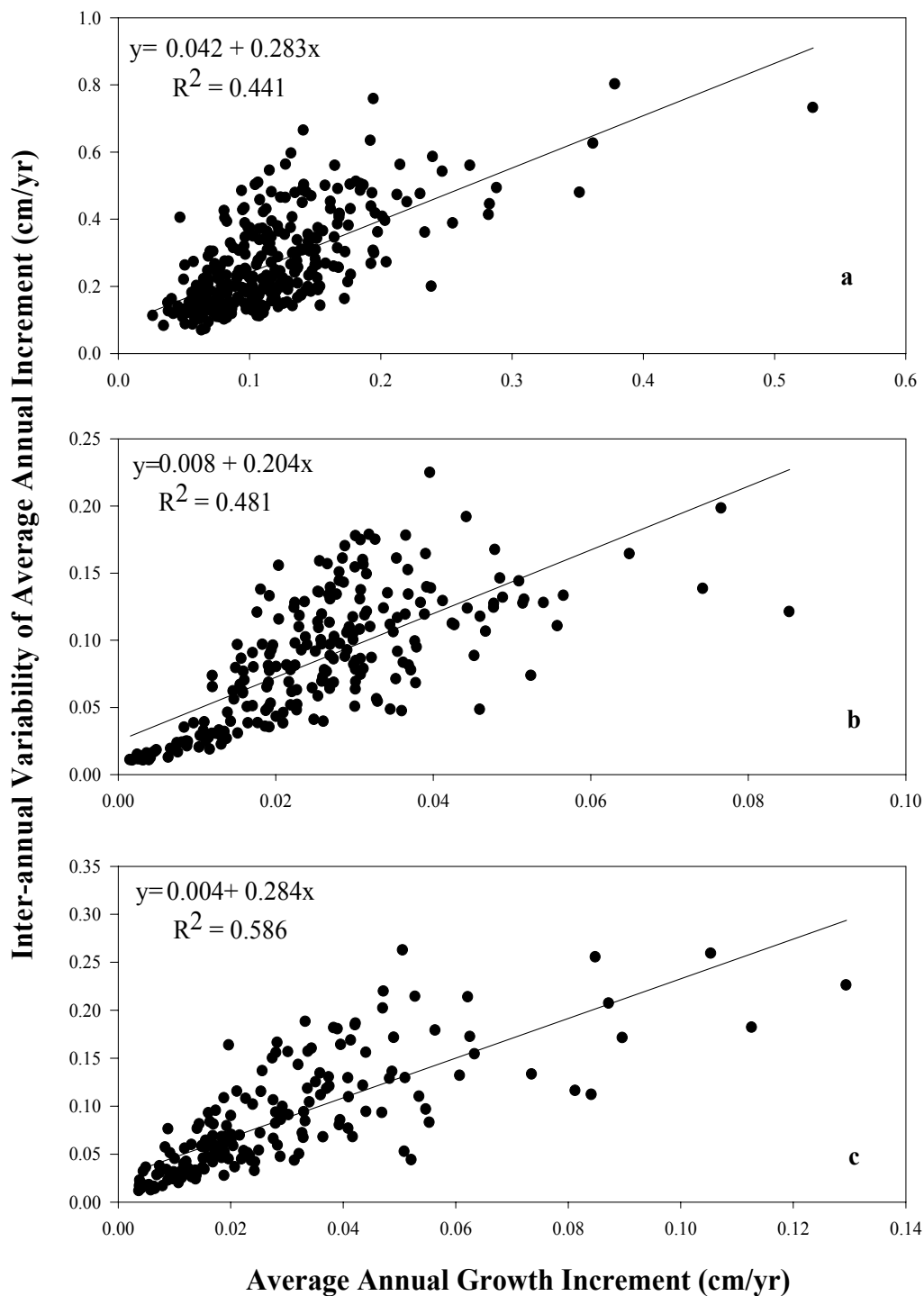


Figure 4.2 Linear regressions illustrating the relationship of increasing inter-annual variability of annual growth increment as mean growth rate increases. Each panel is a simple linear regression of trees from one site (**a**=second-growth, **b**=mature, and **c**=old-growth).

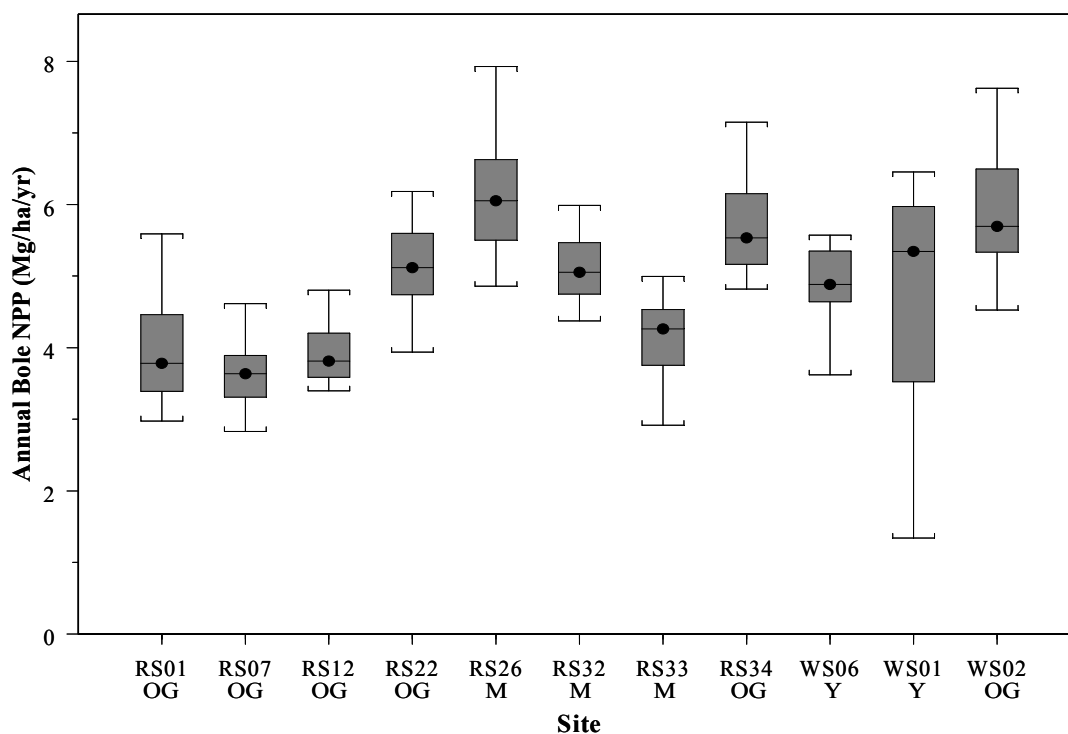


Figure 4.3 Box plots of annual NPP_B (Mg/ha/yr) vs. site and age class for 11 sites sampled in the western Oregon Cascades, H.J. Andrews Experimental Forest, Oregon. Boxes represent the 50th quantile with the black line and dot representing the median NPP_B. Whiskers represent the 25th and 75th quantile. Y=young, M=mature, and OG=old-growth.

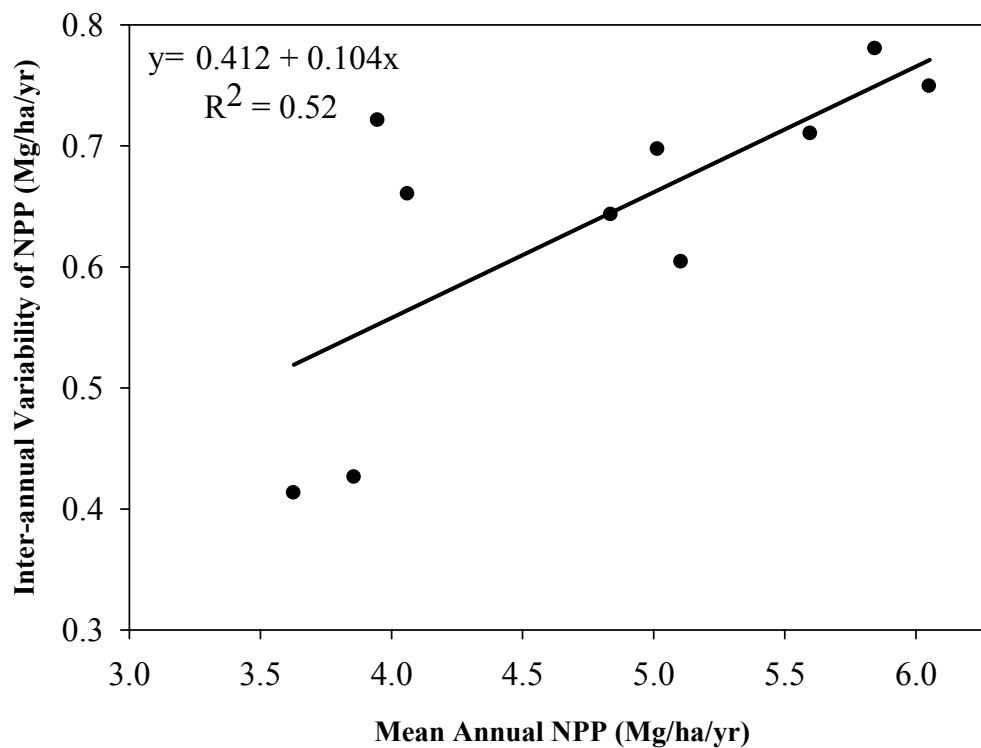


Figure 4.4 Linear regression illustrating the relationship of increasing inter-annual variability of annual NPP_B (Mg/ha/yr) as mean annual NPP_B (Mg/ha/yr) increases across sites on the landscape. Inter-annual variability calculated as the SD of mean annual NPP_B .

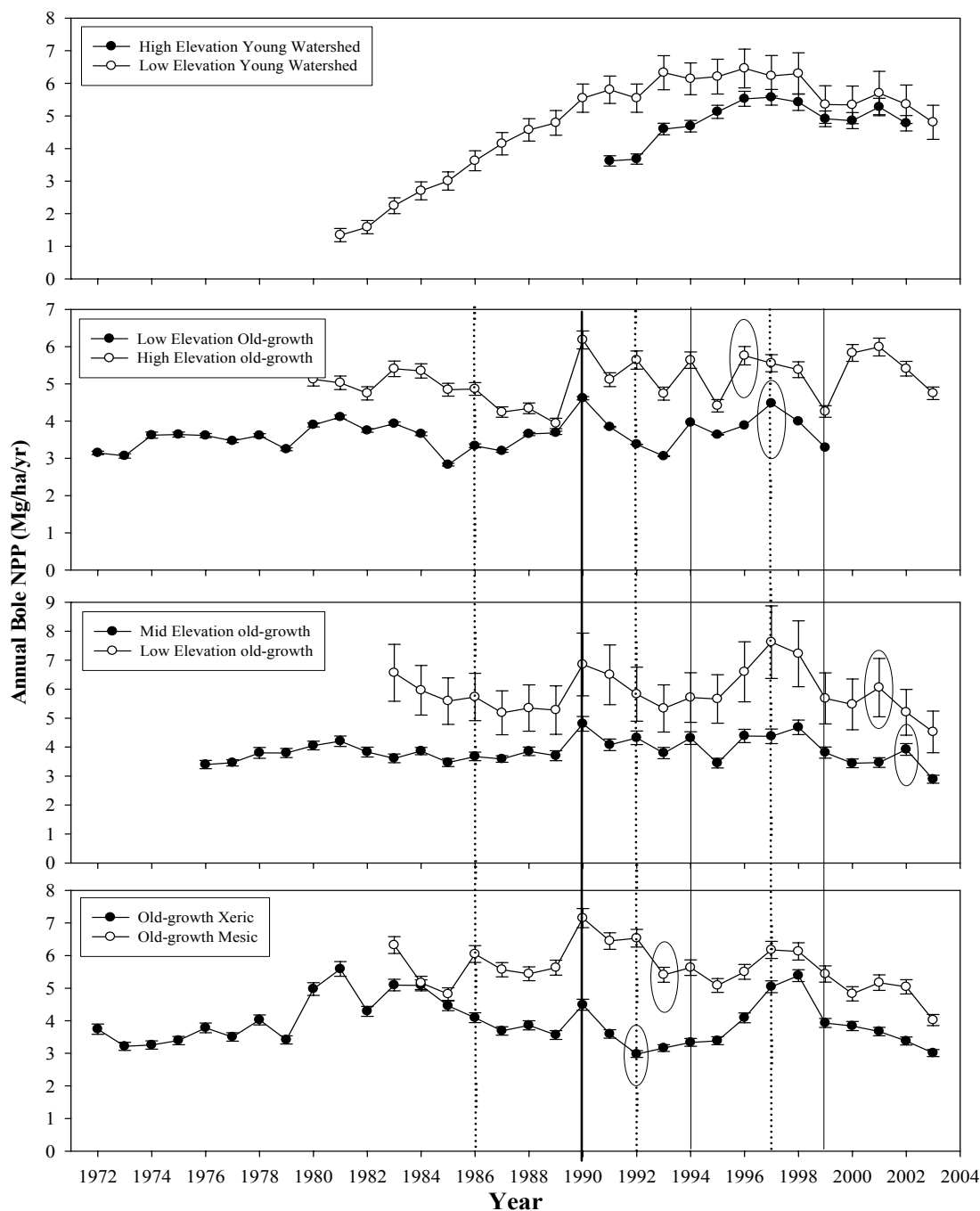


Figure 4.5 Annual NPP_B (Mg/ha/yr) over time for all sites. Panels represent comparisons within age classes. Error bars are the SD of 10,000 Monte Carlo simulations. Vertical solid line indicates high degree of coherence in that year for all sites. When residuals of the second-growth site are calculated and graphically displayed these large peaks were also present. Dotted lines indicate decreased coherence across all sites in that year. Circles indicate possible lags in response of NPP_B between sites in that comparison.

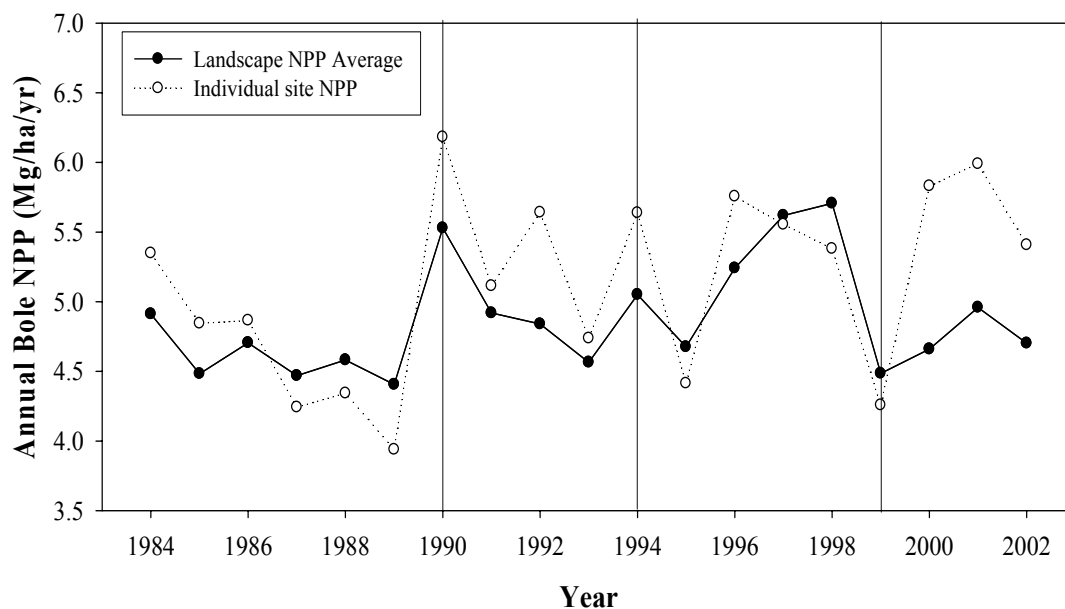


Figure 4.6 Average annual NPP_B across all sites. Solid vertical lines indicate amplification of landscape response due to increased coherence between sites in those years. Peak NPP_B in 1998 is from successive increase of NPP_B across most sites in 1996, 1997, and 1998. In remaining years, landscape NPP_B was modulated.

CHAPTER 5: General Conclusions

Sub-sampling radial growth increment using stratification by tree size and application of a simple random model (Chapter 2) is a valid approach to estimating annual bole biomass increment. Using Monte Carlo uncertainty analysis we determined the error of estimates associated with predicting radial growth increment of non-sampled trees at varying sample sizes. We have shown using this approach that more trees may need to be sampled than previously sampled in other studies. Improvements on the model structure and complexity may allow increased accuracy and precision, as well as smaller sample sizes. This methodology was also sufficient in replicating the patterns of inter-annual variability of live bole biomass increment, a major component of the inter-annual variability of NPP_B .

A multivariate analysis of two small adjacent watersheds of contrasting ages (Chapter 3) displayed similar responses of NPP_B within and between watersheds to environmental variables. Even at the small spatial scale of a watershed, tree NPP_B was not as spatially coherent as would be assumed based solely on physiological and climatic relationships. Comparing NPP_B within the two watersheds indicated that response of NPP_B to differing climatic drivers and differing responses to climatic variability over time, i.e., low spatial coherence. Lack of coherence in some years indicates that climate may be less of an influence on productivity in some years, and/or other stand-level dynamics and environmental factors may be more important within and between watersheds. As spatial scale increases, spatial coherence may be decreasing. Time since disturbance (age class) may also be contributing to decreased spatial coherence of NPP_B .

An unexpected conclusion was that the degree of spatial coherence was not consistent and changed through time. Therefore, the coherence of sites over time is not a simple and strict relationship, instead exhibiting complex behaviors that have implications for scaling estimates of productivity. This pattern has implications for the temporal scale at which coherence is examined, i.e., time step dependency, as well as the measures used to quantify spatial coherence. As these same questions are answered at larger spatial scales (landscape, region, biome) we predict that a decrease of spatial coherence between biological variables such as NPP_B will be seen, although abiotic factors may still be highly correlated.

A comparison of 11 sites indicated that inter-annual variation and spatial coherence of NPP_B between sites across the landscape was much more variable than expected (Chapter 4). This results in complex behavior between sites over time. Local intrinsic factors (i.e., stand dynamics) and spatial proximity were important factors indicated by the lack of coherence over the study period between some sites. Heterogeneity in age classes across of the landscape may be important to modulate affects of future climate change possibilities. Spatial coherence of NPP_B across the landscape was much lower than would be predicted by current models that include only physiological and climatic linkages. As mean growth rates of individual trees and mean site productivity increases, the variability of those rates also increases. As rates of productivity are predicted in the future and response of ecosystem processes is forecasted, taking into account changes in coherence as we scale spatially and temporally may result in more realistic and accurate representations of future NPP_B .

Bibliography

- Acker, S. A., Halpern, C.B., Harmon, M.E., and Dyrness, C.T. (2002). Trends in Biomass accumulation, net primary production, and tree mortality in *Psuedotsuga menziesii* forest of contrasting age. *Tree Physiology* **22**: 213-217.
- Acker, S. A., W. A. McKee, et al. (1998). Long-term research on forest dynamics in the Pacific Northwest: a network of permanent forest plots. *Forest biodiversity in North, Central, and South America and the Caribbean: Research and Monitoring*, Washington, DC, The Parthenon Publishing Group.
- Baines, S. B., K. E. Webster, T. K. Kratz, S. R. Carpenter, and J. J. Magnuson. 2000. Synchronous behavior of temperature, calcium, and chlorophyll in lakes of northern Wisconsin. *Ecology* **81**:815-825.
- Baron, J. S., and N. Caine. 2000. Temporal coherence of two alpine lake basins of the Colorado Front Range, U.S.A. *Freshwater Biology* **43**:463-476.
- Bierlmaier, F. A., and McKee, A. (1989). Climatic Summaries and Documentation for the Primary Meteorological Station, H.J. Andrews Experimental Forest, 1972 to 1984. Gen. Tech. Rep. PNW-GTR-242. Portland, OR, Department of Agriculture, Forest Service, Pacific Northwest Research Station: 56 p.
- Bond-Lamberty, B., C. Wang, et al. (2004). Net primary production of a black spruce wildfire chronosequence. *Global Change Biology* **10**: 473-487.
- Brubaker, L. B. 1980. Spatial patterns of tree growth anomalies in the Pacific Northwest. *Ecology* **61**:798-807.
- Campbell, J., O. Sun, and B. E. Law. 2004. Disturbance and net ecosystem production across three climatically distinct forest landscapes. *Global Biogeochemical Cycles* **18**:1-11.
- Chernick, M. R. (1999). *Bootstrap Methods: A Practitioner's Guide*. New York, John Wiley & Sons, Inc.
- Clark, D. A., S. Brown, D. W. Kicklighter, J. Q. Chambers, J. R. Thomlinson, and J. Ni. 2001. Measuring Net Primary Production in Forests. *Ecological Applications* **11**:356-370.
- Cook, E. R., and L. A. Kairiukstis. 1990. *Methods of Dendroecology. Applications in the Environmental Sciences*. Kluwer Academic Publishers, Dordrecht, Netherlands.

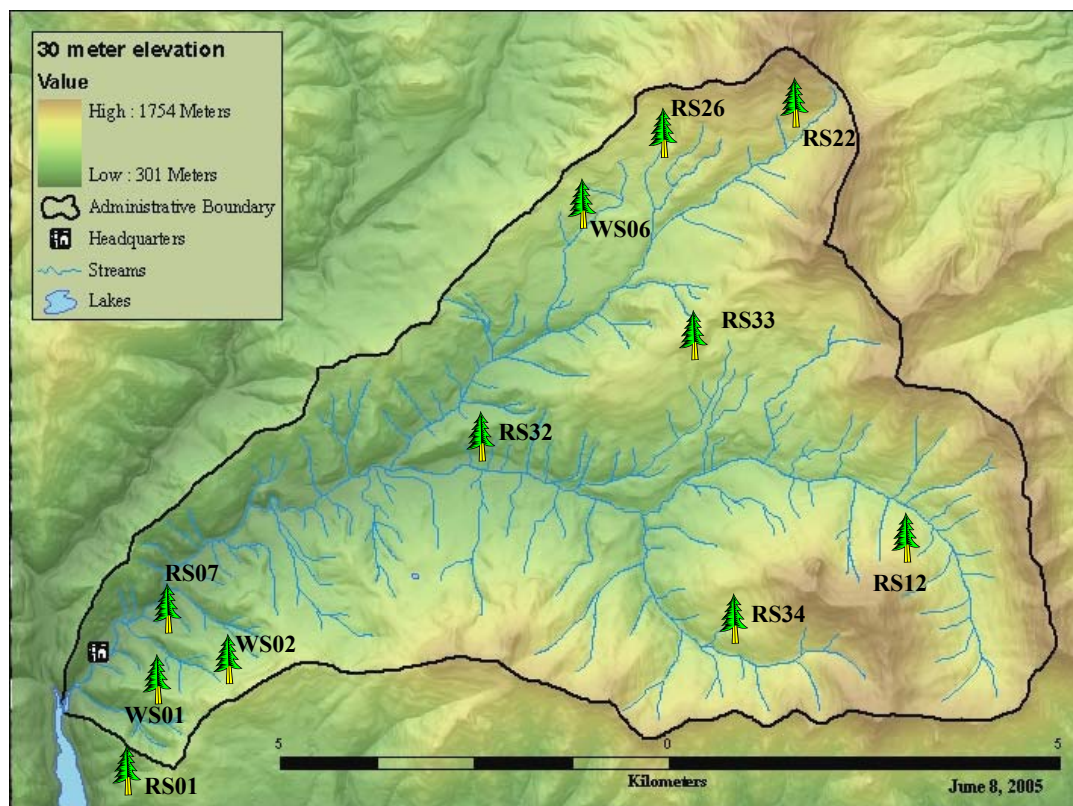
- Cook, E. R., D. M. Meko, D. W. Stahle, and M. K. Cleaveland. 1999. Drought reconstructions for the continental United States. *Journal of Climate* **12**:1145-1162.
- Cook, E. R., et al. 2004. North American Summer PDSI Reconstructions. *in* I. P. W. D. C. f. Paleoclimatology, editor. Data Contribution Series # 2004-045, NOAA/NGDC Paleoclimatology Program, Boulder CO, USA.
- Dixon, R. K., Brown S., Houghton, R.A., Solomon, A.M., Trexler, M.C., and Wisniewski, J. 1994. Carbon Pools and Flux of Global Forest ecosystems. *Science* **263**:185-190.
- Dyrness, C. T. 1973. Early stages of plant succession following logging and burning in the western Cascades of Oregon. *Ecology* **54**:57-69.
- Franklin, J. F. and C. T. Dyrness (1973). Natural vegetation of Oregon and Washington, USDA Forest Service General Technical Report PNW 8. Pacific Northwest Forest and Range Experiment Station.
- Franklin, J. F., H. H. Shugart, and M. E. Harmon. 1987. Tree Death as an Ecological Process. *BioScience* **37**:550-556.
- Fraser, V. D. (2001). Biomass and productivity in an old-growth Douglas-fir/western hemlock stand in the western Cascades of Oregon. Project in Ecology.
- Fritts, H. C. 1976. Tree rings and climate. Academic Press, London, England.
- Fritts, H. C., and T. W. Swetnam. 1989. Dendroecology: a Tool for Evaluating Variations in Past and Present Forest Environments. *Advances in Ecological Research* **19**:111-188.
- Gholz, H. L. 1982. Environmental limits on aboveground net primary production, leaf area and biomass production in vegetation zones of the pacific northwest. *Ecology* **63**:469-481.
- Goulden, M. L., J. W. Munger, et al. (1996). Exchange of Carbon Dioxide by a deciduous forest: Response to interannual climate variability. *Science* **271**: 1576-1578.
- Graumlich, L. J., L. B. Brubaker, and C. C. Grier. 1989. Long-term trends in forest Net primary productivity: Cascade Mountains, Washington. *Ecology* **70**:405-410.
- Grier, C. C., and Logan, R.S. (1977). Old-growth *Pseudotsuga menziesii* communities of a western Oregon watershed: Biomass distribution and production budgets. *Ecological Monographs* **47**: 373-400.

- Grissino-Mayer, H. D. 2001. Evaluating Crossdating accuracy: A manual and tutorial for the computer program COFECHA. *Tree-Ring Research* **57**:205-221.
- Harmon, M. E., Bible K., Ryan, M.G., Shaw, D.C., Chen, H., Klopatek, J., and Xia, L. (2004). Production, respiration, and overall Carbon Balance in an old-growth *Pseudotsuga-Tsuga* Forest Ecosystem. *Ecosystems* **7**: 498-512.
- Holmes, R. L. 1983. Computer-assisted quality control in tree-ring dating and measurement. *Tree Ring Bulletin* **43**:69-78.
- Huxman, T. E., M. D. Smith, P. A. Fay, A. K. Knapp, R. M. Shaw, M. E. Lolk, S. D. Smith, D. T. Tissue, J. C. Zak, J. F. Weltzin, W. T. Pockman, O. E. Sala, B. M. Haddad, J. Harte, G. W. Koch, S. Schwinning, E. E. Small, and D. G. Williams. 2004. Convergence across biomes to a common rain use efficiency. *Nature* **429**:651-654.
- Janisch, J. E. a. H., M.E. (2002). Successional changes in live and dead wood carbon stores: implications for net ecosystem productivity. *Tree Physiology* **22**: 77-89.
- Jenkins, J. C., R. A. Birdsey, et al. (2001). Biomass and NPP estimation for the mid-atlantic region (USA) using plot-level forest inventory data. *Ecological Applications* **11**(4): 1174-1193.
- Knapp, K. A., and Smith, M.D. 2001. Variation among biomes in temporal dynamics of aboveground primary production. *Science* **291**:481-484.
- Kratz, T. K., Deegan, L.A., Harmon, M.E., Lauenroth, W.K. 2003. Ecological Variability in space and time: Insights gained from the US LTER program. *BioScience* **53**:57-67.
- Lamarque, V. C. 1984. Increasing Atmospheric Carbon Dioxide: Tree Ring Evidence for Growth Enhancement in Natural vegetation. *Science* **225**:1019-1021.
- Landsberg, J. J., and R. H. Waring. 1997. A generalised model of forest productivity using simplified concepts of radiation-use efficiency, carbon balance and partitioning. *Forest Ecology and Management* **95**:209-228.
- Law, B. E., O. J. Sun, et al. (2003). Changes in carbon storage and fluxes in a chronosequence of Ponderosa Pine. *Global Change Biology* **9**: 510-524.
- Law, B. E., D. P. Turner, et al. (2004). Disturbance and climate effects on carbon stocks and fluxes across western Oregon, USA. *Global Change Biology* **10**: 1429-1444.
- Magnuson, J.J. 1990. Long-Term Ecological Research and the Invisible Present. *BioScience* **40**:495-501.

- Magnuson, J. J., B. J. Benson, and T. K. Kratz. 1990. Temporal coherence in the limnology of a suite of lakes in Wisconsin, USA. *Freshwater Biology* **23**:145-159.
- McCune, B., and J. B. Grace. 2002. *Analysis of Ecological Communities*. MJM Software, Gleneden Beach, Oregon.
- McCune, B., and D. Keon. 2002. Equations for potential annual direct incident radiation and heat load. *Journal of Vegetation Science* **13**:603-606.
- McCune B., and M. J. Mefford. 1999. *PC-ORD. Multivariate Analysis of Ecological Data*. V.4. MJM Software, Gleneden Beach, Oregon.
- Moore, G. W., B. J. Bond, J. A. Jones, N. Phillips, and F. C. Meinzer. 2004. Structural and compositional controls on transpirations in 40- and 450-year old riparian forests in western Oregon, USA. *Tree Physiology* **24**:481-491.
- Palmer, W. C. 1965. *Meteorological Drought*. U.S. Department of Commerce, Washington, D.C.
- Piutti, E., and A. Cescatti. 1997. A quantitative analysis of the interactions between climate response and intraspecific competition in European beech. *Canadian Journal of Forest Research* **27**:277-284.
- Running, S. W. 1994. Testing Forest-BGC ecosystem process simulations across a climatic gradient in Oregon. *Ecological Applications* **4**:238-247.
- Running, S. W., and J. C. Coughlan. 1988. FOREST BGC, A general model of forest ecosystem processes for regional applications I. Hydrologic balance canopy gas exchange and primary production. *Ecological Modeling* **42**:125-154.
- Running, S. W., and E. R. J. Hunt. 1993. Generalisation of a forest ecosystem process model for other biomes, BIOME-BGC, and an application for global scale models. Academic Press, San Diego.
- SAS Institute (2002). *SAS Version 9.1*. SAS Inc. Cary N.C.
- Schimel, D., Melillo, J., Tian, H., McGuire, D.A., Kicklighter, D., Kittel, T., Rosenbloom, N., Running, S., Thornton, P., Ojima, D., Parton, W., Kelly, R., Skyes, M., Neilson, R., Rizzo, B. 2000. Contribution of Increasing CO₂ and Climate to Carbon Storage by Ecosystems in the United States. *Science* **287**:2004-2006.

- Soranno, P. A., K. E. Webster, J. L. Riera, T. K. Kratz, J. S. Baron, P. A. Bukaveckas, G. W. Kling, D. S. White, N. Caine, R. C. Lathrop, and P. R. Leavitt. 1999. Spatial Variation among Lakes within Landscapes: Ecological Organization along Lake Chains. *Ecosystems* **2**:395-410.
- Swanson, F. J., and R. E. Sparks. 1990. Long-Term Ecological Research and the Invisible Place. *BioScience* **40**:502-508.
- Schweingruber, F. H. 1988. *Tree Rings: Basics and Application of Dendrochronology*. D. Reidel Pub. Company, Dordrecht, Holland.
- Swetnam, T. W., M. A. Thompson, and E. K. Sutherland. 1985. Using dendrochronology to measure radial growth of defoliated trees. USDA Forest Service Cooperative State Research Service.
- Turner, D. P., and G. J. Koerper. 1995. A Carbon Budget for the Conterminous United States. *Ecological Applications* **5**:421-436.
- Turner, D. P., Cohen W.B., Kennedy, R.E. (2000). Alternative spatial resolutions and estimation of carbon flux over a managed forest landscape in Western Oregon. *Landscape Ecology* **15**: 441-452.
- Turner, D. P., Guxy, M., Lefsky, M.A., Van Tuyl, S., Sun, O., Daly, C., Law, B.E. (2003). Effects of land use and fine scale environmental heterogeneity on net ecosystem production over a temperate coniferous forest landscape. *Tellus* **55(B)**: 657-668.
- Turner, D. P. 2005. Personal Communication. *in*.
- Van Tuyl, S., Law, B.E., Turner, D.P., Gitelman, A.I. (2005). Variability in net primary production and carbon storage in biomass across Oregon forests-an assessment integrating data from forest inventories, intensive sites, and remote sensing. *Forest Ecology and Management* **209**: 273-291.
- Webb, W. L., Lauenroth, W.K., Szarek, S.R., Kinerson, R.S. 1983. Primary production and abiotic controls in forests, grasslands, and desert ecosystems in the United States. *Ecology* **64**:134-151.
- White, M. A., P. E. Thornton, S. W. Running, and R. R. Nemani. 2000. Parameterization and sensitivity analysis of the BIOME_BGC terrestrial ecosystem model: Net Primary Production controls. *Earth Interactions* **4**:1-85.
- Yamaguchi, D. K. 1991. A simple method for cross-dating increment cores from living trees. *Canadian Journal of Forest Research* **21**:414-416.

Appendices



Appendix 1.1 Map of H.J. Andrews Experimental Forest showing sampling sites.

Appendix 1.2 Sample Sizes used for uncertainty analysis for each age class.

Site	Sampling Level (% of all Trees in Population)	Number of Trees Sampled
WS06 (Second- growth)	90	280
	80	248
	70	216
	60	184
	50	156
	40	124
	30	92
	20	64
	10	32
RS32 (Mature)	90	144
	80	128
	70	112
	60	96
	50	80
	40	64
	30	48
	20	32
	10	16
RS07 (Old- growth)	90	64
	80	56
	70	48
	60	44
	50	36
	40	28
	30	20
	20	16
	10	8

Appendix 1.3 D-statistics and associated p-values from a Kolmogorov-Smirnov test for normality for Monte Carlo distributions of each model and site at the highest and smallest sample sizes for four different years (**a,b,c,d**).

Site	Model	Largest Sample Size		Smallest Sample Size	
		D-statistic	p-value	D-statistic	p-value
Second-growth	SR	0.0118 ^a	<0.01	0.0161 ^a	<0.01
		0.0223 ^b	<0.01	0.0076 ^b	>0.15
		0.0232 ^c	<0.01	0.0087 ^c	0.0682
		0.0219 ^d	<0.01	0.0069 ^d	>0.15
	SRQ	0.0096 ^a	0.0236	0.0253 ^a	<0.01
		0.0057 ^b	>0.15	0.0184 ^b	<0.01
		0.0060 ^c	>0.15	0.0066 ^c	>0.15
		0.0120 ^d	<0.01	0.0044 ^d	>0.15
Mature	SR	0.0359 ^a	<0.01	0.0110 ^a	<0.01
		0.0334 ^b	<0.01	0.0822 ^b	0.0977
		0.0264 ^c	<0.01	0.0083 ^c	0.0903
		0.0486 ^d	<0.01	0.0294 ^d	<0.01
	SRQ	0.0116 ^a	<0.01	0.0066 ^a	>0.15
		0.0110 ^b	<0.01	0.0152 ^b	<0.01
		0.0129 ^c	<0.01	0.0106 ^c	<0.01
		0.0128 ^d	<0.01	0.0316 ^d	<0.01
Old-growth	SR	0.0591 ^a	<0.01	0.0587 ^a	<0.01
		0.0500 ^b	<0.01	0.0340 ^b	<0.01
		0.0402 ^c	<0.01	0.0059 ^c	>0.15
		0.0614 ^d	<0.01	0.0078 ^d	0.149
	SRQ	0.0489 ^a	<0.01	0.0126 ^a	<0.01
		0.0567 ^b	<0.01	0.0830 ^b	<0.01
		0.0434 ^c	<0.01	0.0131 ^c	<0.01
		0.0265 ^d	<0.01	0.0202 ^d	<0.01

Appendix 1.4 Four different years illustrating the estimate, standard deviation, and upper and lower bounds of biomass increment at varying sample sizes for the second-growth site using the SR model. Estimate of biomass increment with highest accuracy, and the upper and lower bounds that fall within +/- 10% of true biomass increment, are in bold.

True annual Biomass Increment Mg/ha/yr (+/- 10%)	# of Trees Sampled	Estimated Biomass Increment (Mg/ha/yr)	Standard Deviation (SD)	Lower Bound	Upper Bound	
2.814 (2.533-3.095)	280	2.793	0.036	2.733	2.853	
	1991	248	2.771	0.051	2.687	2.854
		216	2.748	0.063	2.644	2.852
		184	2.727	0.074	2.606	2.849
		156	2.708	0.083	2.572	2.845
		124	2.686	0.093	2.533	2.838
		92	2.662	0.102	2.493	2.830
		64	2.643	0.118	2.448	2.837
		32	2.619	0.148	2.375	2.862
3.822 (3.440-4.204)	280	3.774	0.044	3.702	3.845	
	1995	248	3.724	0.061	3.623	3.825
		216	3.674	0.075	3.550	3.798
		184	3.625	0.088	3.480	3.770
		156	3.582	0.097	3.422	3.742
		124	3.530	0.110	3.348	3.712
		92	3.479	0.125	3.273	3.685
		64	3.435	0.142	3.200	3.669
		32	3.383	0.183	3.081	3.685
3.652 (3.287-4.017)	280	3.598	0.051	3.514	3.682	
	1999	248	3.544	0.072	3.425	3.664
		216	3.489	0.090	3.340	3.638
		184	3.435	0.108	3.257	3.612
		156	3.388	0.120	3.190	3.585
		124	3.332	0.138	3.105	3.560
		92	3.278	0.163	3.010	3.547
		64	3.228	0.193	2.911	3.545
		32	3.177	0.264	2.743	3.610

Appendix 1.4 (continued)

True annual Biomass Increment Mg/ha/yr (+/- 10%)	# of Trees Sampled	Estimated Biomass Increment (Mg/ha/yr)	Standard Deviation (SD)	Lower Bound	Upper Bound
	280	3.854	0.057	3.760	3.947
2001	248	3.797	0.081	3.664	3.931
	216	3.739	0.101	3.571	3.906
	184	3.680	0.121	3.481	3.879
3.910 (3.519-4.301)	156	3.631	0.138	3.404	3.858
	124	3.573	0.161	3.309	3.838
	92	3.519	0.187	3.211	3.828
	64	3.464	0.227	3.091	3.838
	32	3.405	0.316	2.885	3.925

Appendix 1.5 Four different years illustrating the estimate, standard deviation, and upper and lower bounds of biomass increment at varying sample sizes for the mature site using the SR model. Estimate of biomass increment with highest accuracy, and the upper and lower bounds that fall within +/- 10% of true biomass increment, are in bold.

True annual Biomass Increment Mg/ha/yr (+/- 10%)	# of Trees Sampled	Estimated Biomass Increment (Mg/ha/yr)	Standard Deviation (SD)	Lower Bound	Upper Bound
1975 3.571 (3.214-3.928)	144	3.532	0.097	3.373	3.691
	128	3.494	0.141	3.262	3.727
	112	3.450	0.172	3.167	3.733
	96	3.410	0.205	3.073	3.746
	80	3.372	0.234	2.988	3.757
	64	3.328	0.261	2.899	3.757
	48	3.290	0.304	2.790	3.790
	32	3.245	0.365	2.645	3.844
	16	3.200	0.496	2.384	4.014
1985 4.269 (3.842-4.696)	144	4.207	0.102	4.040	4.374
	128	4.142	0.145	3.902	4.381
	112	4.073	0.184	3.771	4.375
	96	4.005	0.215	3.651	4.360
	80	3.937	0.251	3.523	4.350
	64	3.871	0.287	3.340	4.343
	48	3.804	0.338	3.250	4.360
	32	3.736	0.409	3.063	4.408
	16	3.673	0.581	2.718	4.628
1995 4.372 (3.935-4.809)	144	4.302	0.107	4.125	4.478
	128	4.227	0.157	3.969	4.485
	112	4.149	0.194	3.831	4.468
	96	4.079	0.228	3.704	4.454
	80	4.000	0.261	3.571	4.430
	64	3.927	0.300	3.433	4.420
	48	3.852	0.347	3.281	4.424
	32	3.774	0.415	3.091	4.457
	16	3.703	0.568	2.768	4.637

Appendix 1.5 (continued)

True annual Biomass Increment Mg/ha/yr (+/- 10%)	# of Trees Sampled	Estimated Biomass Increment (Mg/ha/yr)	Standard Deviation (SD)	Lower Bound	Upper Bound
	144	4.900	0.151	4.652	5.148
1999	128	4.822	0.219	4.463	5.183
	112	4.741	0.276	4.288	5.195
	96	4.663	0.322	4.133	5.194
4.976 (4.478- 5.464)	80	4.584	0.376	3.964	5.203
	64	4.503	0.429	3.799	5.209
	48	4.421	0.497	3.602	5.239
	32	4.341	0.601	3.340	5.342
	16	4.252	0.835	2.878	5.626

Appendix 1.6 Four different years illustrating the estimate, standard deviation, and upper and lower bounds of biomass increment at varying sample sizes for the old-growth site using the SR model. Estimate of biomass increment with highest accuracy, and the upper and lower bounds that fall within +/- 10% of true biomass increment, are in bold.

True annual Biomass Increment Mg/ha/yr (+/- 10%)	# of Trees Sampled	Estimated Biomass Increment (Mg/ha/yr)	Standard Deviation (SD)	Lower Bound	Upper Bound
1975 3.290 (2.961-3.619)	64	3.286	0.139	3.057	3.515
	56	3.276	0.209	2.932	3.620
	48	3.259	0.264	2.824	3.693
	44	3.252	0.291	2.772	3.731
	36	3.240	0.346	2.671	3.809
	28	3.222	0.412	2.544	3.900
	20	3.208	0.504	2.380	4.038
	16	3.190	0.551	2.284	4.096
	8	3.167	0.776	1.891	4.443
1985 2.628 (2.365-2.891)	64	2.623	0.099	2.460	2.786
	56	2.619	0.145	2.380	2.858
	48	2.615	0.185	2.310	2.919
	44	2.605	0.202	2.278	2.944
	36	2.611	0.241	2.209	3.000
	28	2.603	0.284	2.136	3.071
	20	2.605	0.341	2.045	3.166
	16	2.603	0.377	1.984	3.223
	8	2.607	0.524	1.744	3.470
1995 3.657 (3.291-4.023)	64	3.610	0.144	3.373	3.847
	56	3.561	0.210	3.215	3.907
	48	3.511	0.270	3.067	3.955
	44	3.480	0.293	2.998	3.962
	36	3.433	0.345	2.866	4.000
	28	3.378	0.398	2.723	4.034
	20	3.330	0.473	2.553	4.108
	16	3.311	0.525	2.446	4.175
	8	3.255	0.739	2.039	4.471

Appendix 1.6 (continued)

True annual Biomass Increment Mg/ha/yr (+/- 10%)	# of Trees Sampled	Estimated Biomass Increment (Mg/ha/yr)	Standard Deviation (SD)	Lower Bound	Upper Bound
	64	3.256	0.127	3.046	3.465
1999	56	3.181	0.182	2.881	3.480
	48	3.113	0.232	2.732	3.495
	44	3.073	0.254	2.654	3.491
3.318	36	3.003	0.299	2.511	3.494
(2.986- 3.650)	28	2.929	0.343	2.365	3.492
	20	2.861	0.414	2.181	3.542
	16	2.827	0.454	2.080	3.574
	8	2.755	0.634	1.711	3.799

Appendix 1.7 Four different years illustrating the estimate, standard deviation, and upper and lower bounds of biomass increment at varying sample sizes for the second-growth site using the SRQ model. Estimate of biomass increment with highest accuracy, and the upper and lower bounds that fall within +/- 10% of true biomass increment, are in bold.

True annual Biomass Increment Mg/ha/yr (+/- 10%)	# of Trees Sampled	Estimated Biomass Increment (Mg/ha/yr)	Standard Deviation (SD)	Lower Bound	Upper Bound
1991 2.814 (2.533- 3.095)	280	2.816	0.023	2.772	2.860
	248	2.819	0.041	2.751	2.887
	216	2.822	0.053	2.735	2.908
	184	2.824	0.064	2.719	2.930
	156	2.828	0.073	2.705	2.945
	124	2.828	0.085	2.688	2.968
	92	2.826	0.101	2.660	2.991
	64	2.827	0.119	2.630	3.023
	32	2.816	0.167	2.541	3.090
1995 3.822 (3.440- 4.204)	280	3.823	0.030	3.774	3.871
	248	3.824	0.046	3.748	3.899
	216	3.825	0.059	3.727	3.923
	184	3.826	0.071	3.709	3.943
	156	3.824	0.080	3.692	3.956
	124	3.826	0.094	3.672	3.980
	92	3.824	0.109	3.645	4.004
	64	3.823	0.129	3.610	4.035
	32	3.816	0.174	3.529	4.102
1999 3.652 (3.287- 4.017)	280	3.652	0.037	3.592	3.713
	248	3.651	0.060	3.553	3.749
	216	3.651	0.077	3.523	3.778
	184	3.646	0.094	3.492	3.802
	156	3.648	0.110	3.468	3.829
	124	3.643	0.129	3.430	3.856
	92	3.643	0.154	3.390	3.896
	64	3.644	0.186	3.338	3.949
	32	3.648	0.259	3.222	4.073

Appendix 1.7 (continued)

True annual Biomass Increment Mg/ha/yr (+/- 10%)	# of Trees Sampled	Estimated Biomass Increment (Mg/ha/yr)	Standard Deviation (SD)	Lower Bound	Upper Bound
2001 3.910 (3.519-4.301)	280	3.912	0.042	3.843	3.981
	248	3.913	0.065	3.807	4.019
	216	3.913	0.084	3.774	4.052
	184	3.912	0.101	3.746	4.078
	156	3.911	0.120	3.713	4.109
	124	3.912	0.140	3.681	4.142
	92	3.917	0.168	3.640	4.194
	64	3.918	0.210	3.573	4.263
	32	3.922	0.294	3.438	4.405

Appendix 1.8 Four different years illustrating the estimate, standard deviation, and upper and lower bounds of biomass increment at varying sample sizes for the mature site using the SRQ model. Estimate of biomass increment with highest accuracy, and the upper and lower bounds that fall within +/- 10% of true biomass increment are in bold.

True annual Biomass Increment Mg/ha/yr (+/- 10%)	# of Trees Sampled	Estimated Biomass Increment (Mg/ha/yr)	Standard Deviation (SD)	Lower Bound	Upper Bound
1975 3.571 (3.214-3.928)	144	3.582	0.100	3.417	3.747
	128	3.594	0.148	3.351	3.837
	112	3.604	0.184	3.301	3.907
	96	3.613	0.217	3.257	3.969
	80	3.624	0.253	3.209	4.040
	64	3.634	0.298	3.143	4.125
	48	3.646	0.353	3.065	4.227
	32	3.657	0.442	3.929	4.385
16	3.657	0.622	3.633	4.681	
1985 4.269 (3.842-4.696)	144	4.278	0.101	4.112	4.446
	128	4.289	0.144	4.052	4.525
	112	4.297	0.179	4.002	4.592
	96	4.312	0.214	3.960	4.664
	80	4.321	0.251	3.908	4.734
	64	4.323	0.290	3.846	4.800
	48	4.335	0.344	3.770	4.901
	32	4.345	0.420	3.654	5.035
16	4.345	0.591	3.372	5.318	
1995 4.372 (3.935-4.809)	144	4.383	0.104	4.211	4.553
	128	4.390	0.154	4.136	4.643
	112	4.401	0.196	4.079	4.724
	96	4.411	0.235	4.024	4.798
	80	4.419	0.277	3.963	4.874
	64	4.432	0.321	3.905	4.960
	48	4.440	0.375	3.822	5.058
	32	4.455	0.474	3.676	5.234
16	4.455	0.674	3.346	5.564	

Appendix 1.8 (continued)

True annual Biomass Increment Mg/ha/yr (+/- 10%)	# of Trees Sampled	Estimated Biomass Increment (Mg/ha/yr)	Standard Deviation (SD)	Lower Bound	Upper Bound
1999 4.976 (4.478-5.464)	144	4.985	0.155	4.730	5.240
	128	4.995	0.225	4.624	5.366
	112	4.999	0.289	4.524	5.475
	96	5.009	0.344	4.444	5.574
	80	5.020	0.400	4.362	5.678
	64	5.027	0.475	4.245	5.809
	48	5.034	0.561	4.111	5.958
	32	5.057	0.701	3.903	6.211
16	5.053	0.995	3.417	6.689	

Appendix 1.9 Four different years illustrating the estimate, standard deviation, and upper and lower bounds of biomass increment at varying sample sizes for the old-growth site using the SRQ model. Estimate of biomass increment with highest accuracy, and the upper and lower bounds that fall within +/- 10% of true biomass increment are in bold.

True annual Biomass Increment Mg/ha/yr (+/- 10%)	# of Trees Sampled	Estimated Biomass Increment (Mg/ha/yr)	Standard Deviation (SD)	Lower Bound	Upper Bound
1975 3.290 (2.961-3.619)	64	3.348	0.161	3.084	3.613
	56	3.410	0.235	3.023	3.796
	48	3.475	0.295	2.989	3.961
	44	3.413	0.327	2.972	4.046
	36	3.509	0.387	2.938	4.210
	28	3.559	0.466	2.865	4.399
	20	3.636	0.561	2.784	4.629
	16	3.678	0.637	2.700	4.798
	8	3.761	0.907	2.349	5.333
1985 2.628 (2.365-2.891)	64	2.682	0.126	2.475	2.889
	56	2.742	0.185	2.437	3.047
	48	2.793	0.240	2.398	3.189
	44	2.825	0.266	2.387	3.262
	36	2.874	0.321	2.346	3.402
	28	2.936	0.396	2.285	3.587
	20	2.985	0.496	2.169	3.800
	16	3.028	0.576	2.081	3.975
	8	3.088	0.879	1.642	4.534
1995 3.657 (3.291-4.023)	64	3.696	0.159	3.435	3.958
	56	3.737	0.234	3.352	4.121
	48	3.781	0.299	3.289	4.272
	44	3.797	0.328	3.258	4.337
	36	3.847	0.394	3.198	4.495
	28	3.893	0.465	3.128	4.657
	20	3.936	0.578	2.985	4.887
	16	3.974	0.656	2.895	5.054
	8	4.062	0.958	2.487	5.637

Appendix 1.9 (continued)

True annual Biomass Increment Mg/ha/yr (+/- 10%)	# of Trees Sampled	Estimated Biomass Increment (Mg/ha/yr)	Standard Deviation (SD)	Lower Bound	Upper Bound
	64	3.342	0.129	3.129	3.554
1999	56	3.366	0.188	3.057	3.675
	48	3.392	0.240	2.998	3.786
	44	3.402	0.264	2.968	3.837
3.318 (2.986- 3.650)	36	3.433	0.317	2.912	3.953
	28	3.463	0.379	2.834	4.086
	20	3.482	0.465	2.716	4.247
	16	3.512	0.524	2.650	4.373
	8	3.576	0.751	2.341	4.810

Appendix 1.10 Coefficients for equations used to calculate volume and total stem biomass in Mg for five conifer species in the second-growth watersheds, using diameter at breast height measurements (DBH). Total volume equations are in the following form; $\text{volume} = B_0 * (\text{DBH}^{B_1})$. Volume equations are from Brown (1962), wood/bark ratios from Acker (2002) and density values are from TV0097 optical dendrometer data set.

Species	Total Volume (B₀)	Total Volume (B₁)	Wood/bark ratio	Wood Density	Bark Density
<i>Pseudotsuga menziesii</i>	0.0001123560	2.509359	0.71	0.452	0.438
<i>Tsuga heterophylla</i>	0.0003720880	2.259720	0.876	0.421	0.415
<i>Taxus brevifolia</i>					
<i>Thuja plicata</i>	0.0003339420	2.197256	0.918	0.312	0.333
<i>Calocedrus decurrens</i>					

Appendix 1.11 Coefficients for equations used to calculate wood and bark volume and total stem biomass in Mg for seven conifer species in old-growth sites, using diameter at breast height measurements (DBH). Wood and bark volume equations are in the following form; volume= (B₀*(DBH^{B₁}))*Correction Factor (CF). All coefficients and values are from TV0097 optical dendrometer data set.

Species	Wood Volume (B ₀)	Wood Volume (B ₁)	CF	Bark Volume (B ₀)	Bark Volume (B ₁)	CF	Wood Density	Bark Density
<i>Pseudotsuga menziesii</i>								
<i>Pinus lambertiana</i>	0.0002719	2.3323	1.0311	0.0000384	2.4818	1.0834	0.452	0.438
<i>Pinus monticola</i>								
<i>Tsuga heterophylla</i>	0.0001431	2.5353	1.081	0.0000308	2.3474	1.2438	0.421	0.415
<i>Taxus brevifolia</i>							0.600	
<i>Thuja plicata</i>								
<i>Calocedrus decurrens</i>	0.0001641	2.4078	1.0185	0.0000097	2.3631	1.2041	0.312	0.333
<i>Abies procera</i>	0.0000973	2.6043	1.0176	0.0000274	2.4313	1.0824	0.37	0.55
<i>Abies amabilis</i>	0.0000989	2.5942	1.0492	0.000011	2.5677	1.1451	0.40	0.57
<i>Abies concolor</i>	0.0000341	2.7856	1.0302	0.0000131	2.7271	1.0639	0.365	0.59
<i>Tsuga mertensiana</i>	0.0000564	2.6627	1.022	0.0000499	2.3268	1.0351	0.403	0.415

Appendix 1.12 Allometric equations used to calculate height (HT) for three hardwood tree species in both second-growth and old-growth watersheds, using diameter at breast height measurements (DBH). All equations are in the following form $HT = B_0 * (1 - \exp(B_1 * DBH)^2)$.

Species	Site(s)	B ₀	B ₁	B ₂
<i>Acer macrophyllum</i>	WS01/WS02	30.41311	-0.034245	0.682100
<i>Prunus emarginata</i>	WS01/WS02	24.21249	-0.033914	0.891708
<i>Castanopsis chrysophylla</i>	WS01/WS02	40.66479	-0.017775	0.873626

Appendix 1.13 Allometric equations used to calculate total stem biomass (BST) in g for three hardwood tree species in both second-growth and old-growth watersheds, using diameter at breast height measurements (DBH). Equation in the following form; $\ln(BST) = \exp(B_0 + B_1 * \ln(DBH))$.

Species	Site(s)	BIOPAK Equation #	B ₀	B ₁
<i>Alnus rubra</i>				
<i>Arbutus menziesii</i>	WS01/WS02	266	3.97	2.56
<i>Cornus nuttallii</i>				

Appendix 1.14 Allometric equations used to calculate total stem wood volume in g for three hardwood tree species in both second-growth and old-growth watersheds, using diameter at breast height (DBH) and height HT. Equation is in the following form; $\text{volume} = B_0 * (DBH^{B_1}) * (HT^{B_2})$. Wood density values are then used to obtain total stem biomass, bark considered negligible.

Species	Site(s)	B ₀	B ₁	B ₂	Wood Density
<i>Acer macrophyllum</i>	WS01/WS02	0.0000718042	2.224620	0.575610	0.44
<i>Arbutus menzeisii</i>	WS01/WS02	0.0000378129	1.992950	1.015320	0.56
<i>Castanopsis chrysophylla</i>	WS01/WS02	0.0001169607	2.022320	0.686380	0.42

Appendix 1.15 Example SAS code for modeling of increment growth and estimation of NPP_B for a single site.

```

****Import Increment Data****;
OPTIONS PS=200 LS=200;
TITLE 'RS07_biomass';
LIBNAME SAS 'N:\SAS\Updated code_data\rs07';
RUN;
ODS Select ALL;
DATA RS07_all;
    INFILE 'N:\SAS\Updated
code_data\RS07\RS07_coredata_96_allmort.csv'
    FIRSTOBS=2 DELIMITER=', ';
    INPUT studyid $ stand $ plot tag species $ year dbh_last
dbh_died inc1971-inc1999 sampcode;

RUN;
PROC PRINT DATA=RS07_all;
RUN;

*****Single MACRO*****;
%MACRO biomass_sim(data_orig);
%DO n=1 %to 1;
ODS SELECT NONE;
filename myfile1 'F:\DATA\test1.log';
PROC PRINTTO log=myfile1;
run;
Proc means data=RS07_all;
    var dbh_last;
    output out=quarts p25=q1 p50=q2 p75=q3;
    run; PROC PRINT;
run;

****Randomly assign year of death to trees that died previous to
sampling;
data ex2;
    array live{29} live1971-live1999;

    if _N_=1 then set quarts;retain q1 q2 q3;
    set RS07_all;

if sampcode=6 then y=10*ranuni(-1);
    x=round(y,0.1);

    if (sampcode=6) and (x ge 0) and (x lt 5.1) then addyr_2=0;
    if (sampcode=6) and (x ge 5.1) and (x le 10.0) then addyr_2=2;

    if (sampcode=6) and (x ge 0) and (x lt 3.3) then addyr_3=0;
    if (sampcode=6) and (x ge 3.3) and (x lt 6.6) then addyr_3=1;
    if (sampcode=6) and (x ge 6.6) and (x le 10.0) then addyr_3=2;

    if (sampcode=6) and (x ge 0) and (x lt 2.5) then addyr_4=0;
    if (sampcode=6) and (x ge 2.5) and (x lt 5.0) then addyr_4=1;
    if (sampcode=6) and (x ge 5.0) and (x lt 7.5) then addyr_4=2;
    if (sampcode=6) and (x ge 7.5) and (x le 10.0) then addyr_4=3;

```

```

        if (samprcode=6) and (x ge 0) and (x lt 1.6) then addyr_6=0;
        if (samprcode=6) and (x ge 1.6) and (x lt 3.2) then addyr_6=1;
        if (samprcode=6) and (x ge 3.2) and (x lt 4.8) then addyr_6=2;
        if (samprcode=6) and (x ge 4.8) and (x lt 6.4) then addyr_6=3;
        if (samprcode=6) and (x ge 6.4) and (x lt 8.0) then addyr_6=4;
        if (samprcode=6) and (x ge 8.0) and (x le 10.0) then addyr_6=5;

if (samprcode=6) and (year= 16 or 17 or 18 or 19 or 20 or 21) then
yrdead=year;
    if (samprcode=6) and (year=8) then yrdead=year-addyr_2;
    if (samprcode=6) and (year=15) then yrdead=year-addyr_3;
    if (samprcode=6) and (year=12) then yrdead=year-addyr_4;
    if (samprcode=6) and (year=6) then yrdead=year-addyr_6;

do j=1 to 29 by 1;
if (samprcode=6) and j le yrdead then live(j)=1; else live(j)=0;
if (samprcode=1) or (samprcode=0) then live (j)=1;
end;

if (samprcode=1) and (dbh_last gt 0) and (dbh_last lt q1) then
quartile=1;
if (samprcode=1) and (dbh_last ge q1) and (dbh_last lt q2) then
quartile=2;
if (samprcode=1) and (dbh_last ge q2) and (dbh_last lt q3) then
quartile=3;
if (samprcode=1) and (dbh_last ge q3) then quartile=4;

if (samprcode=0) and (dbh_last gt 0) and (dbh_last lt q1) then
quartile=1;
if (samprcode=0) and (dbh_last ge q1) and (dbh_last lt q2) then
quartile=2;
if (samprcode=0) and (dbh_last ge q2) and (dbh_last lt q3) then
quartile=3;
if (samprcode=0) and (dbh_last ge q3) then quartile=4;

if (samprcode=6) and (dbh_died gt 0) and (dbh_died lt q1) then
quartile=1;
if (samprcode=6) and (dbh_died ge q1) and (dbh_died lt q2) then
quartile=2;
if (samprcode=6) and (dbh_died ge q2) and (dbh_died lt q3) then
quartile=3;
if (samprcode=6) and (dbh_died ge q3) then quartile=4;

RUN;PROC PRINT; RUN;
PROC SORT DATA=ex2;
    BY quartile;
RUN;PROC PRINT; RUN;

/* identifies observations in the original dataset */
/* as either sampled or not, for each quartile */
data sampled;set ex2;if samprcode=1;run;PROC PRINT data=sampled;RUN;
/* sampled contains only sampled trees */
/* ex2 contains sampled and unsampled trees */

```

```

*-----Means for quartiles-----;

PROC MEANS Data=sampled; *no print*;
  VAR inc1971-inc1999;
  BY quartile;
  OUTPUT OUT=samp_12avg MEAN=avg_inc1971-avg_inc1999
         STD=sd_inc_1971-sd_inc_1999;
RUN; PROC PRINT; RUN;

*****Makes missing SDS and/or averages zero so model will run*****;

Data samp_12avg2;
set samp_12avg;retain avg_inc1971-avg_inc1999 sd_inc_1971-
sd_inc_1999;
ARRAY oldavgs {29} avg_inc1971-avg_inc1999;
ARRAY avgs {29} navg_inc1971-navg_inc1999;
ARRAY oldsds {29} sd_inc_1971-sd_inc_1999;
ARRAY sds {29} nsd_inc_1971-nsd_inc_1999;
do j= 1 to 29 by 1;
  if oldsds(j)=. then sds(j)=0;
  else sds(j)=oldsds(j);
  if oldavgs(j)=. then avgs(j)=0;
  else avgs(j)=oldavgs(j);
end;
proc print data=samp_12avg2; run;

/***** Increment Prediction start here *****/
/* This macro predicts a growth increment for non-sampled trees */
/* and uses the real increment for the sampled trees */
/* this is done separately for a single quartile */
/* The predicted DBH in each year is then constructed from the */
/* predicted or real growth increments */

%MACRO inc_predict(quart, quart_predict);
options ps= 900 ls=256;
data onemnsd;set samp_12avg;if quartile=&quart;run;proc print
data=onemnsd;run;
data onequart;set ex2;if quartile=&quart;run;proc print; run;

data &quart_predict;
  array rinc{29} inc1971-inc1999;
  array avgs{29} avg_inc1971-avg_inc1999;
  array sds{29} sd_inc_1971-sd_inc_1999;
  array predinc{29} predinc1971-predinc1999;
  array dbhyr{29} dbh_1971-dbh_1999;
  array live{29} live1971-live1999;

set onequart;
  if _N_=1 then set onemnsd;
  retain avg_inc1971-avg_inc1999 sd_inc_1971-sd_inc_1999;

do j=29 to 1 by -1;
  if sampcode=1 then predinc(j)=rinc(j);
end;

do f=29 to 1 by -1;

```

```

    if sampcode=0 then do until (predinc(f) ge 0);
        predinc(f)= avgs(f) + sds(f)*rannor(-1);
    end;end;

do h=29 to 1 by -1;
    if (sampcode=6) and (live(h)=1) then do until (predinc (h) ge 0);
        predinc(h)= avgs(h) + sds(h)*rannor(-1);
    end;end;

if sampcode=1 then do;
    do g=26 to 1 by -1;
        if g=26 THEN dbhyr(g)=dbh_last;
        if g lt 26 then dbhyr(g)=dbhyr(g+1)-(2*predinc(g+1));
    end;
    do k=27 to 29 by 1;
        dbhyr(k)=dbhyr(k-1)+2*predinc(k);
    end;end;

if sampcode=0 then do;
    do k=28 to 1 by -1;
        if k=28 then dbhyr(k)=dbh_last;
        if k lt 28 then dbhyr(k)=dbhyr(k+1)-(2*predinc(k+1));
    end;
    do k=29 to 29 by 1;
        dbhyr(k)=dbhyr(k-1)+(2*predinc(k));
    end;end;

if (sampcode=6) then do;
    do m=yrdead to 1 by -1;
        if m=yrdead then dbhyr(m)=dbh_last;
        if m lt yrdead then dbhyr(m)=dbhyr(m+1)-(2*predinc(m+1));
    end;end;

keep plot sampcode tag species predinc1971-predinc1999 quartile
dbh_1971-dbh_1999;
output;run;
%MEND;

%inc_predict(1, quart1_predict);PROC PRINT;RUN;
%inc_predict(2, quart2_predict);PROC PRINT;RUN;
%inc_predict(3, quart3_predict);PROC PRINT;RUN;
%inc_predict(4, quart4_predict);PROC PRINT;RUN;
data allquart;set quart1_predict quart2_predict quart3_predict
quart4_predict;run;proc print data=allquart;run;

*****CALCULATE BIOMASS*****;
data bmass; set allquart;
    array dbhyr {29} dbh_1971-dbh_1999;
    array ht_yr {29} ht1971-ht1999;
    array wood_vol_yr {29} w_vol1971-w_vol1999;
    array bark_vol_yr {29} b_vol1971-b_vol1999;
    array bmass_yr {29} bmass1971-bmass1999;

```

```

*****CALCULATE HT FOR HARDWOODS ACMA ARME CACH*****;
do j= 1 to 29;

if species= 'ACMA' and dbhyr(j) ge 5.0 then ht_yr(j)=30.41311*(1-
exp(-0.034245*(dbhyr(j)**0.682100)));

if species= 'ARME' and dbhyr(j) ge 5.0 then ht_yr(j)=24.21249*(1-
exp(-0.033914*(dbhyr(j)**0.891708)));

if species= 'CACH' and dbhyr(j) ge 5.0 then ht_yr(j)=40.66479*(1-
exp(-0.017775*(dbhyr(j)**0.873626)));

end;

*****CALCULATE WOOD VOLUME FOR ALL SPECIES*****;
do j= 1 to 29;

if species= 'ACMA' and dbhyr(j) ge 5.0 then wood_vol_yr(j)=
(0.0000718042*(dbhyr(j)**2.224620)*(ht_yr(j)**0.575610));

if species= 'ARME' and dbhyr(j) ge 5.0 then wood_vol_yr(j)=
(0.0000378129*(dbhyr(j)**1.992950)*(ht_yr(j)**1.015320));

if species= 'CACH' and dbhyr(j) ge 5.0 then wood_vol_yr(j)=
(0.0001169607*(dbhyr(j)**2.022320)*(ht_yr(j)**0.686380));

if species= 'PSME' and dbhyr(j) ge 5.0 then wood_vol_yr(j)=
(0.0002719*(dbhyr(j)**2.3323))*1.0311;

if species= 'TSHE' and dbhyr(j) ge 5.0 then wood_vol_yr(j)=
(0.0001431*(dbhyr(j)**2.5353))*1.081;
if species= 'THPL' and dbhyr(j) ge 5.0 then wood_vol_yr(j)=
(0.0001641*(dbhyr(j)**2.4078))*1.0185;

if species= 'TABR' and dbhyr(j) ge 5.0 then wood_vol_yr(j)=
(0.0001431*(dbhyr(j)**2.5353))*1.081;

if species= 'LIDE2' and dbhyr(j) ge 5.0 then wood_vol_yr(j)=
(0.0001641*(dbhyr(j)**2.4078))*1.0185;

if species= 'CADE3' and dbhyr(j) ge 5.0 then wood_vol_yr(j)=
(0.0001641*(dbhyr(j)**2.4078))*1.0185;

if species= 'ABPR' and dbhyr(j) ge 5.0 then wood_vol_yr(j)=
(0.0000973*(dbhyr(j)**2.6043))*1.0176;

if species= 'ABAM' and dbhyr(j) ge 5.0 then wood_vol_yr(j)=
(0.0000989*(dbhyr(j)**2.5942))*1.0492;

if species= 'ABCO' and dbhyr(j) ge 5.0 then wood_vol_yr(j)=
(0.0000341*(dbhyr(j)**2.7856))*1.0302;

if species= 'TSME' and dbhyr(j) ge 5.0 then wood_vol_yr(j)=
(0.0000564*(dbhyr(j)**2.6627))*1.022;

end;

```

```

*****CALCULATE BARK VOLUME*****;
do j= 1 to 29;

if species= 'PSME' and dbhyr(j) ge 5.0 then bark_vol_yr(j)=
(0.0000384*(dbhyr(j)**2.4818))*1.0834;

if species= 'TSHE' and dbhyr(j) ge 5.0 then bark_vol_yr(j)=
(0.0000308*(dbhyr(j)**2.3474))*1.2438;

if species= 'THPL' and dbhyr(j) ge 5.0 then bark_vol_yr(j)=
(0.0000097*(dbhyr(j)**2.3631))*1.2041;

if species= 'TABR' and dbhyr(j) ge 5.0 then bark_vol_yr(j)=
(0.0000308*(dbhyr(j)**2.3474))*1.0311;

if species= 'LIDE2' and dbhyr(j) ge 5.0 then bark_vol_yr(j)=
(0.0000097*(dbhyr(j)**2.3631))*1.0311;

if species= 'CADE3' and dbhyr(j) ge 5.0 then bark_vol_yr(j)=
(0.0000097*(dbhyr(j)**2.3631))*1.0311;

if species= 'ABPR' and dbhyr(j) ge 5.0 then bark_vol_yr(j)=
(0.0000274*(dbhyr(j)**2.4313))*1.0824;

if species= 'ABAM' and dbhyr(j) ge 5.0 then bark_vol_yr(j)=
(0.000011*(dbhyr(j)**2.5677))*1.1451;

if species= 'ABCO' and dbhyr(j) ge 5.0 then bark_vol_yr(j)=
(0.0000131*(dbhyr(j)**2.7271))*1.0639;

if species= 'TSME' and dbhyr(j) ge 5.0 then bark_vol_yr(j)=
(0.0000499*(dbhyr(j)**2.3268))*1.0351;
end;

***CALCULATE BIOMASS using volume and density of wood and bark*****;
do j= 1 to 29;

if species= 'PSME' and dbhyr(j) ge 5.0 then
bmass_yr(j)=(wood_vol_yr(j)*0.452) + (bark_vol_yr(j)*0.438);

if species= 'TSHE' and dbhyr(j) ge 5.0 then
bmass_yr(j)=(wood_vol_yr(j)*0.421) + (bark_vol_yr(j)*0.415);

if species= 'TABR' and dbhyr(j) ge 5.0 then
bmass_yr(j)=(wood_vol_yr(j)*0.600) + (bark_vol_yr(j)*0.415);

if species= 'THPL' and dbhyr(j) ge 5.0 then
bmass_yr(j)=(wood_vol_yr(j)*0.312) + (bark_vol_yr(j)*0.333);

if species= 'LIDE2' and dbhyr(j) ge 5.0 then
bmass_yr(j)=(wood_vol_yr(j)*0.312) + (bark_vol_yr(j)*0.333);

if species= 'CADE3' and dbhyr(j) ge 5.0 then
bmass_yr(j)=(wood_vol_yr(j)*0.312) + (bark_vol_yr(j)*0.333);

```

```

if species= 'ABPR' and dbhyr(j) ge 5.0 then
bmassyr(j)=(woodvolyr(j)*0.37) + (barkvolyr(j)*0.55);

if species= 'ABAM' and dbhyr(j) ge 5.0 then
bmassyr(j)=(woodvolyr(j)*0.4) + (barkvolyr(j)*0.57);

if species= 'ABCO' and dbhyr(j) ge 5.0 then
bmassyr(j)=(woodvolyr(j)*0.365) + (barkvolyr(j)*0.59);

if species= 'TSME' and dbhyr(j) ge 5.0 then
bmassyr(j)=(woodvolyr(j)*0.403) + (barkvolyr(j)*0.415);

if species= 'ACMA' and dbhyr(j) ge 5.0 then
bmassyr(j)=(woodvolyr(j)*0.44);

if species= 'ARME' and dbhyr(j) ge 5.0 then
bmassyr(j)=(woodvolyr(j)*0.56);

if species= 'CACH' and dbhyr(j) ge 5.0 then
bmassyr(j)=(woodvolyr(j)*0.42);

if species= 'ALRU' and dbhyr(j) ge 5.0 then bmassyr(j)=(exp(3.97 +
2.56*log(dbhyr(j))))/1000000;

if species= 'PREM' and dbhyr(j) ge 5.0 then bmassyr(j)=(exp(3.97 +
2.56*log(dbhyr(j))))/1000000;

if species= 'CONU' and dbhyr(j) ge 5.0 then bmassyr(j)=(exp(3.97 +
2.56*log(dbhyr(j))))/1000000;

if species= 'RHPU' and dbhyr(j) ge 5.0 then bmassyr(j)=(exp(3.97 +
2.56*log(dbhyr(j))))/1000000;

end;output;proc print;run;

****CALCULATE BIOMASS ADDED every year FOR Individuals EVERY YEAR****;

Data bmassadded; set bmass;
array bmassyr {29} bmass1971-bmass1999;
array bmassadd {29} bmassadd1971-bmassadd1999;

do j= 1 to 29 by 1;
  if j=1 then bmassadd(j)=0;
  else bmassadd(j)= bmassyr(j)-bmassyr(j-1);
end;
PROC PRINT;RUN;

****SUM BIOMASS added for EVERY YEAR *****;
PROC SORT data=bmassadded;
  run;

PROC MEANS DATA=bmassadded;
  VAR bmassadd1971-bmassadd1999;

  OUTPUT OUT=st_bmassadd sum=stand_bmassadd1971-
stand_bmassadd1999;
PROC PRINT;

```

```
RUN;  
  
***Store Data appended from each simulation in a file***;  
libname store 'N:\SAS\Updated code_data\rs07';  
PROC APPEND DATA=st_bmassadd  
base=store.badd_4quarts_RS07_allmort_10000;  
run;  
ODS SELECT ALL;  
%END;  
%MEND;  
%biomass_sim(RS07_core);run;
```